City Research Online

Citation: Benjamin, S. (1994). Aspects of self stratifying coatings. (Unpublished Doctoral thesis, City, University of London)

Permanent repository link: https://openaccess.city.ac.uk/id/eprint/29328/

Link to published version:

Aspects of Self Stratifying Coatings

by

Susan Benjamin

Submitted for the degree of Doctor of Philosophy
at The City University, UK
wholly carried out at the laboratories of PRA, Teddington, UK

January 1994

ACKNOWLEDGEMENTS

I would like to thank K W Allen for his supervision of this work and PRA for supporting its presentation as a thesis. My grateful thanks are to those of my colleagues at PRA who have encouraged and guided me. I would like to acknowledge the financial support of this programme of research by the CEC and the consortium of industrial sponsors under the BRITE scheme.

ABSTRACT

Liquid unpigmented coatings can be prepared which spontaneously stratify after application to a metallic substrate.

Stratification can be seen to be dependent upon the solubility of pairs of polymers in common solvents; the occurrence of phase separation and subsequent layer formation.

The solubility of commercial resin pairs in common solvents has been studied using the three - dimensional solubility parameter of Hansen. Attempts have been made to extend the use of solubility parameters to the prediction of phase behaviour. However, no clear correlation of stratification with Hansen solubility parameter data has been established. Experimental phase diagrams have been constructed to provide information on phase behaviour.

After the occurrence of phase separation, stratification has been observed to be a surface energy driven process. Stratification has been predicted from surface energy data of resin / solvent solutions with some success.

Experimental stratifying coatings have been characterised using elemental analysis and infra red spectroscopy. Epoxy / acrylic and epoxy / fluorinated-polyether systems can be observed to stratify experimentally. It has been shown that stratification of these systems is improved by curing the epoxy component with a proprietary polyoxypropyleneamine curing agent. The most favourable conditions are a resin ratio of 1:1 and a dry film thickness of at least 100 microns.

Extension to systems containing a protective pigment in the layer at the substrate interface has shown success. Addition of a second pigment proved more difficult. Some success was achieved using a silane coated titanium dioxide pigment which could be located in the fluorinated polyether resin. However, this was an isolated case.

It has been shown that the coatings produced perform at least as well as their two-coat counterparts when subjected to standard paint testing methods.

CONTENTS

ABBREVIATIONS AND SYMBOLS

Abbreviation	**Term**
DSC	Differential Scanning Calorimetry
EDS	Energy Dispersive Spectrometry
FTIR	Fourier Transform Infrared
GC-MS	Gas Chromatography - Mass Spectrometry
GPC	Gel Permeation Chromatography
HATR / FTIR-HATR	Horizontal Attenuated Total Reflectance
MEK	Methyl Ethyl Ketone
MiBK	Methyl iso Butyl Ketone
PAS / FTIR-PAS	Photoacoustic Spectroscopy
PBMA	Poly (butyl methacrylate)
PEMA	Poly (ethyl methacrylate)
PiBMA	Poly (isobutyl methacrylate)
PMMA	Poly (methyl methacrylate)
PVC	Pigment Volume Concentration
SEM	Scanning Electron Microscope
γ	Surface Tension
δ	Solubility Parameter
θ	Contact Angle

1. SURFACE COATINGS

1.1. Surface Coatings - A Brief History

Since his days as a cave dweller man has been using paint to decorate and protect his surroundings[1]. The earliest cave dwellers used naturally occurring materials such as clays and chalks bound together with animal fats to decorate their cave walls with pictures of people and animals. Chemical analysis of cave paintings found in areas of Spain and France showed that the pigments used were mainly based on iron and manganese oxides together with carbon and chalk[2]. Although the paints themselves were of poor durability many pictures have been preserved because of their sheltered position.

Between about 3000 and 600 BC the Egyptians used paints to decorate their palaces, temples and burial chambers[3]. Animal fat binders were replaced with other everyday materials such as gum arabic, gelatine, albumen and beeswax coloured, initially, with yellow or red ochre and chalk. They later extended their knowledge to use arsenic sulphide yellow and malachite green as pigments. The first synthetic pigment, known today as Egyptian Blue, was produced within this period[4].

After the Egyptians, the Greeks and Romans continued to leave painted records of the important events of the time using paints based on molten wax. By this time pigments representing most colours were available employing very diverse materials such as mussels and roots. However, the fifth century AD saw the loss of much of this knowledge when the Roman Empire was overrun by the Barbarians. It was not until the twelfth century that interest in paints and painting was rekindled, primarily in the form of religious paintings in churches. The paints of this era used egg white and casein (solubilised by lime) as binders and a wide range of pigments. The number of available pigmentary colours had increased with travel to the Orient. During this period paint manufacture was considered an art, only carried out by skilled craftsmen using closely guarded recipes.

Towards the end of the 16th century shellac, a naturally occurring resin, was introduced to Europe from India and became used as a finish for interior woodwork. These finishes imitated the Oriental lacquering techniques which were far superior to their European counterparts. Attempts had been made to bring the lacquering techniques of the Orient to Europe but had failed because of the toxicity of the lacquers.

By the 1700's paints were being used for both decorative and protective applications[5] but paint manufacture was still regarded as an art form. The painter himself made his paint on a small scale using simple hand grinding methods with natural oils, such as linseed oil as binders. Linseed oil was initially used in its raw state, but as knowledge increased it was boiled prior to use to remove moisture and other impurities.

During the Industrial Revolution in the mid eighteenth century, demand for paint increased leading to the mechanisation of the paint manufacture process. During this period paint factories began to appear, first in Europe, and later in America[6]. Although early manufacturing equipment was simple it had a tremendous impact on the volume of paint produced compared with previous hand methods. By the 1850's the paint industry was well established in Britain and the existence of over 250 paint factories was recorded[5]. The mechanisation of paint manufacture marked the end of the era of the master painters as ready mixed paint became widely available.

The twentieth century has seen the transformation of the paint industry from an art form to a specialised branch of the world chemical industry. The development of synthetic resins and new solvents has rapidly altered paint technology. Paints today represent a sizeable and diverse industry which has been estimated at some £1.4bn per annum in the UK alone.

1.2. Surface Coatings - An Introduction

Paint and other surface coatings make an invaluable contribution to maintaining the world's architectural and industrial fabric. Their use is universal for protection and / or decoration of metals, masonry, concrete, plastics and wood. Not only do they provide a pleasing finish in terms of both colour and gloss to a wide range of domestic and industrial goods, but also offer heavy-duty protection to cars, ships, chemical plant and structural steel. Coatings can offer a very effective barrier between a vulnerable substrate and a harsh service environment by dramatically prolonging life and reducing maintenance costs.

Traditionally, the term paint described a liquid pigmented coating and was used to distinguish it from a clear varnish or lacquer. Today, however, the word is applied to a wide variety of materials used for coating purposes and the terms paint and surface coating have become almost synonymous.

A paint may generally be considered as having three main components: a pigment, a resin or binder, and a solvent. The exact composition will be dependent upon many factors; including the substrate, the method of application, the service environment and the role of the coating - be it aesthetic or protective.

Pigments generally have a role that may be both protective and decorative. They usually consist of finely divided insoluble solids with a particle size from about 0.2 to 20μm diameter and may be organic or inorganic in nature. Pigments provide colour and opacity or hiding power and also contribute to durability. Specific pigments may be used to inhibit corrosion or reflect sunlight for example. The pigment content in a paint will affect the final properties of the paint film and is usually described in terms of the pigment volume concentration, or PVC[7].

$$PVC = \frac{Volume\ \ of\, Pigment}{Volume\ \ of\, Pigment\ +\ Resin} \qquad \textbf{(1)}$$

In the UK pigments are usually supplied in powder form. However, the particles supplied are usually aggregates of the primary pigment particles produced by the manufacturer. In order for the pigment to play a useful role in the coating these aggregates must be broken down in a process known as dispersion. Dispersion is usually carried out in a machine that subjects the aggregates to shear forces. A variety of equipment is available for pigment dispersion including ball-mills, bead-mills, high speed dispersers and triple roll mills.

The resin binds the pigment particles together and holds them onto the surface in a coherent film. It also provides important barrier properties and is responsible for the mechanical and protective properties of the final paint film. The desired properties (e.g. chemical resistance) of the final coating and the nature of the substrate will determine which resin is used.

Many of the resins in use today are relatively new materials having been introduced this century, most since World War II. This has led to modern high performance coatings based on synthetic polymers. However, more traditional materials such as the alkyd resins, first used in paints in the late 1920's are still very much in demand[8,9].

Resins are often classified into convertible and non-convertible types. Convertible resins dry by undergoing a chemical reaction in the film by the action of oxygen, other chemical reaction, or heat (thermosetting binders). Non-convertible resins dry solely by solvent evaporation.

Solvents dissolve the resin for application and also reduce the viscosity of the paint to suit the application technique. To date, most protective coatings used on metallic substrates contain resins dissolved in organic solvents although water based protective coatings are increasing in market share. Blends of solvents are more commonly used than single solvents in paints to provide the correct application properties in terms of solubility, viscosity and evaporation profile. Solvent blends can also aid the paint in complying with cost limitations and health and safety regulations.

Many different additives can also be used in paints for various reasons. These include prevention of settling of pigment and skin formation in the can, and reducing paint film defects such as segregation of pigment, cracking and formation of pin holes.

1.2.1. Traditional Organic Coatings

Traditional organic coatings for metallic substrates are composed of at least two layers. The primer is generally a pigmented layer applied to the substrate to provide good corrosion protection, adhesion and filling of defects in the substrate. A variety of commercial materials are available for this task including chlorinated rubbers, polyurethanes, modified alkyds and epoxies. The choice of resin is dependent upon the environment and requirements of the coating. A topcoat is applied over the primer to provide good surface properties, weather resistance and decorative appearance. Resins employed as topcoats should reflect the properties of the primer resin in terms of flexibility and hardness. Durable topcoat resins include acrylics, alkyds and polyurethanes. The topcoat can either be pigmented or "clear" depending on the purpose of the coating. Clear topcoats are often employed in automotive applications where a high gloss finish that is also weather resistant is a priority. In some cases in addition to a primer and topcoat intermediate coats may also be used to improve the adhesion and performance of the total system.

1.2.2. Materials used for the Protection of Metallic Substrates

The prime concern when painting ferrous metals is the prevention of corrosion. The Steel Structures Painting Council[10] recommends the use of a solvent borne epoxy coating containing an anti-corrosive pigment for the protection of steel against corrosion. Similar epoxy based coatings are found world-wide protecting bridges, oil platforms, ships and structural steel from damage by sea, weather and atmospheric pollutants.

Epoxy resins have been used for more than 25 years as a standard resin for industrial finishes where superior chemical and corrosion resistance is required. When correctly applied they can have an estimated service life of between 7 and 13 years[11].

Epoxy resins are synthetic resins that are prepared from epichlorohydrin and a dihydroxy compound, usually a diphenol. Often the diphenol used is a compound known as Bisphenol A (diphenylol propane).

Epoxy resins based on epichlorohydrin and Bisphenol A have the following generalised structure[12].

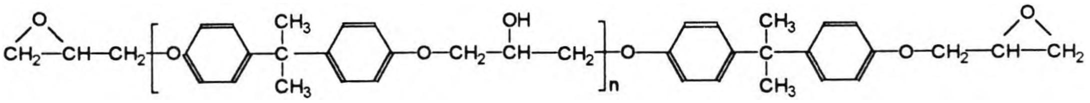

The presence of both epoxy and hydroxyl groups renders the resins very polar, providing excellent adhesion to polar or metallic substrates. Used alone epoxy resins tend to form brittle films and are of relatively low molecular weight, giving poor chemical resistance. Therefore, they are used as film formers when cross-linked with other materials to increase molecular weight and flexibility. The most commonly used curing agents are polyfunctional amines and polyamide resins. Cross-linking takes place through the reactive epoxide rings and hydroxyl groups. The cross-linkages formed are very well separated so a flexible cross-linked film is produced with extremely good chemical resistance. However, the aromatic epoxy resins absorb UV light strongly which leads to degradation, if used as a topcoat on exterior surfaces. It is for this reason that epoxy resins usually find their application in protective primers for metallic substrates.

Anti-corrosive pigments are used in primers for metallic substrates. Common anti-corrosive pigments include red lead, zinc chromate, zinc tetroxy chromate, zinc dust and zinc phosphate. The different pigments protect the substrate by different mechanisms, not all of which are clearly understood.

Zinc phosphate is a white anti-corrosive pigment of low toxicity suitable for use on many metallic substrates. Its ability to inhibit the corrosion of ferrous substrates was discovered in the mid 1950's but it was not routinely used in paints until the 1970's[13,14,15]. Since then it has replaced many of the more toxic lead and chromate based corrosion inhibiting pigments whose use has become limited by legislation. The structure of the pigment grade of zinc phosphate has been determined to be $Zn_3(PO_4)_2.2H_20$.

Iron oxide pigments are often added to metal primers as inert pigments which play a reinforcing role in the coating. The presence of hydroxyl groups is thought to slow down metal corrosion.

1.2.3. Self-Stratifying Coatings

An ideal protective coating would combine in a single coat the protective and decorative properties of a conventional multi-coat system. One route to such a system would be a self-stratifying coating in which primer and top coat resins are applied in a single coat but form distinct functional layers after application. The layer forming at the substrate would provide protective properties, where required, as well as good adhesion to the substrate; while the layer forming at the air interface would provide decorative properties as well as protection against the environment. A coating of this type would have obvious economic benefits from lower labour costs as it could be applied in a single coat instead of two or three coats applied using conventional methods. It has been estimated that in a typical maintenance operation the cost of the labour required represents up to 84% of the total cost. Self-stratifying systems potentially have all the benefits of two coat systems whilst reducing the burden of their application costs.

Self-stratifying coatings also have possible technological advantages. It is conceivable that instead of two distinct and discrete layers forming after application a film would form with a high concentration of one resin at the air interface, a high concentration of the other resin at the substrate interface and a concentration gradient across the film. The presence of a concentration gradient would provide all the advantages of a dual resin system but would eliminate the definite inter-coat boundary which is often the point of failure in conventional coatings.

The feasibility of producing a multilayer coating system which can be applied in a single operation has already been demonstrated during the past 17 years[16, 17, 18, 19, 20]. The systems devised depend on the mutual incompatibility of two or more components in a mixture of polymers or oligomers. Funke[16] described a system where a mixture of powders form distinct layers when heat cured above their melting points. Verkholantsev[17] extended the theory to two oligomers dissolved in a common solvent, where phase separation can occur as the solvent evaporates with subsequent layer formation. Both studies show that the resultant film performs better than would be expected if the different components were applied separately. This is thought to be due to the formation of a transitional layer containing significant concentrations of both components as phase inclusions. Such a layer removes the problem of adhesion between separately applied layers.

The present study aimed to develop guidelines for the formation of liquid stratifying coatings containing two incompatible resins in a common solvent or solvent blend. The coatings would be designed for metallic substrates and would employ materials that are typically used with success in traditional two coat systems. In order to achieve this it would be necessary to study the processes involved in multilayer formation.

2. INTRODUCTION

2.1. Self-Stratifying Coatings

2.1.1. Introduction

The concept of a self-stratifying coating is a relatively new one. Less than twenty years ago Funke[21] made reference to a multilayered surface coating that was formed on a metallic substrate when a mixture of two polymer powders was heat cured. There have been two main studies carried out in this field since : a continuation of the work of Funke[16, 18] using powder coatings and a separate study into multilayer formation from solvent borne oligomer systems[17, 22, 23, 24].

2.1.2. Multilayer Formation From Polymer Powders

Funke[16, 21] showed that multilayer formation can occur on metallic substrates when mixtures of polymer powders were heat cured. Suitable polymers were found to be mixtures of an epoxy powder and polybutyl methacrylate powder.

A pre-requisite for multilayer formation from polymer powders was found to be their limited compatibility which caused phase separation to occur during film formation. The order of the layers did not appear to be influenced by the relative densities of the two components but by the affinity of one of the components for the substrate. It was found that the separation of the layers could be improved by cross-linking one of the resin components.

The resultant coatings showed the characteristics of both polymers, good adhesion to the substrate from the epoxy and good weather resistance from the acrylic.

The subject was further explored by Murase and Funke[18] using similar epoxy / acrylic powder mixtures. In order to determine the compatibility of polymer powders they used a compatibility parameter (P) (Equation 2) which was determined from turbidity measurements and assumed to be related to the free energy of mixing.

$$P = \frac{\Delta m}{m_1 + m_2 + m_s + \Delta m} \tag{2}$$

where:

P = the compatibility parameter of the two powders

m_1, m_2, m_s = the weights of components 1 and 2 and solvent

Δm = the weight of added solvent required to produce mixing or demixing

P was found to correlate well with the observed phase separation behaviour of the polymer powders after heat curing. This was assessed by viewing through an optical microscope having first pigmented one of the layers with carbon black for ease of identification. P was found to be positive for a one phase to two phase change and negative for a two phase to a one phase change. The compatibility of polymer powders was also found to be dependent on molecular weight.

A second parameter that was found useful for the prediction of multilayer formation was the multilayer parameter (H). This parameter was quantified by measuring the height of the rise of a molten polymer in a glass capillary in a given time. The value obtained for H was found to be related to both the surface energy and the viscosity of the polymer. The ratio of the multilayer parameters (H) of two polymer powders often indicated whether substrate wetting and coverage and multilayer formation would occur. For successful multilayer formation a ratio of 1.5 or above was found to be desirable.

A combination of epoxy and acrylic powders was described. After heat curing, the epoxy resin, which has the higher surface energy, was found predominately at the substrate interface, whereas the acrylic resin, of lower surface energy, was found predominately at the air interface.

2.1.2.1. Practical Systems

This work became the subject of several patents. British patent 1 570 540[19] gives examples of polymer powder mixtures which were claimed to form multilayer coatings when heat cured. Use was made of the compatibility parameter (P) and the multilayer parameter (H) whose magnitude was claimed to be dependent on the surface energy ,viscosity and molecular weight of the molten polymer.

This patent claimed that for multilayer formation to occur the surface energy difference between the polymers in the fused state must be greater than 0.2 J cm^{-1} and the multilayer parameter ratio of the two polymers 1.5 or greater. Suitable resins for these systems were found to be polyester or epoxy powders for the high surface energy component and olefins or acrylic powders for the low surface energy component.

British patent 2 046 765 A[25] claimed the formation of a multilayered coating from a slurry of a solid polymer powder of low surface energy (e.g. an olefin) and a film forming resin of higher surface energy (e.g. epoxy) in a volatile organic compound that wets, but does not substantially swell or dissolve the polymer powder (iso or normal octane, a mixture of iso hexane and iso octane...). The multilayer was formed after heating the powder above its melting point. The films were claimed to have good delamination strength, high corrosion resistance and strong adhesion to metal substrates. The coatings were successfully applied by brush, spray, electrostatic spray and dip coating producing dry film thicknesses of between 30 and 200μm.

2.1.3. Multilayer Formation From Solvent Borne Systems

Verkholantsev[22] aimed to develop multilayer coatings which would have improved properties compared to classical two coat systems. It was envisaged that interlayer adhesion would no longer be a problem for this new generation of coating materials. The coatings described by Verkholantsev were formed from solutions of two incompatible oligomers or one oligomer and one polymer in a blend of at least two organic solvents.

Phase separation was considered to be a necessity for multilayer formation[24]. A homogeneous solution of the two oligomers can phase separate either by solvent evaporation or by chemical reaction; for example by curing one of the oligomers. Phase separation operates either by a binodal or spinodal mechanism. A binodal mechanism produces a new phase consisting of discrete droplets which have to coalesce to form a layered structure. A spinodal phase separation mechanism produces interpenetrating polymer networks. In this case the final film may not show the type of phase separation which occurred as the structure has sufficient time to transfer to a simpler system in a surface energy driven process. In all cases both of the separating layers were found to include both polymers but in differing ratios.

A compatibility parameter (β) was used in an attempt to assess the compatibility between pairs of oligomers using literature solubility parameter data[17] (Equation 3). It was considered that a value of $\beta < 0.07$ J cm^{-3} would indicate compatibility. However, this was found to be unreliable[18] presumably because literature values for solubility parameters vary considerably according to the method of determination[26].

$$\beta = (\delta_1 - \delta_2)^2 \quad \textbf{(3)}$$

where:-

δ_1, δ_2 = the literature solubility parameters of the two components.

The systems studied contained an epoxy resin which predominated in the high surface energy phase at the substrate and either oligodiene urethane diepoxide (ODUD) or perchlorovinyl resin (PCVR) which predominated at the air interface. The solvent used was either xylene or a 4:3 mixture of xylene and acetone[23].

It was shown that the rate and degree of layer separation could be increased by several factors:-

The use of binder compositions far removed from equal concentration ratios was found to enhance layer separation. Films with the best protective properties were formed using 20% PCVR and 80% epoxy (by weight). Selectively cross-linking <u>one</u> of the binder components with a cross-linking agent as a fourth component was also found to be beneficial. In some cases even causing one phase systems to form multilayers on curing.

The rate of evaporation of solvent was found to be an important factor in thinner films. At thicknesses of less than 200 μm epoxy aniline resin (EAR) / ODUD oligomer systems did not form multilayers above a given rate of solvent evaporation. It was considered that a slow rate of solvent evaporation would produce better separation as the phases would have a low viscosity for a longer period. This would allow longer for separation to occur before the structure becomes frozen as viscosity increases.

The nature of the substrate was found to be an important parameter since the order of the layers is dependent on the selective wetting of the substrate by one of the components. The relative order of the multilayer formed was not dependent on the density of the separate polymers except in very thick films. Multilayer epoxy / acrylic coatings could be formed at thicknesses of up to 700 μm on steel, 600 μm on glass and 500 μm on mica. Above these thicknesses the heavier acrylic layer tended to form at the substrate.

These coatings were described by Verkholantsev[24] as being comparable to conventional organic coatings containing between three and five separately applied coats when subjected to standard paint durability tests.

2.1.4. Summary

It is apparent that in order to obtain an insight into the processes of self-stratification from solvent borne liquid pigmented systems areas of study should include those of resin solubility, compatibility and surface energy.

Resin combinations used for a stratifying coating need to be soluble in a common solvent or solvent blend at similar concentrations to those used in surface coatings. Phase separation would occur after application and the two phases would then separate into distinct layers in what would appear to be a surface energy driven process.

2.2. Polymer Solubility

2.2.1. Practical Solubility

Early ideas on practical solubility generally followed the maxim that *like dissolves like* leading to a situation involving much trial and error. Several attempts have since been made to derive simple practical methods that would predict solubility.

Early practical tests for the solubility of resins in solvents included the kauri-butanol test which involved titrating kauri resin in butanol with a hydrocarbon solvent until turbidity was observed. Other similar empirical tests included the aniline point, solvent index and dilution ratio[27].

Hildebrand and Scott[28] made the first attempt to relate the thermodynamic properties of regular (non-polar) solutions to solubility by defining a quantity they termed the solubility parameter (δ_{Hild}) which can be used to predict solubility in a semi-quantitative manner.

δ_{Hild} is defined as the square root of the cohesive energy density (potential energy per unit volume) of a pure substance (Equation 4).

$$\delta_{Hild} = \sqrt{\frac{\Delta E}{V_m}} \qquad \textbf{(4)}$$

where:-

ΔE = the energy of vaporisation

V_m = the molar volume

Hildebrand and Scott were able to obtain single point values of the solubility parameters of pure liquids from molar energy of vaporisation and molar volume data. However, it is not possible to determine solubility data for non-volatile substances such as polymers or resins by this method.

Burrell[29] made two additions to Hildebrand's concept to make it of practical use for surface coatings. He recognised that hydrogen bonding was at least as important to the cohesive energy density as dispersion forces. He therefore grouped solvents into three classes based on their ability to form hydrogen bonds; namely poor, moderate and strong.

Burrell also suggested two ways to determine experimentally solubility data for polymers[30]. Both methods determined a range of solubility instead of a single point.

The first method used a "solvent spectrum" containing solvents with different solubility parameters within each hydrogen bonding class[29,30]. These were used to assess solubility by placing the polymer in contact with the solvent and observing whether a solution resulted. The solubility range of the polymer would encompass the solvents which dissolved the polymer.

The second method was based on the ability of a solvent to "swell" a lightly cross-linked version of the polymer. The amount of swelling will be greatest for the solvent with the solubility parameter closest to that of the polymer[30]. The percentage increase in volume due to swelling was determined visually.

The results from either method can be used to predict the solubility of the polymer in other solvents of similar hydrogen bonding character.

2.2.2. Three Dimensional Solubility Parameters

Several proposals have been made to extend the single point values of Hildebrand and Scott to three components.

Crowley, Teague and Lowe[31,32] described a system used to predict the solubility of cellulose esters at 3% concentration. The three components were based on the Hildebrand solubility parameter (δ_{Hild}), the dipole moment (μ) and the spectroscopic hydrogen bonding parameter (γ) based on the work of Gordy[33]. Solubility was determined experimentally and drawn in three dimensions or represented on two dimensional contour diagrams. However, the three dimensional models were not symmetrical so it was necessary to have a series of two dimensional contour maps for each polymer before the results could be used in a predictive manner.

Nelson, Hemwell and Edwards[34] described a three dimensional system based on the Hildebrand solubility parameter (δ_{Hild}), the fractional polarity (p) and the net hydrogen bond accepting index (θ_A) which was described in terms of the spectroscopic value for hydrogen bonding and a constant that is -1 for simple alcohols, 0 for glycol ethers and +1 for all other solvents. Solvents were further classified as non hydrogen bonding, hydrogen bond acceptors, hydrogen bond donors or solvents which can be either donors or acceptors.

The most commonly used system within the field of surface coatings is that of Hansen[35, 36] who extended the single term solubility parameter of Hildebrand into three separate terms.

The three terms are due to the various interactions that occur between molecules and which together form the cohesive energy density. The first term (δ_d) is due to the dispersion or London forces that arise from fluctuating atomic dipoles caused by the presence of a positive nucleus surrounded by a cloud of electrons. Such interactions exist in all molecules but are assumed to be the only ones present in saturated hydrocarbons.

The second term (δ_p) is due to either the interaction of permanent dipoles with each other or permanent dipoles inducing temporary dipoles in other molecules.

The last term (δ_h) is caused by the ability to form hydrogen bonds.

The total solubility parameter (δ_t) is calculated from the dispersion (d), polar (p) and hydrogen bonding (h) contributions (Equation 5).

$$\delta_t = \sqrt{\delta_d^2 + \delta_p^2 + \delta_h^2} \qquad \textbf{(5)}$$

For pure solvents the dispersion component can be calculated via the homomorph concept. This relies on the assumption that a hydrocarbon solvent of a similar size and shape will have the same energy of vaporisation as the solvent of interest if the active groups were disregarded. The difference between the solvent's energy of vaporisation and that of the hydrocarbon gives a measure of the contributions of the polar and hydrogen-bond interactions.

Hansen assumed that the polar and hydrogen bonding contributions together made up the active portion of the molecule (δ_a) (Equation 6). Actual values for δ_p and δ_h were arbitrarily determined after carrying out solubility tests and values of δ_p and δ_h chosen to provide the most coherent solubility volumes[35].

$$\delta_a = \sqrt{\delta_p^2 + \delta_h^2} \qquad \textbf{(6)}$$

Three-dimensional solubility parameter data for solvents obtained from physical data are readily available from literature[37,38]. However, similar data for polymers are scarce and the values obtained from different sources and methods vary considerably[26]. Data for commercial resins are even scarcer. In most cases the parameters for polymers or commercial resins must be determined experimentally by assessing the solubility of the polymer in a range of solvents of known three dimensional solubility parameters, being classified as soluble or non-soluble in each solvent. The Hansen solubility parameters of solvents used for the determination are plotted as points on a three dimensional grid having D, P and H as axes, representing δ_d, δ_p and δ_h. It is then possible to determine a sphere which encompasses only those solvents which dissolved the polymer and excludes all non-solvents. In order to obtain a sphere rather than an oblate spheroid it is necessary to increase the scale on the δ_d axis by a factor of two.

The calculation may be carried out using a computer program[39] which determines a sphere of minimum radius (R) which contains all those solvents which dissolved the polymer but excludes those solvents which did not. A value representing the quality of the fit (D_{tot}) is also obtained. For a perfect fit where every good solvent lies inside the sphere and every non-solvent outside the sphere this value will be unity. However, for every good solvent that lies outside the sphere and every bad solvent that lies inside the sphere D_{tot} will decrease.

Using this information it is possible to predict whether a solvent will dissolve a polymer by the location of the solubility parameter of the solvent in relation to the solubility sphere of the polymer. It is also possible to obtain information about common solvents for pairs of polymers. If the solubility spheres of the two polymers overlap then solvents or solvent blends lying in the overlap region should be common solvents for both polymers. However, it should be noted that a common solvent lying in the overlap region does not necessarily mean that a mixture of the two polymers in this solvent will be homogeneous as a dispersion of one solution in the other could result.

In a study by Hansen, solubility predictions based on the three dimensional solubility parameter yielded a 97.5% certainty[37]. However, attempts were made to improve on Hansen's system.

Huyskens *et al*[40] made two major criticisms of Hansen's work. First, Hansen considered entropy changes as constant for a given polymer dissolving in any solvent, whereas the entropy change on dissolution is not constant (Equation 7) but is dependent on other factors including the molar volume of the solvent .

$$S_B = \frac{-\Delta H_{transfer}}{RT} + \frac{\Delta S_{transfer}}{R} \qquad \textbf{(7)}$$

where:-

S_B = The dissolving power of the polymer

The term $-\Delta H_{transfer}$ takes into account the heat absorbed by the system when one mole of B transfers from its own phase into solution. The term $\Delta S_{transfer}$ denotes the corresponding change in entropy.

The other main criticism Huyskens had for Hansen's approach was in his use of a single hydrogen bonding term to represent both proton acceptor and donor sites. Huyskens therefore introduced a "structuration factor" (b_S) which was zero for solvents which do not form hydrogen bonds, -1 for solvents which form long single hydrogen bond chains (e.g. alcohols, phenols) and -2 for solvents where double chains are formed (e.g. water, diols).

A modified equation was proposed to take account of these factors. However, like Hansen's approach, Huyskens' dissolving power is dependant on the volume fraction of the polymer and is only valid at the concentration and temperature at which it was determined.

In the absence of polymer-solvent and polymer-polymer hydrogen bonds the equation takes the form:

$$S_m = -A\frac{-V_m}{RT}(1-\Phi_p)^2(\delta_s-\delta_p)^2 + (0.5+b_s)(1-\Phi_p)\frac{V_m}{V_s} \qquad \textbf{(8)}$$

where:

S_m = Dissolving power of solvent
A = Constant for a given polymer at a given temperature
V_m = Molar volume of repeat unit of polymer
R = Gas constant
T = Absolute temperature
Φ_p = Solubility of polymer in solvent at a given volume fraction
δ_p, δ_s = Modified solubility parameter of polymer and solvent
b_s = Structuration factor

If polymer - solvent hydrogen bonds are present then a further term must be added to Equation 8. This term relates to the stability of the polymer - solvent hydrogen bond.

If polymer - polymer hydrogen bonds are present an additional term must be subtracted from Equation 8. This term depends on the stability constant, k_{pp}, of the segment - segment hydrogen bonds.

Huyskens[40] tested seventy eight systems for solubility / insolubility. Use of predictions based on Hansen's approach yielded 61 correct results, whereas using predictions based on Huyskens revised method 77 correct results were reported.

The problem with this approach is that this equation only holds at concentrations of a few percent, above this further terms not specified by Huyskens must also be added. This approach is therefore of limited use in the coatings industry. Another limitation of this approach is that it is only valid if the degree of polymerisation is so large that the influence of the end groups on the dissolving power can be neglected. In many cases in the surface coatings field resin materials only consist of a few repeating units so the effect of the end groups should not be neglected.

2.2.3. Group Contribution Methods

The UNIFAC (Uniquac Functional Groups Activity Coefficients) method[41,42] uses group interaction parameters to predict activity coefficients in binary and multi-component mixtures with good accuracy. Existing data are used to predict the behaviour of systems for which no experimental data are available. A knowledge of the group interaction parameters can be used for the prediction of single point solubility parameters.

The method assumes that a physical property of a substance is the sum of contributions made by the molecule's functional groups, a group being any convenient structural unit e.g. CH_3. It also assumes that the different functional groups interact with each other in a unique manner irrespective of the molecule in which they are situated. The UNIFAC method uses experimentally obtained activity coefficient data to characterise the interactions between pairs of groups which may then be used to predict activity coefficients for other systems which have not been experimentally studied but contain the same functional groups.

It is necessary to have data containing two adjustable parameters per pair of functional groups. These represent the contributions to the activity coefficient made by differences in particle size and molecular interactions (Equation 9).

$$\ln \gamma_i = \ln \gamma_i^C + \ln \gamma_i^R \qquad \textbf{(9)}$$

The superscript *C* in Equation 9 represents the combinatorial contribution to the activity coefficient due to differences in size and shape between the groups and *R* represents a residual contribution to the activity coefficient due to energetic interactions.

These interactions together form a matrix of published group interaction parameters which are periodically updated and extended[41,43]. In order to use the UNIFAC method, data for the groups of interest must be amongst those published. However, certain groups, for example those containing C-F groups are still missing from the UNIFAC system. This means that UNIFAC is not suitable for fluorinated resins such as the Lumiflon range of fluorinated polyethers. Epoxy groups have also yet to be included in the UNIFAC data set.

2.2.4. Other Methods

Koehnen and Smolders[44] predicted solubility parameter data from molar attraction constants and other physical properties. Similar methods[43] have also been used to predict phase equilibria where little or no experimental data are available.

Another method of determining the solubility parameters of polymers practically involves viscosity measurements[26, 45, 46]. The solvation of a polymer by a "good" solvent leads to the polymer having an open extended shape with high viscosity, whereas the same polymer solvated by a "poor" solvent leads to a more coiled shape with a lower viscosity. Thus if a polymer is dissolved in a series of mixtures of two solvents of known solubility parameter one of these mixtures will have its solubility parameter closest to that of the polymer. This mixture will also have the highest viscosity. The single point solubility parameter of the polymer may therefore be determined from a knowledge of the solubility parameter of the solvent mixture. However, this method is limited to high molecular weight polymers at low concentrations.

2.2.5. Summary

Self-stratification from a pair of resins in a common solvent or solvent blend requires that the resins are soluble in the solvent at concentrations similar to those used within the surface coatings industry. This requires a knowledge of the solubility behaviour of resin pairs in solvents or solvent blends.

This section has reviewed the variety of methods that exist for the determination of solubility parameters. The use of literature values is inadvisable since they vary considerably due to the different methods of determination.

Methods based on the UNIFAC group contribution theory rely on published data for the groups that are of interest. A requirement is that the structure of the resin of interest is known in order to estimate the contribution made by each group. Unfortunately, the exact composition of many commercial resins has not been revealed.

Huyskens' approach is only valid if the degree of polymerisation is large enough to make the effect of the end groups negligible, which limits its usefulness in surface coatings. The determination of solubility parameters via viscosity measurements is also limited to high molecular weight polymers at low concentrations.

The three dimensional solubility parameter method of Hansen which, although much criticised for oversimplification, provides a relatively simple method of semi-quantitative solvent selection.

2.2.6. Prediction of Stratification Based on Solubility Parameters

The formation of a stratifying coating would require some incompatibility between the resin pair as phase separation is a route to stratification. Hansen solubility sphere data for resins is potentially useful in determining resin compatibility and ultimately stratification.

It could be considered that a pair of resins with a large overlapping volume would have many common solvents and the resins themselves would be similar in nature. A small common volume would suggest few, if any, common solvents as the resins become more dissimilar. It has already been seen that the solubility sphere radius generally decreases with increasing resin concentration. As the radius decreases the overlap volume between a pair of resins will also decrease until either the resins no longer overlap, or one resin becomes insoluble in the other. Either route would lead to phase separation.

Experimental data on solution appearance, film appearance, and solids at the point of phase separation has been studied in order to gain further information on the relationship between solubility parameter data and resin compatibility.

There are several ways of representing three-dimensional Hansen Solubility Parameter data in order to attempt to correlate solubility parameters with other properties.

The volume of the region of overlap (C) between the solubility spheres of two resins may provide information on the compatibility of the resins. The larger the common volume between two resins the more compatibility might be expected between them. The volume of the overlap can be calculated from the equation[47]:-

$$C = \frac{1}{3}\pi[P_1^2(3R_1 - P_1) + P_2^2(3R_2 - P_2)] \qquad \textbf{(10)}$$

where:

C = The volume of the overlap of the spheres
P_1, P_2 = The height of the sphere segments (Figure 1)
R_1, R_2 = The radii of the spheres

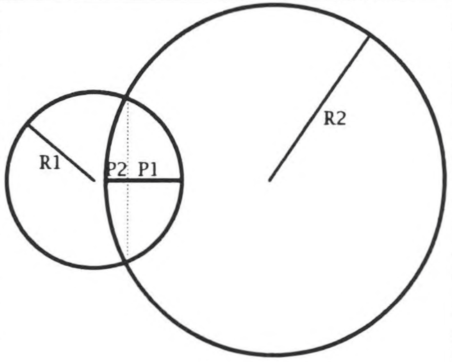

Figure 1. Overlap between Solubility Spheres.

In order to compare the relative sizes of the common volume between different pairs of resins the volume of the overlap may be expressed as a percentage of the volume of the smaller sphere (Equation 11).

$$V = 100\frac{C}{\frac{4}{3}\pi R_1^{\ 3}} \qquad \textbf{(11)}$$

where:

V = The overlap volume as a percentage of the volume of the smaller sphere
C = The overlap volume of the spheres (Equation 10)
R_1 = The radius of the smaller sphere

The distance between the centres of two solubility spheres (D) is probably also important when considering resin compatibility and tendency to stratify.

A small value of D would indicate that the resins are potentially very compatible with a large common volume and many common solvents.

A value of D that is less than the smaller radius indicates that both spheres have their centres within the larger sphere and could be expected to be very similar in nature and potentially compatible.

Conversely, a large value of D would indicate potential incompatibility as the common volume between the two resins decreases until D is larger than the sum of the two radii and no common volume exists.

D may be calculated from:-

$$D = \sqrt{4(d_1 - d_2)^2 + (p_1 - p_2)^2 + (h_1 - h_2)^2} \qquad \textbf{(12)}$$

where:

D = The distance between the centres of the solubility spheres
d_1, d_2 = The Hansen Solubility Parameter d values for the two resins
p_1, p_2 = The Hansen Solubility Parameter p values for the two resins
h_1, h_2 = The Hansen Solubility Parameter h values for the two resins

It would appear that the radii of the two spheres (R_1, R_2) and the distance between the sphere centres (D) are important functions when considering the compatibility of two resins. R_1, R_2 and D can all represented in the function B in the following equation:-

$$B = \frac{V_1 + V_2}{D} \qquad \textbf{(13)}$$

where:

V_1, V_2 = The volumes of the two spheres
D = The separation of the sphere centres

Hansen Three Dimensional Solubility Parameter data were correlated with experimental data which had been obtained from phase diagrams and stratification studies in order to determine if solubility parameters can be used in the prediction of stratification.

2.3. Miscibility of Polymer Solutions

2.3.1. Thermodynamics of Mixing

Miscibility in polymer solutions is controlled by thermodynamic factors[48,49,50,51]. Spontaneous miscibility implies that the Gibbs free energy of mixing, ΔG_{mix}, is negative or zero (Equation 14).

$$\Delta G_{mix} = (\Delta H_{mix} - T\Delta S_{mix}) \leq 0 \qquad \textbf{(14)}$$

where ΔH_{mix} and ΔS_{mix} are the enthalpy and the entropy of mixing respectively and T the absolute temperature.

For the mixing of polymer solutions ΔS_{mix} is always positive providing a negative contribution to ΔG_{mix} and hence favourable to the mixing process. This value is very small in the case of mixing of polymer solutions and generally decreases as the molecular weight of the components increases.

It is generally the magnitude of the enthalpy term (ΔH_{mix}) that determines miscibility which is seen to decrease with increasing molecular weight.

The result of the contributions by ΔS_{mix} and ΔH_{mix} to ΔG_{mix} is that incompatibility of chemically dissimilar polymers is the rule and compatibility the exception, especially for polymers of high molecular weight[26].

The expression for the Gibbs free energy of mixing can be generalised to multi-component systems according to Flory and Huggins[48,52].

$$\frac{\Delta G}{RT} = \sum n_i \ln \varphi_i + \sum \chi_{ij} \varphi_i \varphi_j \sum x_i n_i \qquad \textbf{(15)}$$

where:

$\sum n_i \ln \varphi_i$ = "combinatorial entropy term" due to the increased number of system configurations in the mixture compared to the pure components.

$\sum \chi_{ij} \varphi_i \, \varphi_j \sum x_i n_i$ = "interaction energy (enthalpy) term"

n_i = the number of moles of component i

φ_i = its volume fraction

χ_{ij} = the Flory-Huggins interaction parameter

x_i = the ratio of the molar volume of component i to that of a reference component

The summation over i and j being over all different pairs i, j.

Although the Flory-Huggins theory represents the main features of polymer solution thermodynamics, the theories are strictly only valid for regular solutions and make the following assumptions.

(i) that the mixing process is endothermic or athermal

(ii) the components are randomly distributed

(iii) the volumes are additive

(iv) χ_{ij} is a constant

(v) the energy of interaction between i and j is assumed to be equal to the geometric mean of the interaction forces of the pure components i and j.

These theories are therefore unable to describe mixtures containing components which could interact with each other. Unfortunately, this also renders them of little use to the types of polymers commonly used in surface coatings.

The interaction parameter (χ) is both temperature and concentration dependent due to large free volume differences between polymer and solvent. A revised theory was developed to account for these differences, however, although superior to the original Flory-Huggins theory, the Prigogine-Flory theory requires additional experimental data to determine the new parameters it introduces.

The other major problem with the Flory-Huggins theory is its inability to describe mixtures where specific interactions such as hydrogen bonding occur. The revised Flory-Huggins expression can be further modified by an extra term whose value is determined by the relative strength of the specific interactions and the entropy changes accompanying the formation of the various types of complexes formed[53,54,55,56,57,58,59]. This term however, has a very complex form and its calculation is tedious.

Whichever model is used to study phase behaviour some experimental data are required. This is usually obtained from measurements of osmotic pressure, chemical activities, infinite dilution activity coefficients or liquid-liquid equilibria. Unfortunately, very little data are currently available especially for the types of commercial resins encountered in surface coatings.

To overcome these problems predictive methods using group contribution methods may be used.

2.3.2. UNIFAC Group Contribution Methods

An alternative route is a group contribution model such as UNIFAC described in Section 2.2.3. Information on phase behaviour may be obtained from the activity coefficients where data for the groups of interest are available.

2.3.3. Phase Diagrams

The phase behaviour of ternary polymer, polymer, solvent systems at equilibrium is often represented using a phase diagram (Figure 2).

Three areas on a ternary phase diagram can be defined: stable, metastable and unstable. The boundary between the stable one phase region and the metastable composition is called the ***binodal***. The binodal is the limit of stability of the homogeneous phase. Within the binodal region growth originates from nuclei and depends on time and diffusion rate.

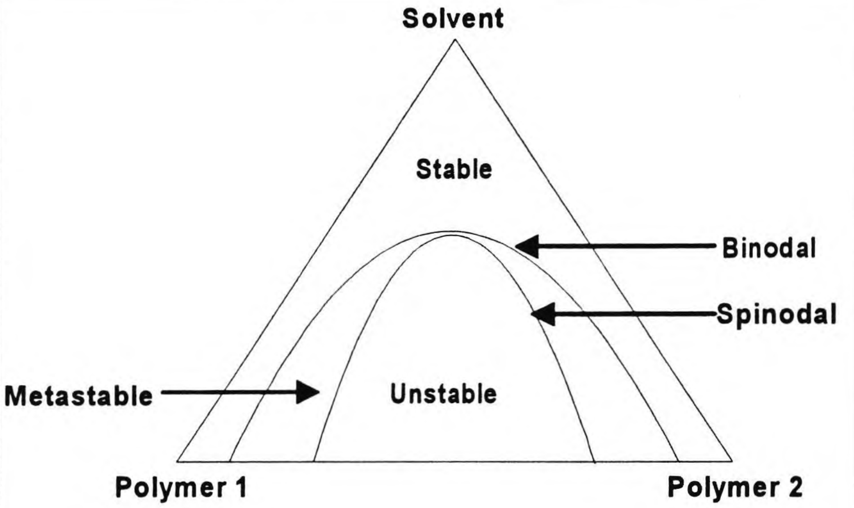

Figure 2. Ternary Phase Diagram

The boundary between the metastable and the unstable regions is called the ***spinodal***. Phase separation is spontaneous within the spinodal region and results in continuous decomposition into two phases with a high level of interconnectivity. The growth originates from small amplitude composition fluctuations which are always present in the equilibrium liquid state.

Practical information about phase diagrams for particular polymer, polymer, solvent combinations can be gained by determining the areas of stability and instability using a light scattering technique.

It should be noted however, that the phase diagram represents the system at equilibrium and thus can only provide accurate information about the initial and final states of the system. Between these points the system will not be in equilibrium due to heat and mass exchanges and only very approximate information may be gained. A drying paint film could be far removed from equilibrium due to compositional changes as the solvent evaporates increasing the percentage solid matter. The solvent composition will also change with evaporation as the more volatile solvent in the blend preferentially evaporates.

2.3.4. Summary

Accurate prediction of the phase behaviour of resin / resin / solvent blends is imperative for the successful formulation of self-stratifying coatings. It would appear from the methods reviewed in this section that methods predicting miscibility based on the Flory-Huggins theory are far too complex to be considered of practical use for the types of commercial resins and solvents commonly used in surface coatings.

The use of the UNIFAC group contribution principle may be a useful predictive tool for the calculation of activity coefficients where data for the groups of interest are available. From activity coefficients information on phase behaviour may be obtained.

Practical information on phase behaviour may be obtained by constructing phase diagrams from experimental data, which, although they only represent the system at equilibrium may contain useful information.

2.4. Surface Energy

2.4.1. Solution Surface Energy

Many methods exist which can be used for the direct measurement of the energy of a solution surface. The du Noüy ring method is a well established technique. A horizontal ring usually made of platinum is dipped into a liquid surface and then raised slowly. The force exerted on the ring increases until the ring is detached from the liquid surface. The theory assumes that both the inner and outer radii of the ring may be regarded as equal and that the inner and outer menisci approach verticality together and this corresponds to the point of rupture. Thus the force applied at the point of rupture is given by:

$$f = 4\pi R\gamma \tag{16}$$

Therefore the surface energy (γ) of the solution may be determined.

$$\gamma = \frac{f}{4\pi R} \tag{17}$$

where R is the radius of the ring.

It has been suggested that the assumptions made by this method are not always valid and tables of correction factors have been prepared[60].

Many other methods exist which may be used for the direct measurement of solution surface energy including the Wilhelmy Plate method, pendant drop method, and sessile drop method.

2.4.2. Solid Surface Energy

It is not possible to make a direct measurement of the surface energy of a solid. However, it can be estimated by measuring the contact angles of liquids on the solid surface. The contact angle of a liquid phase (l), with a surface energy γ_l, on a solid surface (s), with surface energy γ_s, can be represented using Young's equation (neglecting the spreading pressure Π_e):

$$\gamma_s - \gamma_{sl} - \gamma_l \cos\theta = 0 \qquad \textbf{(18)}$$

where γ_{sl} is the solid / liquid interfacial energy.

Spontaneous spreading of the liquid over the solid will occur when the contact angle between them is zero which occurs when:

$$(\gamma_s - \gamma_{sl}) \geq \gamma_l \qquad \textbf{(19)}$$

2.4.2.1. Critical Surface Energy

The critical surface energy (γ_c) of a solid is usually defined as the surface energy of a liquid which will just wet the solid surface[61]. It can be calculated by measuring the contact angles of a homologous series of liquids and extrapolating to zero contact angle according to Zisman[62]. The critical surface energy is often used as an approximation of the solid surface energy but the value obtained will depend on the series of liquids used for the determination.

2.4.2.2. Determination of Solid Surface Energy

An alternative route to the surface energy of a solid surface is the equation of state method conceived by Neumann[63,64,65,66]. The method allows the solid surface energy to be calculated from a single contact angle measurement and assumes that the same value would be obtained if different liquids were used.

In order to calculate the solid surface energy the Young Equation:

$$\gamma_{sl} = \gamma_{sv} - \gamma_{lv} \cos\theta \qquad \textbf{(20)}$$

Is combined with an equation of state of the form:

$$\gamma_{sl} = f(\gamma_{sv}, \gamma_{lv}) \qquad \textbf{(21)}$$

This gives two equations with which to obtain the two unknowns γ_{sv} and γ_{sl}.

This method would predict that all liquids with the same total surface energy would have the same contact angle on a given substrate. It disregards the separate disperse and polar contributions to the surface energy and completely characterises the surface in terms of the total surface energy. This method does, however, provide a very quick and easy method of measuring approximate solid surface energies.

An alternative route is that of Good and Girifalco[67,68] who stated that the interfacial energy between two apolar phases can be calculated from the surface energies of the two individual phases:

$$\gamma_{12} = \gamma_1 + \gamma_2 - 2\sqrt{\gamma_1 \gamma_2} \qquad \textbf{(22)}$$

which may also be expressed:

$$\gamma_{12} = \left(\sqrt{\gamma_1} - \sqrt{\gamma_2}\right)^2 \qquad \textbf{(23)}$$

Departures from regularity can be allowed for using a correction factor, Φ, which can be included in Equation 22[69].

$$\gamma_{12} = \gamma_1 + \gamma_2 - 2\Phi\sqrt{\gamma_1\gamma_2} \tag{24}$$

This equation takes into account that the two phases may be of different nature, *for example* polar / apolar. However, in systems where hydrogen bonds form interactions can be established which lead to serious disagreements between experimental and calculated values.

Fowkes[70,71] suggested that total surface energy , γ, could be resolved into several components such that $\gamma = \gamma^d + \gamma^i + \gamma^p + \gamma^h \ldots$ where d represents dispersion (London) forces, i represents induction (Debye) forces, p represents dipole-dipole interactions and h represents hydrogen bond forces. It has been generally recognised that induction forces can be neglected and the dipole-dipole interaction is generally negligible so that[72]:

$$\gamma = \gamma^d + \gamma^a \tag{25}$$

where *a* represents donor / acceptor interactions.

Wu[73] extended this work to produce equations for polar and non-polar interactions across interfaces. The harmonic mean equation is favoured over the geometric-harmonic mean and the geometric mean for polymers and other low energy systems. For an interface between two materials, 1 and 2, the interfacial energy according to the harmonic mean is given by:

$$\gamma_{12} = \gamma_1 + \gamma_2 - \frac{4\gamma_1^d\gamma_2^d}{\gamma_1^d + \gamma_2^d} - \frac{4\gamma_1^p\gamma_2^p}{\gamma_1^p + \gamma_2^p} \tag{26}$$

Using Equation (26) and Young's Law, the surface energy of the unknown can be calculated if the contact angle with two reference liquids are known.

An alternative method of determining the solid surface energy of polymers is to calculate the donor / acceptor characteristics instead of the disperse and polar contributions to the interaction. This can be done using a method derived by van Oss et al[74,75,76,77,78] who modified the Fowkes equation[70,71] by showing that a single expression could be used for d, p and i terms:

$$\gamma^{LW} = \gamma^{d} + \gamma^{p} + \gamma^{i} \qquad \textbf{(27)}$$

where LW stands for Lifshitz - van der Waals interactions.

γ^{p} is small because of a tendency towards mutual cancellation in a condensed phase and this is also assumed to be true in reasonably concentrated solutions.

Fowkes[72] showed that γ^{h} can be treated as acid - base interactions (AB) so that the total surface energy is given by:

$$\gamma = \gamma^{LW} + \gamma^{AB} \qquad \textbf{(28)}$$

At an interface the contribution to interfacial energy from LW interactions is given by:

$$\gamma_{12}^{LW} = \gamma_{1}^{LW} + \gamma_{2}^{LW} - 2\sqrt{\gamma_{1}^{LW}\gamma_{2}^{LW}} = \left(\sqrt{\gamma_{1}^{LW}} - \sqrt{\gamma_{2}^{LW}}\right)^{2} \qquad \textbf{(29)}$$

but a different equation is required for γ_{12}^{AB}.

The acid base contribution to the surface energy may be divided into electron acceptor, γ_{i}^{+}, and electron donor, γ_{i}^{-}, components:

$$\gamma_i^{AB} = 2\sqrt{\gamma_i^+\gamma_i^-} \qquad (30)$$

For a 'monopolar' substance:

$$\sqrt{\gamma_i^+\gamma_i^-} \ll \gamma_i^{LW} \qquad (31)$$

and the total surface energy can be approximated by γ^{LW}.

At an interface, the equation for a non-negligible polar component of interfacial energy is:

$$\gamma_{12} = \left(\sqrt{\gamma_1^{LW}} - \sqrt{\gamma_2^{LW}}\right)^2 + 2\left(\sqrt{\gamma_1^+} - \sqrt{\gamma_2^+}\right)\left(\sqrt{\gamma_1^-} - \sqrt{\gamma_2^-}\right) \qquad (32)$$

$$\gamma_{12}^{AB} = 2\left(\sqrt{\gamma_1^+} - \sqrt{\gamma_2^+}\right)\left(\sqrt{\gamma_1^-} - \sqrt{\gamma_2^-}\right) \qquad (33)$$

The total interfacial energy is then the sum of the LW and AB terms:

Substituting into Young's equation enables the $\gamma^{LW}, \gamma^+, \gamma^-$, components to be calculated from contact angles using standard liquids or solids:

$$(1 + \cos\theta)\gamma_l = 2\left(\sqrt{\gamma_s^{LW}\gamma_l^{LW}} + \sqrt{\gamma_s^+\gamma_l^-} + \sqrt{\gamma_s^-\gamma_l^+}\right) \qquad (34)$$

For each sample there are three unknowns, therefore three reference liquids are required to characterise a solid. The total surface energy of the solid surface is then:

$$\gamma_s = \gamma_s^{LW} + 2\sqrt{\gamma_s^+\gamma_s^-} \qquad (35)$$

Table 1 shows the values of some potential test liquids.

Solvent	γ^{TOT}	γ^{LW}	γ^{+}	γ^{-}
Water	72.8	21.8	25.5	25.5
Methylene Iodide	50.8	50.8	0	0
α-Bromonaphthalene	44.4	43.6	0	0
Glycerol	64.0	34.0	3.92	57.4
Formamide	58.0	39.0	2.28	39.6
Decane	23.8	23.8	0	0
MEK	24.6	24.6	0	24.0
CCl_4	26.8	26.8	0	0
$CHCl_3$	27.3	27.3	3.8	0
THF	27.4	27.4	0	15
Hexadecane	27.5	27.5	0	0
Toluene	28.3	28.3	0	2.7
Benzene	28.9	28.9	0	2.3
Ethyl Glycol	48.0	29.0	3.0	30.1

Table 1. LW and AB Components for Several Liquids[78]

2.4.3. Summary

This section has reviewed the various methods available for the direct measurement of solution surface energy and the indirect determination of the surface energy of solids from contact angle measurements. A knowledge of surface energies will be required to assess whether resin pairs have the potential for stratification.

2.4.4. Prediction of Stratification Based on Surface Energy

For stratification to occur in a thin film containing two phases two conditions must be fulfilled:

A) One component must spontaneously wet the substrate,

B) The total surface and interfacial energy of the layer sequence must be the lowest possible.

The total surface energy of the system is proportional to the area of the surfaces and interfaces. Layer formation from a system containing a dispersion of one phase in another will lead to a reduction in surface area and hence surface energy. Therefore, layer formation should be favoured for purely geometric reasons. However, it is still necessary to study which criteria need to be satisfied to ensure that the layers form in the correct order and that the layers are continuous (Figure 3).

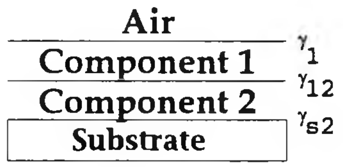

Figure 3

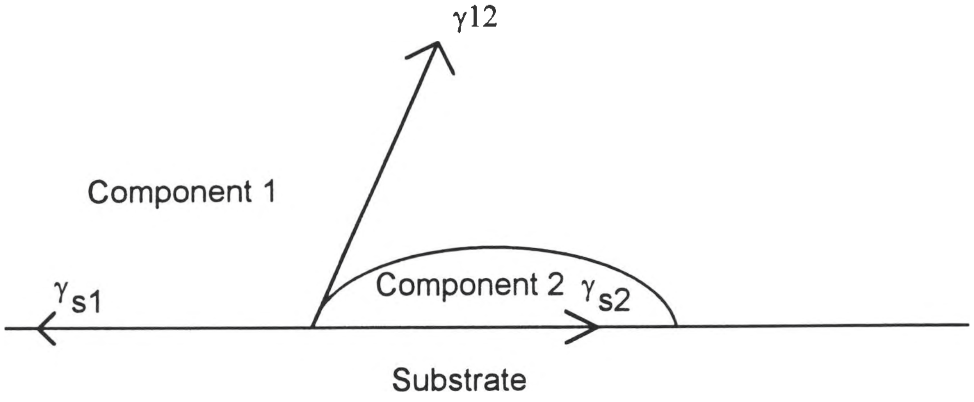

Figure 4

Condition (A) is satisfied when the contact angle (θ) between one of the separating phases and the substrate is zero. Young's equation states that (neglecting the spreading pressure π_e) (Figure 4):

$$\gamma_{s1} - \gamma_{s2} - \gamma_{12}\cos\theta = 0 \qquad \textbf{(36)}$$

where γ_{s1} is the solid /phase 1 interfacial energy , γ_{s2} is the solid / phase 2 interfacial energy and γ_{12} is the interfacial energy between phases 1 and 2. When component 2 wets the surface, displacing component 1 from the surface, then the contact angle, θ, is zero and:

$$\left(\gamma_{s1} - \gamma_{s2} - \gamma_{12}\right) \geq 0 \qquad \textbf{(37)}$$

This means that wetting of the substrate is best achieved by a large difference between the solid / liquid surface energies of the two components and a small interfacial energy between the two liquid components.

It should also be noted that the surface energy of the system must decrease for spontaneous wetting. This can be stated as:

$$\gamma_s > \gamma_{s2} + \gamma_{12} + \gamma_1 \quad \textbf{(38)}$$

or:

$$\gamma_s - \gamma_{s2} - \gamma_{12} - \gamma_1 > 0 \quad \textbf{(39)}$$

where γ_s is the surface energy of the substrate in contact with air.

Condition B states that the most favourable layer sequence will be the one giving rise to the lowest total surface energy. For the sequence in Figure 3 the total energy is given by:

$$\gamma_{s2} + \gamma_{12} + \gamma_1 \quad \textbf{(40)}$$

For the alternative sequence, the total energy is:

$$\gamma_{s1} + \gamma_{12} + \gamma_2 \quad \textbf{(41)}$$

Therefore, the required layer sequence is the most favourable when (41) > (40) or:

$$\gamma_{s1} - \gamma_1 - \gamma_{s2} + \gamma_2 > 0 \quad \textbf{(42)}$$

In most cases this is probably the equivalent of saying that the phase with the lowest surface energy will migrate to the air interface.

It is evident, therefore, that the prediction of stratification based on surface energies requires a knowledge of the surface energy of the two separating phases and their interfacial energy plus their interfacial energy with the substrate.

The surface energy of solution phases will be changing continuously as the solvent evaporates. It may be possible to estimate their value from the surface energy of the solid polymer and the solution concentration. However, a simpler route would be to use the surface energy of the pure polymer in place of the surface energy of the solution to acquire some idea of the tendency of the system to stratify.

Similarly, the interfacial energies will not be static but values determined from pure materials could be used to give estimated values. Solid / liquid interfacial energies cannot be measured directly but can be calculated from the surface energies of the solid and liquid.

The conditions for stratification can therefore be summarised as:

$$(\gamma_{sl} - \gamma_{s2}) \geq \gamma_{12} \qquad \textbf{(37)}$$

$$\gamma_2 - \gamma_{s2} - \gamma_1 + \gamma_{s1} > 0 \qquad \textbf{(42)}$$

$$\gamma_s - \gamma_{s2} - \gamma_{12} - \gamma_1 > 0 \qquad \textbf{(39)}$$

In order to solve these equations $\gamma_{s1}, \gamma_{s2}, \gamma_{12}, \gamma_1$ and γ_2 must all be known. γ_1 and γ_2 may be directly calculated but the other terms must be obtained using indirect methods.

These terms can be calculated using the Harmonic Mean method of Wu (Equation 26) for any combination of substrate and resins if the dispersive and polar contributions to the surface energy are known. This enables the prediction of stratification for any resin pair / substrate combination.

$$\gamma_{12} = \gamma_1 + \gamma_2 - \frac{4\gamma_1^d \gamma_2^d}{\gamma_1^d + \gamma_2^d} - \frac{4\gamma_1^p \gamma_2^p}{\gamma_1^p + \gamma_2^p} \qquad \textbf{(26)}$$

2.5. Objectives

The objectives of this research could be summarised as follows:

1. The formulation of experimental self-stratifying coatings on the basis of a preliminary screening of resin families, in particular to develop liquid pigmented systems. Self-stratifying systems were to be developed for steel substrates. Research would be focused on the systematic study of the variables governing stratification, taking into account the choice of materials, their concentration and level of use as well as temperature, film thickness and other external factors.

2. The characterisation of promising self-stratifying coatings at both the film formation and dry film stages. This systematic characterisation would consist of instrumental analysis to determine the presence and extent of stratification; standard performance tests to assess the physico-mechanical properties of dry films; and environmental tests to evaluate the durability and ageing behaviour of applied coatings

A series of main tasks arising from the research objectives were identified:-

2.5.1. Task 1 - Formulation

2.5.1.1. Selection of Materials

A range of commercial resins were to be selected after discussion with industrial sponsors. Suitable resins were to be selected for steel substrates from resins that perform well as either primers or topcoats in conventional two coat protective coatings. Epoxies, polyolefins, polyesters, halogenated resins and nitrogen containing resins were considered likely to be the main candidates. Choice of solvent blends, after solubility requirements of the resins, was to be based on such properties as volatility, evaporation rates and viscosity, whilst also taking into consideration environmental acceptability. Pigments were to be selected either for protective (anti-corrosive or durability) or aesthetic properties. Measurement of the physical properties of the materials was to be carried out where required.

2.5.2. Task 2 - Characterisation of Experimental Formulations

2.5.2.1. Preparation of Experimental Formulations

Initially unpigmented systems were to be prepared to observe the stratification effect. Optimum formulation parameters were to be determined by continuous experimentation.

2.5.2.2. Instrumental Analysis

Analytical techniques were to be employed to establish the presence and extent of stratification, both at the film formation stage and in dry films.

Attenuated total reflectance infra red spectroscopy (ATR) appeared an ideal method for the determination of stratification. Although normally used to examine the upper surface of films a recently developed overhead cell for used with Fourier transform infra-red spectroscopy allows the examination of the interface with the substrate. For supporting evidence on dry films additional analytical techniques were to be used including optical microscopy, electron microscopy (SEM-EDS), gas chromatography / mass spectrometry (GC-MS)

2.5.2.3. Physical Testing

Physical testing was to be used to confirm the performance properties of stratified films and was to be assessed using standard laboratory test methods for solvent borne coatings. Paint systems with pigmented base coats and clear topcoats were to be considered satisfactory for certain applications.

Tests were to include those for adhesion, hardness, flexibility, solvent resistance and scratch resistance. Comparison was to be made with control samples applied using conventional two coat methods.

2.5.2.4. Weathering Tests

The ageing behaviour of these optimised experimental coatings was determined by standard laboratory exposure tests.

3. EXPERIMENTAL

3.1. Source of Materials

3.1.1. Resins

The resins selected for use, their types and suppliers are shown in Table 2.

Tradename	Resin Type	Supplied as	Supplier
Epikote 828	Bisphenol-A Epoxy	Liquid	Shell UK Ltd
Epikote 1001	Bisphenol-A Epoxy	Solid	Shell UK Ltd
Epikote 1004	Bisphenol-A Epoxy	Solid	Shell UK Ltd
Epikote 1007	Bisphenol-A Epoxy	Solid	Shell UK Ltd
Epikote 1009	Bisphenol-A Epoxy	Solid	Shell UK Ltd
Neocryl B700	Thermoplastic Acrylic (PiBMA)	Solid	ICI Resins
Neocryl B728	Thermoplastic Acrylic (PMMA)	Solid	ICI Resins
Neocryl B804	Thermoplastic Acrylic (PBMA)	Solid	ICI Resins
Neocryl B811	Thermoplastic Acrylic (PMMA)	Solid	ICI Resins
Neocryl B813	Thermoplastic Acrylic (PEMA)	Solid	ICI Resins
Crodaplast AC-500	Thermosetting Acrylic	60% in xylene/butanol	Croda Resins Ltd
Crodaplast AC-550	Thermosetting Acrylic	60% in xylene	Croda Resins Ltd
Lumiflon LF200	Fluorinated Polyether	60% in xylene	ICI Resins
Lumiflon LF916	Fluorinated Polyether	65% in xylene	ICI Resins
Alloprene R10	Chlorinated Rubber	Solid	ICI Resins
Synolac 6016	Short Oil Alkyd	50% in xylene	Cray Valley Products
Synolac 9090	Short Oil Alkyd	50% in xylene	Cray Valley Products
VAS 9223	Long Oil Alkyd	84% in WS	Resinous Chemicals
Plastokyd AC-4X	Acrylic Modified Alkyd	50% in xylene	Croda Resins Ltd
Hythane 9	Urethane Alkyd	Liquid	Croda Resins Ltd
Plastokyd SC-7	Siliconised Polyester	55% in BCA	Croda Resins Ltd
Plastokyd SC-140	Siliconised Alkyd	40% in xylene	Croda Resins Ltd
Plastokyd SC-400	Siliconised Epoxy Ester	50% in AH	Croda Resins Ltd
Plastoprene 1S	Cyclised Rubber	Solid	Croda Resins Ltd
Hypalon 20	Chlorosulphonated Polyethylene	Solid	Dupont

WS = white spirit　BCA = butyl cellosolve acetate　AH = Aromosol H (ICI)

Table 2. Resins selected for use on metallic substrates

The Epikote series of epoxy resins were selected as typical primer resins. All other resins were selected as topcoat resins.

In order to obtain epoxy resins of intermediate molecular weight four mixtures of commercial Epikote resins were also studied. These were:-

"Epikote 901"	Epikote 828 : Epikote 1001 1:1 by weight
"Epikote 903"	Epikote 828 : Epikote 1001 1:3 by weight
"Epikote 781"	Epikote 828 : Epikote 1007 1:1 by weight
"Epikote 783"	Epikote 828 : Epikote 1007 1:3 by weight

The mixtures were prepared by weighing the appropriate amount of each resin into a screw top jar. The resin mixture was then dissolved using an appropriate solvent to give total resin solids of 40 - 50% as required. Dissolution was effected using an oscillating shaker.

3.1.2. Solvents

Solvents used were technical grade unless otherwise stated and obtained from Merck Ltd (Table 3). Solvents were used as received.

Solvent	Abbreviation
xylene	Not abbreviated
methoxy propanol	DPM
methyl iso butyl ketone	MiBK
methyl ethyl ketone	MEK
n-butyl actetate	Not abbreviated

Table 3. Solvents

3.1.3. Pigments

Table 4 shows the pigments selected for use.

Type	Grade & Type	Supplier
Titanium Dioxide	R-SM2 (uncoated grade)	Tioxide Europe Ltd
Titanium Dioxide	R-FC5 (alumina coating)	Tioxide Europe Ltd
Titanium Dioxide	RTC-90 (alumina coating)	Tioxide Europe Ltd
Zinc Phosphate	Delaphos 2M	ISC Alloys
Red Iron Oxide	130B	Bayer

Table 4. Pigments selected for use on metal substrates

3.1.4. Substrates

The substrates used are listed in Table 5. Household aluminium foil and glass panels were used for laboratory testing and analysis. The aluminium foil was laid over a glass panel with the less shiny side uppermost to give a flat and uniform substrate. Both glass and aluminium foil were cleaned with acetone prior to use. Plain steel and aluminium panels were used for physical and environmental testing and were abraded and solvent cleaned prior to use.

Type	Supplier	Other Information
Plain steel panels	The Q-Panel Company	0.25 x 76 x 152 mm
Aluminium panels	The Q-Panel Company	0.6 x 76 x 152 mm
Glass panels	Feltham Glassworks	2 x 100 x 150 mm
Household aluminium foil	Woolworths plc	

Table 5. Substrates

3.1.5. Additives

The additives used are listed in Table 6.

Tradename	Supplier	Description	Purpose
Jeffamine D230	Texaco Ltd	polyoxypropyleneamine	Cross-linking agent for epoxy resins
Cymel 303	American Cynamid	hexamethoxymethyl-melamine	Cross-linking agent for Lumiflon resins
Versamid 115	Cray Valley Products	Polyamide Resin	Cross-linking agent for epoxy resins
Amine "A"*	Aldrich Chemical Co.	4,4'-methylenebis-(cyclohexyl)amine	Cross-linking agent for epoxy resins
Anti Terra-U	Byk Chemie GmBH	A solution of a salt of unsaturated polyamine amides and higher molecular weight acidic ester	Pigment Dispersing Aid
Neocryl B700	ICI	Poly iso butyl methacrylate	Thickener
AMEO*	Dynamit Nobel	Aminopropyl triethoxy silane	Adhesion Promoter
IBTEO*	Dynamit Nobel	Isobutyl triethoxy silane	Adhesion Promoter

*abbreviated by PRA - sold under the generic name

Table 6. Additives

3.2. Characterisation of Raw Materials

3.2.1. Substrates

3.2.1.1. Surface Energy

Surface energy measurements of substrates were made via the measurement of contact angles using a Livereel Contact-θ-Meter at 23°C / 65% relative humidity which is described fully in Section 3.5.8.1. Measurements were made using water and methylene iodide on uncleaned, solvent cleaned, abraded and flamed steel surfaces and solvent cleaned glass panels and aluminium foil and are the mean of three readings.

3.2.2. Resins

3.2.2.1. Molecular Weight and Glass Transition Temperature

Molecular weights were determined using gel permeation chromatography (GPC) described in Section 3.5.4 and glass transition temperatures by differential scanning calorimetry (DSC) (Section 3.5.6).

3.2.2.2. Solid Surface Energy

Surface energy measurements of solid resins were determined from contact angles using a Livereel Contact-θ-Meter at 23°C / 65% relative humidity (Section 3.5.8.1). The resins were cast as a film on a glass microscope slide from a suitable organic solvent and conditioned at 23°C / 65% RH for two weeks prior to measurement. Some solvents attacked the resin films preventing measurement of the contact angle so a range of solvents was selected. Water and methylene iodide were used wherever possible, but if the film showed any signs of deterioration methylene iodide was replaced with either glycerol, formamide or bromonaphthalene. The results were the mean of three determinations.

3.2.2.3. Solution Surface Energies

Surface energy measurements of resin solutions in organic solvents at various concentrations were determined using a Krüss K10T digital tensiometer equipped with a Wilhelmy Plate as described in Section 3.5.8.2. The resins were dissolved or diluted as necessary in a suitable organic solvent to provide solids (by mass) of between 40% and 50%.

3.2.2.4. Solubility Parameters

The solubility parameters of the resins as received were determined at solids contents of between 10 and 60% as described in Section 3.5.7.

3.2.3. Solvents

Literature solubility parameter values were used[83].

Surface energy measurements were made using a Krüss K10T digital tensiometer equipped with a Wilhelmy Plate (Section 3.5.8.2).

3.3. Preparation, Application & Characterisation of Unpigmented Systems

Binary combinations of resins in solution were mixed on a 1:1 (by mass on resin solids) basis, curing agents added if appropriate before being cast onto an acetone cleaned metal substrate using a block applicator to give nominal dry film thicknesses of 100μm unless otherwise stated.

The films were dried at room temperature or cured in a convection oven according to the following schedules:

Curing Agent	Curing Schedule
No curing agent	2 weeks at room temperature
Amine "A"	30 minutes at 140°C
Jeffamine D-230	24 hours room temperature followed by 60 minutes at 110°C
Versamid 115	60 minutes at 100°C
Cymel 303	60 minutes at 110°C

Table 7. Curing Schedules

	Parts of Resin : Parts of Curing Agent (by weight)			
	Amine "A"	**Jeffamine D-230**	**Versamid 115**	**Cymel 303**
Epikote 828	5:1	10:3	1:2.2	-
Epikote 1001	6:1	10:1.2	1:1.1	-
Epikote 1004	6:1	10:0.6	1:0.5	-
Epikote 1007	10:1	10:0.3	1:0.3	-
Lumiflon LF200	-	-	-	100:3

Table 8. Curing Schedules

Where both Cymel 303 and Jeffamine D-230 curing agents were used in the same formulation, trials were carried out to determine an optimum curing schedule for both components which was found to be 24 hours at room temperature followed by 60 minutes at 110°C.

After drying / curing the films were characterised using FTIR-HATR, FTIR-PAS and electron microscopy. Scanning electron microscopy (SEM) was used to detect layer formation and SEM in conjunction with energy dispersive spectrometry (SEM-EDS) used when one of the resins used was Lumiflon as the chlorine in this resin can be detected by this technique.

Optical microscopy was used to follow changes in selected systems as they dried. A small portion of the sample was spread across a microscope slide and viewed at approximately 50x magnification. The changes were permanently recorded using a video cassette recorder.

3.4. Preparation, Application & Characterisation of Pigmented Systems

Pigments were dispersed into resin solutions using a ball-mill. Glass beads were used as the grinding medium and the mixture was milled for 24 hours. The pigment dispersion was then mixed with a second resin solution at a 1:1 ratio (by mass on resin solids). Curing agents were added and the whole system mixed using a ball mill for a further one hour. The system was applied to a metallic substrate to give a nominal dry film thickness of 100 μm and dried / cured as for unpigmented systems.

Films were characterised using FTIR-HATR or FTIR-PAS.

Electron microscopy was used to detect layer formation and SEM-EDS used to detect the location of the pigment in the cross-section.

Optical microscopy was used to follow changes in selected liquid pigmented systems with drying. A small portion of the sample was spread across a microscope slide and viewed at approximately 50x magnification. The changes were permanently recorded using a video cassette recorder. Cross sections of dried samples were also viewed using an optical microscope. Cross-sections of films were cut with a scalpel blade and mounted in plasticine on a microscope slide for viewing.

3.5. Analytical and Test Methods

3.5.1. Fourier Transform Infrared Spectroscopy

Fourier transform infrared (FTIR) measurements were made using a Bio-Rad FTS60 FTIR spectrometer. Unless otherwise stated spectra were recorded from

4000 cm^{-1} to 400 cm^{-1} using a moving mirror velocity of 5cms^{-1}, a zero fill factor of 1 or 2, 512 scans and a resolution of 4cm^{-1}.

3.5.1.1. Horizontal Attenuated Total Reflectance Spectroscopy

Films were initially characterised using horizontal attenuated total reflectance infrared spectroscopy (FTIR-HATR) (Figure 5) using zinc selenide crystals with 45° or 60° angles. In some cases this technique enabled measurement of spectra at the bottom and top surfaces of the film. The bottom surfaces were measured by casting a film directly on the HATR crystal. The films were allowed to dry before the spectrum was measured. The top surfaces were measured by casting the film onto steel strips or aluminium foil and after drying clamping the top surface against the HATR crystal. To obtain spectra good contact is required between the film and the HATR crystal, so very soft films which were disrupted during contact and very brittle films which cracked during contact were difficult to measure by this technique.

Figure 5. FTIR-HATR Unit

3.5.1.2. Photoacoustic Spectroscopy

Films were subsequently characterised using photoacoustic infrared spectroscopy (FTIR-PAS)[79,80,81]. This is a non-destructive technique which allows measurement of the top surface of a dry film. Sample preparation is minimal and involves cutting a small portion of the film approximately 10mm in diameter to fit into the photoacoustic cell. The sample is surrounded by a coupling gas, usually nitrogen or helium in a small cell containing a sensitive microphone. The sample absorbs modulated electromagnetic radiation which, after absorption is emitted from the sample surface in the form of heat. The heat causes fluctuations in temperature at the sample surface which causes a small boundary layer of the gas to expand and contract. The boundary gas layer acts as an acoustic piston on the bulk of the gas which carries the pressure changes to the microphone. The microphone detects small pressure changes.

An electrical signal is generated which, after being Fourier transformed, is recorded as an infra red spectrum.

3.5.2. Electron Microscopy - Energy Dispersive Spectrometry

Scanning Electron Microscopy - Energy Dispersive Spectrometry (SEM-EDS) studies were made using an ISI 100A scanning electron microscope equipped with an Energy Dispersive Analysis of X-Rays (EDAX) EDS detector. Unless otherwise stated an accelerating voltage of 20kV and magnifications of up to x1000 were used.

Top surfaces of dry films were studied by attaching a 1cm x 1cm (approx.) portion of the dry film on aluminium foil to a standard aluminium microscope stub using conductive adhesive. The samples were then gold coated using an Emscope SC 500 sputter coater.

Cross sections of films were cut using a new scalpel blade and mounted edge on in a gripping stub designed to hold biological specimens[82]. The samples were gold coated as before.

3.5.3. Optical Microscopy

Optical microscopy was carried out using a Leitz Laborlux 12ME stereo microscope. The system was also fitted with a Panasonic F15 CCD camera and Aiwa F125 VHS video cassette recorder to allow recording of continuously changing samples e.g. drying films. A Polaroid TX-1000 video printer was also available to enable recording of static samples viewed using the microscope.

3.5.4. Gel Permeation Chromatography

Gel permeation chromatography (GPC) was carried out by Croda Resins Ltd and ICI Resins. Croda Resins used a Waters chromatograph containing either ultrastyragel or mixed bed columns. Samples were introduced at either 1% or 10% in THF using a solvent flow rate of 1 ml/min. The detector used was a Waters R401 differential refractometer. Polystyrene standards were used for calibration. ICI Resins introduced the samples in solution in THF using a 1ml/min solvent flowrate.

3.5.5. Gas Chromatography - Mass Spectrometry

Gas chromatography - mass spectrometry (GC-MS) was carried out using a Hewlett Packard 5890A gas chromatograph in conjunction with a Hewlett Packard 5970B mass spectrometer. The gas chromatograph was fitted with an HP5 capillary column (25m long, 0.2mm internal diameter, coated with 0.11μm 5% cross linked phenyl methyl silicone).

The injector port was held at 250°C. The temperature program consisted of 35°C for 5 minutes then 10°C / min to 240°C until completion of run.

Resin solutions were mixed with methanol in order to precipitate the resin. The solvent mixture was then decanted off and introduced into the chromatograph via a micro syringe. Typically 0.5μl samples were used.

3.5.6. Differential Scanning Calorimetry

The glass transition temperature was determined on the solid resins as received and the solution resins after casting as films and drying for two weeks at 23°C / 65% relative humidity. A Mettler TA3000 liquid nitrogen cooled DSC equipped with a TC Processor unit was used for the determinations. Measurements were carried out from -20°C increasing to 150°C at 2°C / minute using approximately 25 mg of solid resin .

3.5.7. Solubility Parameters

The solubility parameters of resins were determined experimentally using the three-dimensional approach of Hansen[35,36]. The resins were placed in up to 56 solvents (Appendix 1) of known solubility parameter[83] at concentrations of between 10% and 60% solids and after four weeks assessed as either soluble or non-soluble. In some cases a borderline classification was also necessary. A computer program written at PRA was used to calculate a sphere of minimum radius which encompassed only those solvents found to dissolve the resin.

3.5.8. Surface Energy

3.5.8.1. Solid Surfaces

The surface energy of solid surfaces was calculated from the contact angles of reference liquids on the surface using the harmonic mean method of Wu[73]. Samples were conditioned at 23°C / 65% relative humidity for two weeks prior to testing. Contact angles were measured using a Livereel Contact-θ-Meter at 23°C / 65% relative humidity. Measurements were made at intervals of typically 10, 30 and 60 seconds and the contact angle at zero time found by extrapolation. The results are the mean of three determinations.

3.5.8.2. Solutions

Solution surface energy measurements were made using a Wilhelmy plate at 25°C. A Krüss K10T digital tensiometer was used to make the measurements. The temperature was controlled using a water jacket. The glass sample containers were cleaned with organic solvent to remove traces of the resin prior to cleaning with chromic acid and distilled water. The Wilhelmy plate was cleaned in a Bunsen flame prior to each measurement.

3.5.9. Interfacial Energy

The interfacial energy existing between pairs of solutions was measured using a Wilhelmy plate and Krüss K10T tensiometer.

3.5.10. Phase Diagrams

Phase diagrams were determined experimentally by determining the mixing or demixing points between pairs of resins in a common solvent or solvent blend using a light scattering technique. Solvent was added to two phase resin mixtures until a sudden drop in scattering was observed. Three resin ratios (1:4, 1:1 and 4:1) in various solvents were compared. Phase diagrams were constructed which usually contained areas where the mixture was single phase, areas where the mixture was heterogeneous and areas that were not able to be determined due to the high viscosity of many of the resins at high concentrations.

3.5.11. Percentage Non - Volatile Matter

A portion of the liquid sample was heated in an aluminium dish at 105°C for three hours. From the weight loss on heating the percentage solids and percentage volatile matter was determined according to BS 3900 : Part B2[84].

3.5.12. Gloss

The test was performed on a paint film on a steel substrate. Gloss measurements were carried out according to BS 3900 : Part D5[85]. The measurements were made at an angle of 60°, using a Rhopoint gloss meter calibrated using Rhopoint standards and are the average of six readings.

3.5.13.Pencil Hardness

The test was performed on a paint film on a steel substrate. Pencil hardness was carried out according to ASTM D-3363[86]. A pencil from a series representing a range of hardness levels was held firmly against a paint film at a 45° angle and pushed away from the operator in a smooth stroke. The process was started with the hardest pencil and continued down the scale of hardness until the pencil which did not cut into or gouge the film was reached. The hardness of this pencil (e.g. 4H) was quoted as the pencil hardness of the film. The range of pencils used was from 6B (softest) to 6H (hardest).

3.5.14.Pendulum Damping

The test was performed on a paint film on a steel substrate. Measurements were carried out using the König pendulum, which would give a 6° to 3° damping time of 250 ± 10 seconds on a polished glass panel. The time recorded for the test panels was the time taken, in seconds, for the amplitude to fall from 6° to 3° according to BS 3900 Part E5[87].

3.5.15.Cross Cut Adhesion

The test was performed on a paint film on a steel substrate. Eight parallel cuts 2mm apart were made first in one direction and then a second set perpendicular to the first set. Adhesive tape was attached to the cut portion of the film, smoothed to ensure good contact then steadily pulled off. The cut area of the panel was viewed and classified from 0 to 5 (where 0 is best) according to the pictorial representations in BS 3900 : Part E6[88].

3.5.16.Bend Test

The test was performed on a paint film on a soft aluminium substrate. The test panel and coating were bent using a conical mandrel test apparatus. The coating was then examined for the extent of cracking from the small end of the mandrel according to BS 3900 : Part E11[89].

3.5.17.Resistance to Liquids

The test was performed on a paint film on a steel substrate. The test was carried out according to BS 3900 : Part G5[90] using method 3. A drop of a test solvent was spotted onto the panel and left for 10 minutes. After this time the solvent was rinsed off with methanol and the degree of deterioration noted.

3.5.18.Artificial Weathering (QUV)

The test was performed on a paint film on a steel substrate. Panels were subjected to continuous 4 hourly UV / condensation cycles using a Q-Panel Company QUV Accelerated Weathering Tester and UVA lamps (315-400 nm).

3.5.19.Artificial Weathering (Marr)

The test was performed on a paint film on a steel substrate. Panels were weathered in a Marr Enclosed Carbon Arc Weatherometer according to BS 3900 : Part F3[91]. The panels were subjected to water atomisation and a drying fan in cycles whilst exposed to UV light produced by a carbon arc.

3.6. Appendix 1

3.6.1. Solvents Used for Determining Hansen Solubility Parameters

Solvent	δd	δp	δh
Acetone	15.5	10.4	7.0
Acetophenone	19.6	8.6	3.7
Benzaldehyde	19.4	7.4	5.3
1,3-Butanediol	16.6	10.0	21.5
1-Butanol	16.0	5.7	15.8
γ-Butryrolactone	19.0	16.6	7.4
Butyl Acetate	15.8	3.7	6.3
Carbon Tetrachloride	17.8	0.0	0.0
Chlorobenzene	19.0	4.3	2.0
Chloroform	17.8	3.1	5.7
Cyclohexanol	17.4	4.1	13.5
Cyclohexanone	17.8	6.3	5.1
Diacetone Alcohol	15.8	8.2	10.8
o-Dichlorobenzene	19.2	6.3	3.3
Diethyl Ether	14.5	2.9	5.1
Diethylene Glycol	16.2	14.7	20.5
Dimethyl Sulphoxide	18.4	16.4	10.2
Dimethyl Formamide	17.4	13.7	11.3
1,4-Dioxane	19.0	1.8	7.4
Dipropylene Glycol Methyl Ether	15.5	5.7	11.2
Dipropylene Glycol Dimethyl Ether (DMM)	14.9	2.1	3.8
Dipropylene Glycol n-Butyl Ether (DPnB)	14.8	2.5	8.7
Dipropylene Glycol	15.9	20.2	18.4
Ethanol	15.8	8.8	19.4
Ethanolamine	17.0	15.5	21.2
Ethyl Acetate	15.8	5.3	7.2
Ethylene Glycol Monomethyl Ether	16.2	9.2	16.4
Ethylene Glycol Monobutyl Ether	16.0	5.1	12.3
Ethylene Glycol Monoethyl Ether Acetate	15.9	4.7	10.6
Ethylene Glycol Monoethyl Ether	16.2	9.2	14.3
Ethylene Dichloride	19.0	7.4	4.1
Ethylene Glycol	17.0	11.0	26.0

Formamide	17.2	26.2	19.0
Glycerol	17.4	12.1	29.3
Hexane	14.9	0.0	0.0
Isophorone	16.6	8.2	7.4
Methanol	15.1	12.3	22.3
Methyl Ethyl Ketone	16.0	9.0	5.1
Methyl iso-Butyl Ketone	15.3	6.1	4.1
Methylene Dichloride	17.8	3.9	5.5
Nitrobenzene	20.0	8.6	4.1
Nitromethane	15.8	18.8	5.1
2-Nitropropane	16.2	12.1	4.1
Propylene Glycol Monomethyl Ether	15.6	6.3	11.6
Propylene Glycol Diacetate	15.8	3.5	8.8
Propylene Glycol Monobutyl Ether	14.9	2.4	10.7
Propylene Glycol Dimethyl Ether (MM)	15.2	4.6	4.2
Propylene Carbonate	20.0	18.0	4.1
Propylene Glycol Methyl Ether	15.6	7.2	13.6
Propylene Glycol	16.8	9.4	23.3
Tetrahydrofuran	16.8	5.7	8.0
Toluene	18.0	1.4	2.0
Trichloroethylene	18.0	3.1	5.3
Tripropylene Glycol n-Butyl Ether (TPnB)	14.8	1.7	7.9
Tripropylene Glycol Methyl Ether (TPM)	15.1	3.5	11.5
o-Xylene	17.8	1.0	3.1

4. UNPIGMENTED SYSTEMS

4.1. Characterisation of Materials

All materials were selected after discussion with the industrial sponsors of this project and are typical of those which perform well in conventional commercial anti-corrosive primers and durable top coats for steel substrates.

4.1.1. Substrates

The nature of the substrate and its surface energy have important implications for stratification. The surface energy of the substrate may affect the direction of layer formation. It may also prevent layer formation if neither of the separating phases can spontaneously wet it. This work is only concerned with the protection of steel substrates. Steel plate is not a suitable substrate for many analytical techniques so glass plate and aluminium foil were also considered.

Type	Supplier	Other Information
Plain steel panels	The Q-Panel Company	0.25 x 76 x 152 mm
Aluminium panels	The Q-Panel Company	0.6 x 76 x 152 mm
Glass panels	Feltham Glassworks	2 x 100 x 150 mm
Household aluminium foil	Woolworths plc	

Table 9. Substrates

4.1.1.1. Substrate Surface Energies

The surface energies of the majority of the commercial resins used for this study were experimentally found to be between 30 and 40 mN m^{-1} (Table 13). Clean metal surfaces are reported to have a high surface energy but an untreated steel panel was found to have a surface energy of only

41.3 mN m^{-1} (Harmonic Mean). A high substrate surface energy should favour stratification so attempts were made to increase the surface energy of the steel panel using surface preparation methods. Degreasing with acetone marginally improved the measured surface energy (Table 10), but degreasing with xylene had virtually no effect at all, presumably due to the deposition of organic residues. Abrading the surface with 200 grade wet and dry paper caused a significant increase in the surface energy which is probably due to removal of heavily contaminated surface oxides. Acetone cleaned glass plates and aluminium foil were found to have surface energies similar to that of abraded steel and were thus used as substrates for laboratory analysis and testing.

It was found that for steel substrates a very high surface energy that would easily be wetted by a polymer solution could only be achieved by cleaning the surface in a flame. However, as well as being impractical commercially, absorption of material from the atmosphere reduced the energy to below that of water within two hours.

			Equation of State		Harmonic Mean		
Substrate	θ_{H_2O}	θ_{MI}	γ_s mN m^{-1}	γ_{sl} mN m^{-1}	γ^d mN m^{-1}	γ^p mN m^{-1}	γ^T mN m^{-1}
Uncleaned Steel	90	37.4	30.7	30.7	36.5	4.8	41.3
Acetone Cleaned	85	42.4	33.3	26.9	28.7	15.6	44.3
Abraded Steel	33	25	62.7	1.7	32	34	68
Flamed Steel :-							
(0 hours after flaming)	0						
(2 hours after flaming)	7		72.3	0			
(3 hours after flaming)	10		71.7	0.02			
(4 hours after flaming)	15		70.4	0.1			
(24 hours after flaming)	37		60.8	2.5			
(96 hours after flaming)	62		46.1	12			
Aluminium Foil	47	33	55.0	5.3	30.3	27.5	57.8
Glass Slide	39.4		59.3	3.1			

θ_{MI}, θ_{H_2O} Contact angle with methylene iodide / water

Table 10. Surface Energies of Various Substrates.

The method of surface preparation that was used for steel panels involved abrasion followed by solvent cleaning with xylene. This is consistent with commercial methods of surface preparation.

4.1.2. Resins

A range of resins was selected for use that was representative of the types of commercial resins that perform well in conventional anti-corrosive coatings for metallic substrates. A series of epoxy resins of various molecular weights were selected as typical primer materials. These resins provide good adhesion to metallic substrates and excellent chemical resistance. The epoxy resins also have high surface energies compared to many other resins. A variety of materials were selected as typical topcoat materials which would exhibit good weather resistance and durability. These included alkyd and acrylic resins with a range of surface energies which in most cases were lower than that of the epoxy resins.

Incompatibility between resin pairs increases with increasing molecular weight. Since incompatibility is thought to be a route to stratification an understanding of the compatibility of resin pairs is vital. In order to obtain accurate information on the actual resin batches used for this study molecular weights were determined experimentally (Table 11).

4.1.2.1. Molecular Weight and Glass Transition Temperatures

The molecular weights and glass transition temperatures are shown in Table 11 (the resin types are listed in the experimental section)

Tradename	Resin Type	M_n	M_w	M_w/M_n	T_g
Epikote 828	Bisphenol-A Epoxy	293	379	1.293	-20
Epikote 1001	Bisphenol-A Epoxy	934	2304	2.467	30
Epikote 1004	Bisphenol-A Epoxy	1813	4783	2.638	53
Epikote 1007	Bisphenol-A Epoxy	3119	9114	2.922	72
Neocryl B-700	Thermoplastic Acrylic (PiBMA)	85772	156741	1.827	63
Neocryl B-728	Thermoplastic Acrylic (PMMA)	39073	71563	1.831	117
Neocryl B-804	Thermoplastic Acrylic (PBMA)	123399	222909	1.806	30
Neocryl B-811	Thermoplastic Acrylic (PMMA)	23706	39181	1.653	116
Neocryl B-813	Thermoplastic Acrylic (PEMA)	27133	44841	1.653	60
Crodaplast AC500	Thermosetting Acrylic	6334	19475	3.075	31
Crodaplast AC550	Thermosetting Acrylic	2290	8446	3.689	7
Lumiflon LF200	Fluorinated Polyether	15009	42952	2.862	38
Lumiflon LF916	Fluorinated Polyether	10239	25513	2.492	27
Plastokyd SC7	Siliconised Polyester	3038	22688	7.468	-9
Plastokyd SC140	Siliconised Alkyd	3183	90366	28.391	30
Plastokyd SC400	Siliconised Epoxy Ester	3357	22165	6.602	21
Plastokyd AC-4X	Acrylic Modified Alkyd	2781	54213	19.496	19
Alkyd VAS 9223	Long Oil Alkyd	4985	14278	2.864	-15
Hythane 9	Urethane Alkyd	2033	4144	2.039	-10
Synolac 6016	Short Oil Alkyd	2542	17017	6.690	-11
Synolac 9090	Short Oil Alkyd	2244	28900	12.880	
Plastoprene 1S	Cyclised Rubber	6946	25400	3.657	102
Hypalon 20	Chlorosulphonated Polyethylene	39991	77052	1.927	-27

Table 11. Resin Types and Physical Properties

4.1.2.2. Solid Surface Energies

Previous work carried out on powder coatings showed the importance of the surface energies of the resin components in the prediction of stratification. In order to determine the influence of resin surface energy on stratification the surface energies of the solid resins were determined experimentally. These data are not generally available for commercial resins.

The solid surface energies of the resins were determined from contact angle data using the Equation of State method of Neumann and the Harmonic Mean method of Wu. Contact angles were determined on thin films cast from suitable solvents after conditioning at 25°C / 65% Relative Humidity for two weeks. The results are presented in Table 12.

Although both the Equation of State and Harmonic mean methods show similar trends in total surface energies, the absolute values are different. As the Harmonic Mean method is more widely used in the surface coatings field and is more useful for calculating interfacial energies it was decided to concentrate on this method.

	Harmonic Mean			Equation of State
Resin	γ^d	γ^p	γ^T	γ^T
Epikote 828 (Amine Cured)	33.7	10.8	44.5	38.0
Epikote 1001	36.1	9.3	45.4	44.7
Epikote 1004	34.1	11.5	45.6	45.0
Epikote 1007	34.4	9.4	43.8	42.9
Neocryl B700	28.2	2.6	30.8	32.2
Neocryl B728	30.2	12.0	42.2	39.8
Neocryl B804	24.7	9.7	34.4	33.3
Neocryl B811	30.5	13.9	44.4	44.4
Neocryl B813	27.6	10.2	37.8	36.1
Crodaplast AC500	29.4	12.0	41.4	38.9
Crodaplast AC550	32.1	8.6	40.7	37.3
Lumiflon LF200	26.3	10.1	36.4	36.4
Lumiflon LF916	27.2	10.5	37.7	35.8
Plastokyd SC7	27.9	10.1	38.0	36.4
Plastokyd SC140	27.2	9.8	37.0	36.6
Plastokyd SC400	26.3	11.2	37.4	35.2
Plastokyd AC4X	27.8	10.8	38.6	36.6
Alkyd VAS 9223	29.1	10.2	39.3	37.8
Hythane 9	26.3	13.4	39.7	39.7
Synolac 6016	30.5	14.0	44.5	40.0
Synolac 9090	33.6	11.7	44.3	35.4
Plastoprene 1S	31.9	13.2	45.1	41.0
Alloprene R10	40.9	6.1	47.0	47.0
Hypalon 20	32.1	8.6	40.7	40.0

Table 12. Surface Energies of Resins

An alternative method of calculating the surface energy of solid resins from contact angles is to calculate the donor / acceptor characteristics instead of the disperse and polar contributions to the interaction. This method was used to calculate solid surface energies of resins where it was possible to obtain contact angles with three or more reference liquids (Table 13).

In general the total values obtained by this method are similar to the values obtained from the Harmonic Mean and the Equation of State methods (Table 12). All resins studied showed much higher donor properties than acceptor. None of the resins showed significant acid characteristics.

This method, however, does not appear to offer any advantage over the Harmonic Mean method of calculation of surface energy and requires additional experimental data. Therefore, the Harmonic Mean method has been used as the method of calculation from this point.

Resin	θ_W	θ_{Gly}	θ_F	θ_{MI}	θ_B		γ_s^{LW}	γ^+	γ^-	γ_s^{tot}
Epikote 1001	79.4		61.0	29.5	15.1		44.0	.171	7.91	46.3
Epikote 1004	76.0		59.0	32.0	17.7		43.2	.09	9.99	45.1
Epikote 1007	80.0		57.9	33.9	13.5		43.2	.02	6.41	43.9
Neocryl B700		88.0	75.0	60.0			28.6	0.5	0.79	29.9
Neocryl B728	76.4		58.9	41.3	19.9		40.7	.007	9.5	41.2
Neocryl B804		82.5	72.9	56.0	42.0		32.7	0.46	4.03	35.4
Neocryl B811	72.4		59.6	39.2	19.1		41.3	.07	11.86	43.1
Neocryl B813	73.0	67.0	61.0	47.0	34.0		35.9	.002	13.98	36.2
Lumiflon LF200	90.0		67.0	56.0			30.9	.27	2.40	32.5
Lumiflon LF916	90.0		69.0	50.0			34.3	.37	1.40	35.7
Plastokyd SC7	83.0		74.0	48.5	25.4		35.1	0.68	11.79	40.8
Plastokyd SC140	80.0		74.0	50.5	23.0		34.0	.72	15.35	40.6
Plastokyd SC400	80.5		74.3	51.0	29.4		33.7	.69	14.92	40.1
Plastokyd AC-4X	80.4		64.4	48.0	29.3		35.4	.21	5.99	37.6
Hythane 9	83.0	79.0	66.0	51.0	34.4		33.7	.008	7.90	34.2
Synolac 6016X	77.0	71.0	60.0	41.0			39.1	.004	9.44	39.5
Synolac 9090X	83.0	72.0	65.0	36.0	24.0		41.6	.22	6.68	44.0
Alloprene R10	85.0		64.7	22.8			46.9	.58	5.13	50.3
Hypalon 20	83.0		70.1	40.7	46.4		39.3	.28	5.38	41.8
Crodaplast AC500	81.0		73.0	43.4	34.6		37.8	1.05	13.5	45.3
Crodaplast AC550	85.0		74.0	41.3	40.0		37.0	.83	9.8	42.7
Alkyd VAS 9223	85.0		74.0	45.6	20.4		36.7	0.79	9.8	42.3

θ_W	Contact Angle with Water
θ_{Gly}	Contact Angel with Glycerol
θ_F	Contact Angle with Formamide
θ_{MI}	Contact Angle with Methylene Iodide
θ_B	Contact Angle with Bromonaphthalene
γ_s^{LW}	Lifshitz-Van der Waals Contribution to Solid Surface Energy
γ^+	Electron Acceptor Contribution
γ^-	Electron Donor Contribution
γ_s^{tot}	Total Solid Surface

Table 13. Surface Energies of Resins

4.1.2.3. Solution Surface Energies

The surface energy of resin / solvent solution phases will change continuously as the solvent evaporates. In order to predict stratification from surface energy data it was necessary to predict the surface energy of polymer solutions at various concentrations. The surface energies of a series of resin / solvent solutions at various concentrations were determined experimentally.

It was found that when a resin is dissolved in a solvent or solvent blend the surface energy of the solution is dominated by the solvent except at high resin concentrations. This is illustrated in Figure 6 which shows a plot of surface energy against concentration for Epikote 828 (a low molecular weight epoxy) in methyl iso butyl ketone (MiBK). At high resin concentrations, a small addition of solvent produces a large decrease in the solution surface energy. At 50% resin solids the surface energy is dominated by the solvent and further dilution has a small effect on the solution surface energy.

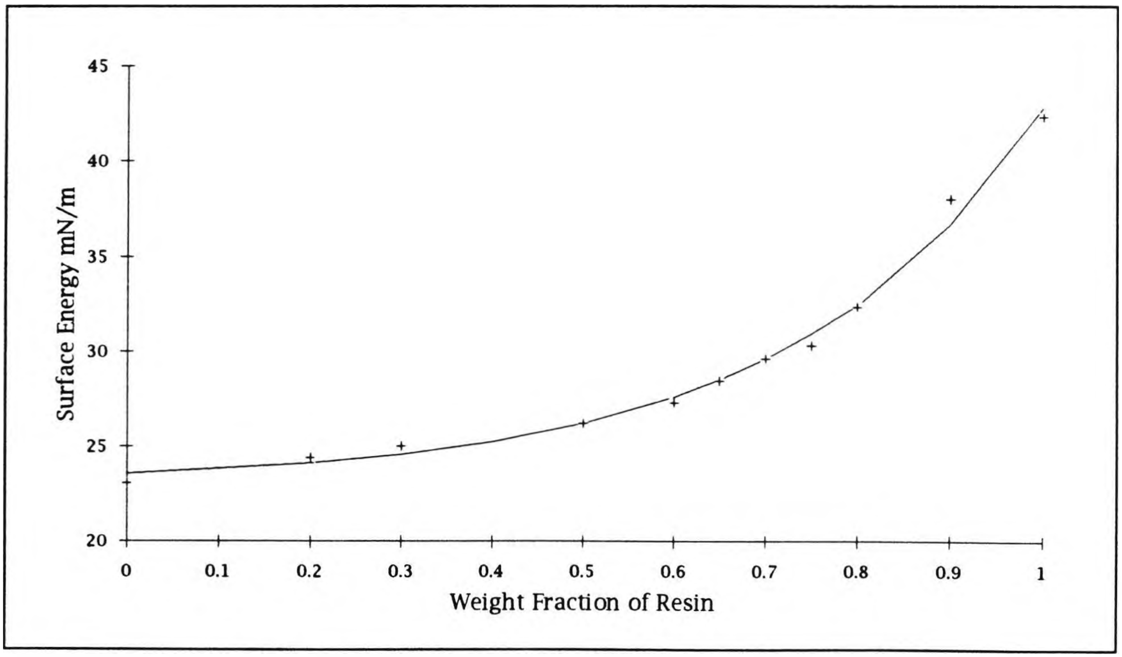

Figure 6. Experimental Surface Energy for Epikote 828 / MiBK Solutions.

Because Epikote 828 is a low molecular weight liquid resin it was possible to measure its surface energy at all resin concentrations. However, this is not the case for all the other resins studied where viscosity prevents measurement above about 40% resin solids. Attempts were made to use surface energy data obtained at measurable concentrations to predict that at higher resin concentrations.

An empirical formula which describes the surface energy / concentration relationship was derived based on curves for 17 systems. The best fit to the experimental data was given by:

$$T_m = T_s + A\exp^{Bf} \tag{43}$$

where:

T_m = Surface energy of the solution
T_s = Surface energy of the solvent
f = Weight fraction of the solvent
A, B = Constants

A, can be calculated from the best fit of the experimental data or using the solid resin surface energy (T_r which is determined from contact angle data) using $T_r - T_s\ (f = 0)$ but B must be derived from the experimental data obtained from measurements made at low resin concentrations. The values for A and B from the best fit of the experimental data for the systems studied are listed in Table 14.

This formula uses surface energy data collected at low resin concentrations to estimate the surface energy at higher concentrations where measurement is not possible due to high viscosity. Its use enables the surface energy of the separating phases to be followed as solvent evaporation takes place and may be useful in the prediction of stratification. Figure 7 shows the results using this method for Epikote 1001. It is seen that the results at low concentrations are in close agreement with the measured surface energy data.

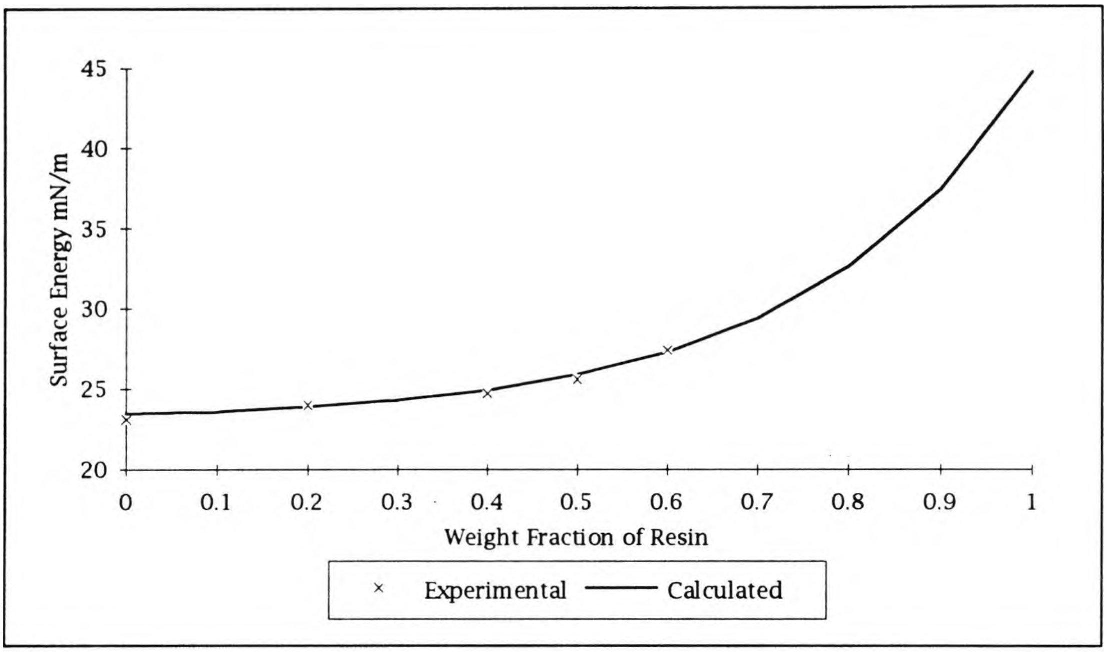

Figure 7. Surface Energy of Epikote 1001 in MiBK

These data alone can only be used to describe the surface energy of the resin solutions. In order to use the data to predict stratification, the disperse and polar components of the surface energy must be known. These cannot be measured directly but can be calculated if we assume they vary in a similar way to the total surface energy. It is possible to calculate values for a polar and disperse contribution to the A coefficient of the solution, A^p and A^d respectively, using:

$$\begin{aligned} A^p &= T_r^p - T_s^p \\ A^d &= T_r^d - T_s^d \end{aligned} \qquad \textbf{(44)}$$

Using the experimentally determined value for B, the variation of the polar and disperse components of the surface energy of the solution can be calculated at any concentration.

Resin	**Solvent**	**A**	**B**
Epikote 828	Xylene	14.6	-3.1
	Methyl iso-Butyl Ketone	19.7	-3.1
	n-Butyl Acetate	17.8	-3.7
	Methoxy Propanol	15.5	-3.4
Epikote 1001	Methyl iso-Butyl Ketone	21.6	-3.0
	n-Butyl Acetate	20.8	-4.2
Epikote 1004	Methyl Ethyl Ketone	21.1	-4.3
	n-Butyl Acetate	20.4	-3.5
Epikote 1007	Methyl Ethyl Ketone	21.6	-4.5
	n-Butyl Acetate	20.9	-3.7
Lumiflon LF916	Xylene	9.3	-4.3
Lumiflon LF200	Methyl iso-Butyl Ketone	13.3	-4.7
Neocryl B700	n-Butyl Acetate	7.7	-3.4
Neocryl B728	n-Butyl Acetate	15.2	-2.2
Neocryl B804	n-Butyl Acetate	8.2	-2.3
Neocryl B811	n-Butyl Acetate	16.1	-3.6
Neocryl B813	n-Butyl Acetate	11.5	-3.0

Table 14. Constants A and B

4.1.2.4. Solubility Parameters

The experimentally determined Hansen solubility parameters for resins at similar concentrations to those used practically in the surface coatings industry are shown in Table 15. Figures in italics indicate that this resin was supplied in solution and a correction has been made for the addition of this solvent to the test solvents.

Table 15 shows that the radii of the solubility spheres of similar resins at the same concentration generally decrease with increasing molecular weight as the resin becomes increasingly difficult to dissolve. As the resin concentration increases the radius of the solubility sphere generally decreases. δ_h also decreases significantly. This may be due to the number of sites involved in intramolecular H-bonding increasing with concentration, thus leaving less sites available for hydrogen bonding with the solvent. These effects are seen most clearly among the Epikote epoxy resins.

Resin	conc.	δd	δp	δh	Radius	Dtot
Epikote 828	60%	16.6	14.0	2.8	14.9	1.00
	30%	16.3	16.4	1.9	16.7	0.89
Epikote 1001	60%	15.8	16.3	3.3	16.4	0.94
	40%	16.3	13.1	6.3	10.9	0.89
	20%	18.8	13.6	8.9	12.0	0.96
	10%	18.1	11.4	9.0	9.1	0.89
Epikote 1004	60%	17.7	10.1	7.6	9.8	0.81
	30%	18.5	9.3	8.0	9.6	0.90
Epikote 1007	30%	18.6	10.6	8.1	8.8	0.92
Epikote 1009	60%	17.0	9.6	8.5	7.6	0.73
	30%	19.8	10.6	10.3	9.7	0.90
	10%	19.0	9.1	10.7	8.0	0.85
Neocryl B-700	10%	17.0	4.6	7.6	9.5	1.00
	30%	17.1	5.9	0.7	7.3	0.92
Neocryl B-728	10%	17.8	10.4	2.9	9.6	0.97
	30%	17.2	7.2	3.5	4.8	0.91
Neocryl B-804	10%	20.6	3.5	7.2	12.8	1.00
	30%	18.1	5.7	0.0	8.5	0.96
Neocryl B-811	10%	17.6	10.1	5.8	9.4	0.94
	30%	17.5	5.5	3.8	4.5	0.94
Neocryl B-813	10%	16.5	8.7	5.0	10.4	0.97
	30%	16.9	7.8	0.5	7.3	0.92
Crodaplast AC500	10%	17.6/*17.8*	6.9/*6.4*	4.5/*4.7*	11.1/*10.7*	1.0/*1.0*
	30%	20.6/*21.2*	3.4/*1.4*	10.5/*10.7*	14.0/*12.3*	0.98/*1.0*
Crodaplast AC550	10%	16.0/*16.3*	11.4/*10.6*	7.7/7.4	14.0/*12.9*	0.97/*0.97*
	30%	16.0/*16.3*	11.4/*10.6*	7.7/*7.4*	14.0/*12.9*	0.97/*0.97*
Lumiflon LF200	10%	19.5/*18.5*	4.6/*5.4*	8.0/*6.9*	11.4/*9.9*	1.0/*1.0*
	30%	18.8/*20.1*	7.3/*4.4*	4.5/*3.2*	9.7/*8.5*	0.94/*0.96*
Lumiflon LF916	10%	18.3/*17.5*	5.3/*6.8*	11.5/*10.5*	14.0/*12.5*	1.0/1.0
	30%	16.6/*18.1*	5.8/*3.9*	10.1/*8.3*	8.8/*8.8*	0.97/0.97

Table 15. Calculated Hansen Solubility Parameters for Resins

Resin	conc.	δd	δp	δh	Radius	Dtot
Plastokyd SC7	30%	24.2/*20.1*	8.1/*5.7*	8.9/*5.3*	20.0/*20.0*	0.92/*0.95*
Plastokyd SC140	30%	22.3/25.2	12.3/*9.2*	5.2/*3.7*	20.0/*20.0*	0.85/*0.90*
Plastokyd SC400	10%	17.6	6.9	4.5	11.14	1.00
	30%	23.7	0.47	10.3	20.0	0.98
Plastokyd AC4X	30%	23.9	7.8	8.8	19.9	0.984
Alkyd VAS 9223	10%	16.0	6.3	6.5	10.0	1.00
	30%	10.6	11.4	4.4	19.9	1.00
	60%	10.3	10.7	4.9	18.7	1.00
Synolac 6016	10%	19.9/*20.4*	5.8/*4.9*	7.5/*7.1*	11.3/*11.1*	1.0/*1.0*
	30%	16.0/*16.9*	11.3/*9.1*	7.7/*6.8*	13.9/*10.8*	0.99/*0.99*
Synolac 9090	10%	20.1/*21.0*	9.5/*8.8*	9.7/*9.2*	14.7/*13.8*	0.96/*0.96*
	30%	19.7/18.0	13.1/*9.9*	5.1/*5.0*	17.0/*10.7*	1.0/*1.0*

Table 15 (continued). Calculated Hansen Solubility Parameters for Resins

Once the solubility sphere for a resin has been calculated it is possible to determine the separation of the solubility sphere of a resin and a solvent relative to the calculated radius (S_{rel}). This is a measure of the 'dissolving power' of the solvent for the resin and is derived from the relationship in Equation 45. The results for Epikote 1009 along with the results of the experimental solubility tests are shown in Table 16. All those solvents with a value of S_{rel} less than unity should be good solvents for the resin, while those with a value greater than unity are outside the solubility sphere of the resin and thus regarded as non-solvents.

$$S_{rel} = \frac{\sqrt{4(\delta_d^s - \delta_d^p)^2 + (\delta_p^s - \delta_p^p)^2 + (\delta_h^s - \delta_h^p)^2}}{R} \qquad \textbf{(45)}$$

where:

S_{rel} = The "dissolving power" of the solvent for the resin

R = The calculated radius of the resin's solubility sphere

$\delta_d^s, \delta_p^s, \delta_h^s$ = The Hansen 3-D Solubility Parameter values for the solvent

$\delta_d^p, \delta_p^p, \delta_h^p$ = The Hansen 3-D Solubility Parameter values for the resin

These data enables the prediction of good solvents for a particular resin. Table 16 shows that the experimental results are generally in good agreement with those predicted from the solubility sphere of Epikote 1009. For 90% of the 48 solvents used for the determination the experimental and predicted results are in agreement.

SOLVENT	Solubility	S_{rel}
Acetone	Insoluble*	0.959
Acetophenone	Soluble	0.712
Benzaldehyde	Soluble	0.616
1,3-Butanediol	Insoluble	1.330
1-Butanol	Insoluble	1.090
γ-Butryrolactone	Soluble	0.714
Butyl Acetate	Insoluble	1.170
Carbon Tetrachloride	Insoluble	1.540
Chlorobenzene	Insoluble	1.090
Chloroform	Borderline	0.996
Cyclohexanol	Insoluble*	0.896
Cyclohexanone	Soluble	0.811
Diacetone Alcohol	Soluble	0.870
o-Dichlorobenzene	Insoluble*	0.855
Diethyl Ether	Insoluble	1.460
Diethylene Glycol	Insoluble	1.360
Dimethyl Sulphoxide	Soluble	0.673
Dimethyl Formamide	Soluble	0.609
1,4-Dioxane	Soluble	0.966
Dipropylene Glycol Methyl Ether	Not Used	1.130
Dipropylene Glycol Dimethyl Ether (DMM)	Not Used	1.500
Dipropylene Glycol n-Butyl Ether (DPnB)	Insoluble	1.340
Dipropylene Glycol	Insoluble	1.530
Ethanol	Insoluble	1.270
Ethanolamine	Insoluble	1.360
Ethyl Acetate	Insoluble	1.040
Ethylene Glycol Monomethyl Ether	Not Used	0.989
Ethylene Glycol Monobutyl Ether	Not Used	0.993
Ethylene Glycol Monoethyl Ether Acetate	Soluble*	1.010
Ethylene Glycol Monoethyl Ether	Soluble	0.868
Ethylene Dichloride	Soluble	0.738
Ethylene Glycol	Insoluble	1.720

* indicates disagreement between experimental and predicted results, i.e. predicted non solvent lying inside the solubility sphere or predicted solvent lying outside the solubility sphere.

Table 16. Calculated Solubility Sphere for Epikote 1009.

SOLVENT	Solubility	S_{rel}
Formamide	Insoluble	1.920
Glycerol	Insoluble	2.030
Hexane	Insoluble	1.830
Isophorone	Not Used	0.772
Methanol	Insoluble	1.590
Methyl Ethyl Ketone	Not Used	0.971
Methyl iso-Butyl Ketone	Insoluble	1.220
Methylene Dichloride	Borderline	0.703
Nitrobenzene	Soluble	0.671
Nitromethane	Insoluble	1.310
2-Nitropropane	Insoluble	1.000
Propylene Glycol Monomethyl Ether	Soluble	1.000
Propylene Glycol Diacetate	Not Used	1.120
Propylene Glycol Monobutyl Ether	Insoluble	1.320
Propylene Glycol Dimethyl Ether (MM)	Soluble*	1.300
Propylene Carbonate	Soluble	1.000
Propylene Glycol Methyl Ether	Soluble	0.976
Propylene Glycol	Insoluble	1.480
Tetrahydrofuran	Borderline	0.837
Toluene	Insoluble	1.330
Trichloroethylene	Soluble	1.000
Tripropylene Glycol Methyl Ether (TPnB)	Insoluble	1.410
Tripropylene Glycol Methyl Ether (TPM)	Insoluble	1.220
o-Xylene	Not Used	1.300

* indicates disagreement between experimental and predicted results, i.e. predicted non solvent lying inside the solubility sphere or predicted solvent lying outside the solubility sphere.

Table 16 (continued). Calculated Solubility Sphere for Epikote 1009.

4.1.3. Solvents

A range of commercial organic solvents was selected that satisfy the solubility requirements of the resins selected. Wherever possible a "universal solvent" blend was used to dissolve pairs of polymers. This blend (abbreviated to XDM) contained methyl iso butyl ketone (MiBK), xylene and methoxy propanol (50:30:20 w/w).

4.2. Stratification Studies

4.2.1. Characterisation of Unpigmented Systems

Individual resins were generally dissolved at 50% solids in methyl iso butyl ketone (MiBK), xylene and methoxy propanol (50:30:20 w/w). Resin pairs comprising one epoxy resin in conjunction with one topcoat resin were then combined at a ratio of 1:1 on weight of resin solids, and mixed using an orbital shaker. Films were applied to acetone cleaned aluminium foil using a block applicator to give nominal dry film thicknesses of 100μm and dried at 23°C / 65% relative humidity for two weeks prior to analysis.

Each Epikote resin (generally used as a primer) was initially studied in combination with every other resin to give a total of 80 combinations.

4.2.1.1. SEM - EDS

Scanning electron microscopy - energy dispersive spectrometry (SEM-EDS) was used to study cross sections of unpigmented films in order to detect stratification. This was only possible where the two resins could be distinguished by this method. Epikote and Lumiflon resins could be distinguished because the Lumiflon resin, a fluorinated polyether, also contains several percent chlorine which can be detected by EDS. An example of the electron micrograph and the elemental map for chlorine from an Epikote 1001 / Lumiflon LF200 system are shown in Figures 8 and 9. The micrograph clearly shows separation of the coating into distinct layers. On the elemental map the chlorine appears as bright dots in the areas where it is detected which corresponds on the micrograph to the portion of the film containing Lumiflon found at the air interface.

In some cases with other resin pairs layering could be detected visually by SEM but analysis of the layers by SEM-EDS was not possible as neither resin contained any distinguishable elements.

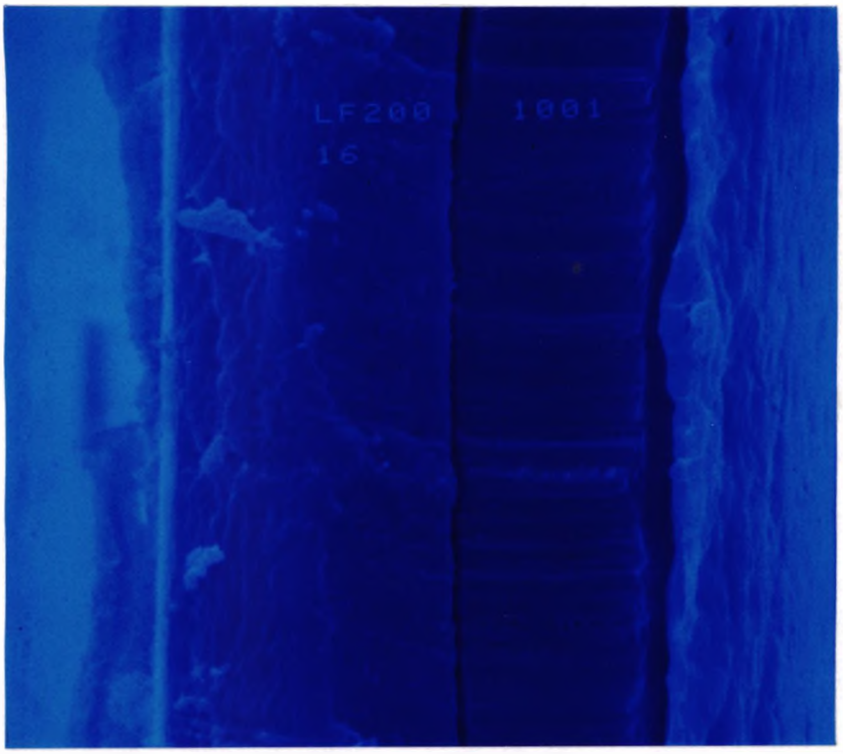

Figure 8. Electron micrograph - Epikote 1001 / Lumiflon LF200

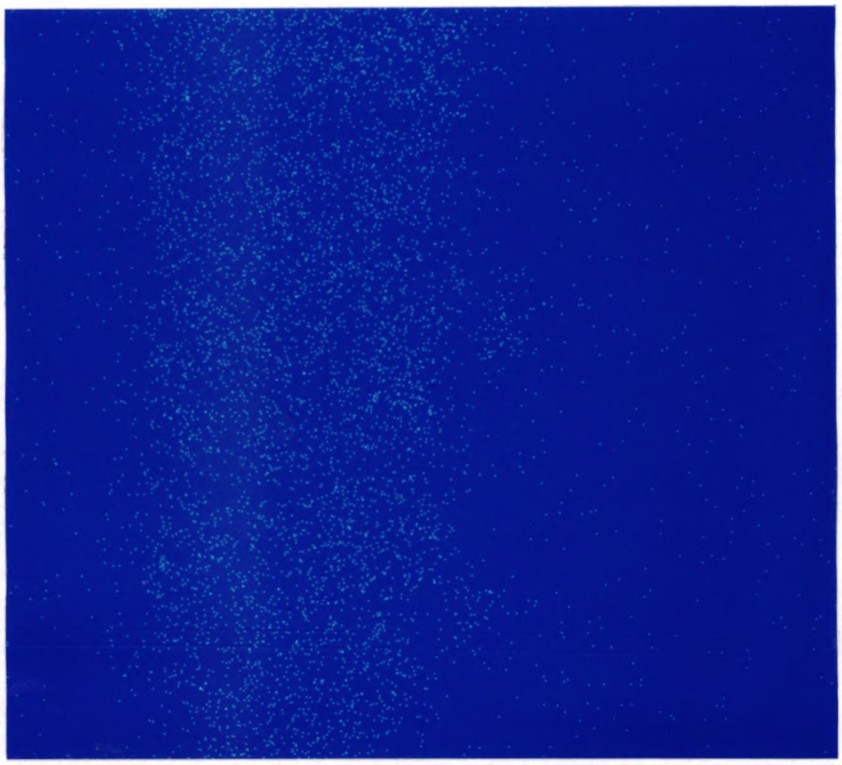

Figure 9. Elemental map for chlorine - Epikote 1001 / Lumiflon LF200

4.2.1.2. FTIR

The top surface of the coatings was analysed using Fourier Transform Infra Red spectroscopy (FTIR) with a horizontal attenuated total reflectance accessory (HATR).

To facilitate analysis of the results a visual ranking system for the degree of stratification from FTIR results was devised as follows:

Rank	Description
0	**No Stratification**
1	**Slight Stratification** (different concentration at each interface)*
2	**Partial Stratification** (increased concentration of resin 2 at air interface)
3	**Good Stratification** (high concentration of resin 2 at air interface)
4	**Full Stratification** (only resin 2 at air interface)

* This rank was only used where spectra of both surfaces were measured by FTIR-HATR

Figure 10. FTIR Ranking System

Figure 11 shows a typical FTIR-Horizontal Attenuated Total Reflectance (HATR) spectrum obtained for an Epikote 1001 / Lumiflon LF200 system. The spectra of the pure resins are included for comparison. As this system does not contain a curing agent both the top and bottom surfaces of the dry film were measured. The spectra show that the top surface consists almost entirely of Lumiflon LF200 distinguished by the strong band at 1125cm^{-1}, whereas the bottom surface although mostly Epikote does contain some Lumiflon.

Figure 12 shows a typical FTIR-HATR spectra obtained for an Epikote 1001 / Neocryl B700 system. Here also the top surface is seen to be almost entirely Neocryl B700 whilst the layer at the substrate, whilst mostly Epikote, does contain some Neocryl B700.

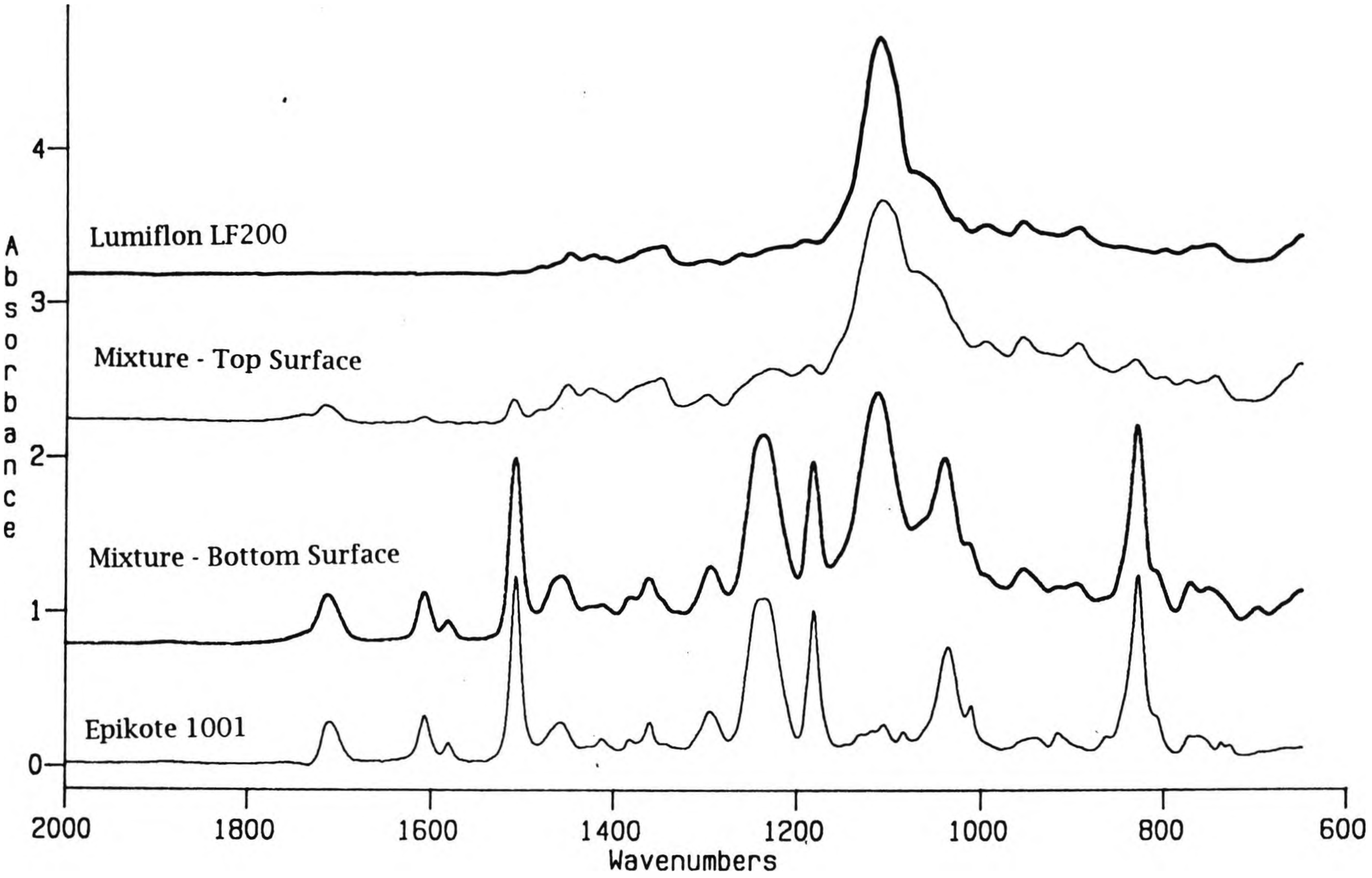

Figure 11. FTIR-HATR Spectrum
Unpigmented Epikote 1001 / Lumiflon LF200 Coating

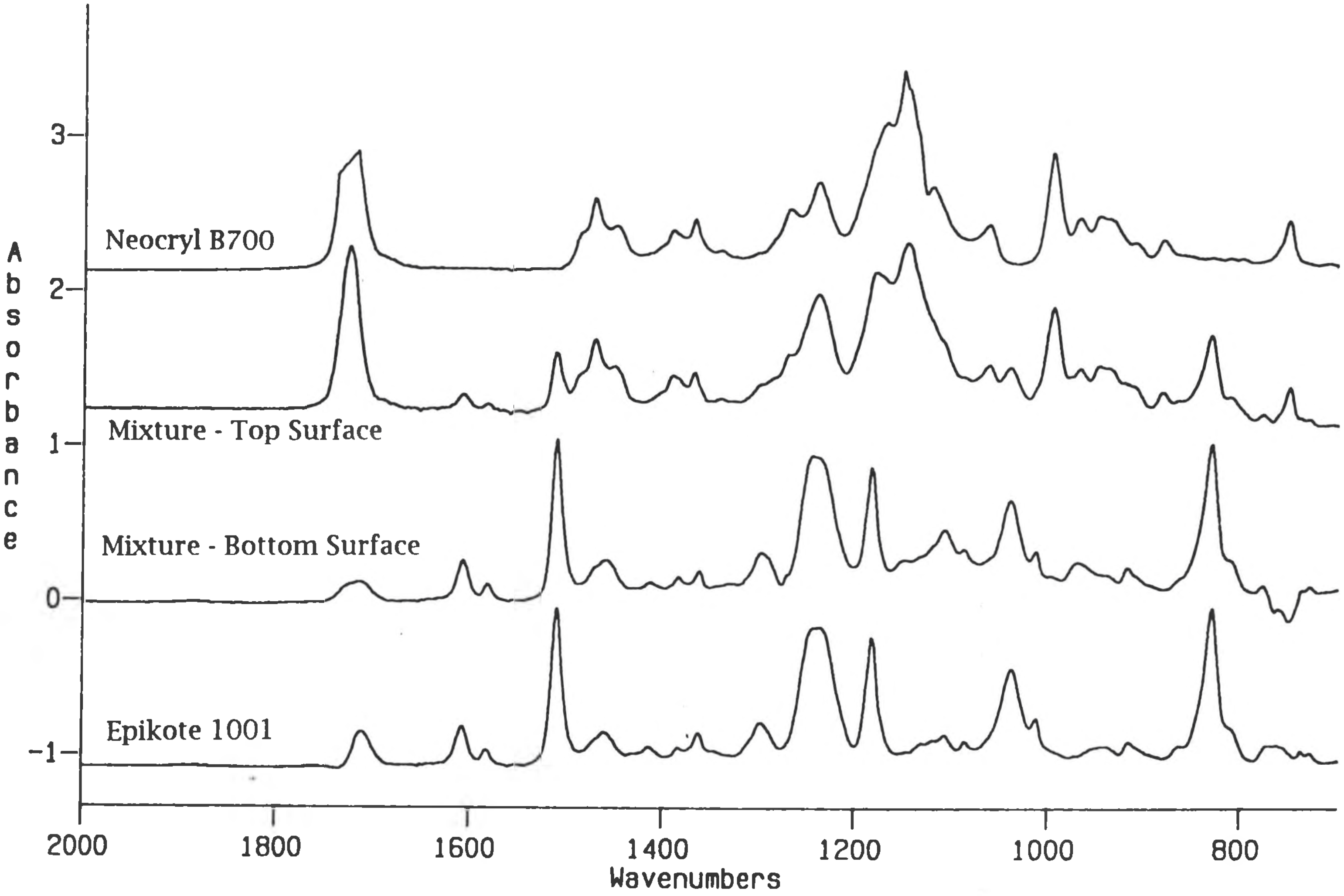

Figure 12. FTIR-HATR Spectrum
Unpigmented Epikote 1001 / Neocryl B700 Coating

4.2.2. Results

The FTIR results from the study of unpigmented systems without addition of curing agent are shown in Table 17. In many cases combinations which included Epikote 828 as the epoxy resin were still tacky after two weeks preventing analysis by FTIR-HATR. For non-cured resin combinations which would remain soluble both the top and bottom surfaces of the film were measured. The bottom surface was measured by casting the film directly on the HATR crystal and allowing it to dry before measurement. Only the top surface of cured systems was measured. The topcoat resins in Table 17 are listed in order of increasing surface energy (Harmonic Mean). The FTIR results are listed using the ranking scheme in Figure 10.

Resin 2	Surface Energy	No curing agent			
		Epikote			
		828	1001	1004	1007
Neocryl B-700	30.8	1	3	3	3
Neocryl B-804	34.4	3	2	2	2
Lumiflon LF200	36.4		4	4	4
Plastokyd SC140	37.0		0	0	0
Plastokyd SC400	37.4		1	1	0
Lumiflon LF916	37.7		4	4	4
Neocryl B-813	37.8	0	1	1	1
Plastokyd SC7	38.0		0	1	1
Plastokyd AC-4X	38.6		1		1
Alkyd VAS 9223	39.3		3	3	3
Hythane 9	39.7		2	1	0
Crodaplast AC-550	40.7	0	0	1	3
Hypalon 20	40.7		1	2	0
Crodaplast AC-500	41.4	2	3	3	4
Neocryl B-728	42.2	0	0	0	0
Synolac 9090	44.3		0	(1)	0
Neocryl B-811	44.4	0	0	(2)	0
Synolac 6016	44.5		1	0	(1)
Plastoprene 1S	45.1		2	0	0

Legend

Figures in parentheses indicate that some stratification had occurred but resin 2 went to the substrate interface and the epoxy resin to the air interface.

Table 17. Infrared (FTIR-HATR) Studies on Unpigmented Systems

4.2.3. Factors Affecting Stratification

4.2.3.1. Curing the Epoxy Resin

Used alone epoxy resins tend to form brittle films and are of relatively low molecular weight, giving poor chemical resistance. Therefore, they are generally only used as film formers when cross-linked with other materials to increase molecular weight and flexibility. For this study three amine type curing agents were selected that would represent a range of properties. "Amine A" was selected as its structure closely resembles that of an epoxy resin, Versamid 115 is a commercial polyamide resin of low polarity and Jeffamine D-230 a commercial polar polyoxypropyleneamine curing agent.

The effect of curing one of the resin components is seen in Table 18. The polar curing agent Jeffamine D230 shows the most improvement to stratification when compared to systems with no curing agent or with a curing agent of low polarity (Versamid 115).

Resin 2	"Amine A"				Jeffamine D230				Versamid 115			
	Epikote				Epikote				Epikote			
	828	1	4	7	828	1	4	7	828	1	4	7
Neocryl B-700	0	4	4	4	2	3	4	4	3	3	4	4
Neocryl B-804	0	2	4	4	0	3	4	4	0	0	0	0
Lumiflon LF200	0	4	4	4	2	4	4	4	0	3	4	4
Plastokyd SC140	0	0	0	2	0	0	3	4	0	0	0	0
Plastokyd SC400	0	2	0	0	0	3	3	3	0	0	0	0
Lumiflon LF916	0	4	2	4	3	3	3	4	0	2	3	3
Neocryl B-813	0	2	2	2	0	0	2	4	2	2	2	3
Plastokyd SC7	0	2	2	2	0	0	2	4	0	0	0	2
Plastokyd AC-4X	0	2	2	2	0	0	2	2	0	0	0	3
Alkyd VAS 9223	0		2	4	3	3	3	4	3	2	3	4
Hythane 9	0		2	2	3	3	3	3	3	2	3	4
Crodaplast AC-550	0	0	2	2	0	0	2	4	0	0	0	2
Hypalon 20	0		0	0		0	2	3	0	0	0	0
Crodaplast AC-500	0	0	4	4	0	0	0	2	0	0	0	2
Neocryl B-728	0	2	2	0	0	0	0	2	0	2	3	3
Synolac 9090	0		2	2	0	0	2	2	0	0	0	2
Neocryl B-811	0	2	2	2	0	0	0	3	(2)	0	2	3
Synolac 6016	0		2	0		0	0	2	0	0	0	3
Plastoprene 1S	0	0	2	0			0	0	0	0	0	0

Legend

Epikote 1 = Epikote 1001 Epikote 4 = Epikote 1004 Epikote 7 = Epikote 1007

Amine "A"= 4,4' methylenebis(cyclohexyl)amine

Figures in parentheses indicate that some stratification had occurred but resin 2 went to the substrate interface and the epoxy resin to the air interface.

Table 18. Infrared (FTIR-HATR) Studies on Unpigmented Systems

4.2.3.2. Epoxy Molecular Weight

The molecular weight of the epoxy resins increases in the order 828, 1001, 1004 and 1007. Table 17 shows that the molecular weight has an effect on stratification but the effect is more clearly seen in Table 18. Stratification is generally seen to improve with increasing epoxy molecular weight. This is because the resin pairs become more incompatible with increasing molecular weight.

This correlates well with work carried out on powder coatings[18] where the molecular weight was seen to be an important parameter in stratification.

4.2.3.3. Surface Energy

The series of Epikote resins used for this study have surface energies of around 45 mN m^{-1}. Generally, the resins chosen as suitable for topcoat materials have surface energies lower than that of the epoxies.

The surface energy difference between the two resins is considered to be an important factor in assessing whether stratification will occur. In Tables 17 and 18 the topcoat resins are listed in order of increasing solid surface energy as determined from contact angle data by the Harmonic Mean method. For a given epoxy resin most films showing a tendency towards stratification are found towards the top of the tables where there is a larger surface energy difference between the two resins. This effect is seen most clearly in the cured systems.

Figure 13 shows FTIR-HATR spectra for an Epikote 1001 / Neocryl B728 combination along with the reference spectra of the pure resins. In this case the spectra of the top and bottom surfaces are both shown to contain a mixture of resins and stratification is not observed. There is a solid surface energy difference of just 3.2mN m^{-1} between Neocryl B728 and Epikote 1001, whereas for a Neocryl B700 and Epikote 1001 combination which is observed to stratify experimentally there is a surface energy difference of 10.0 Nm^{-1}. This suggests that a large surface energy difference between the resins favours stratification.

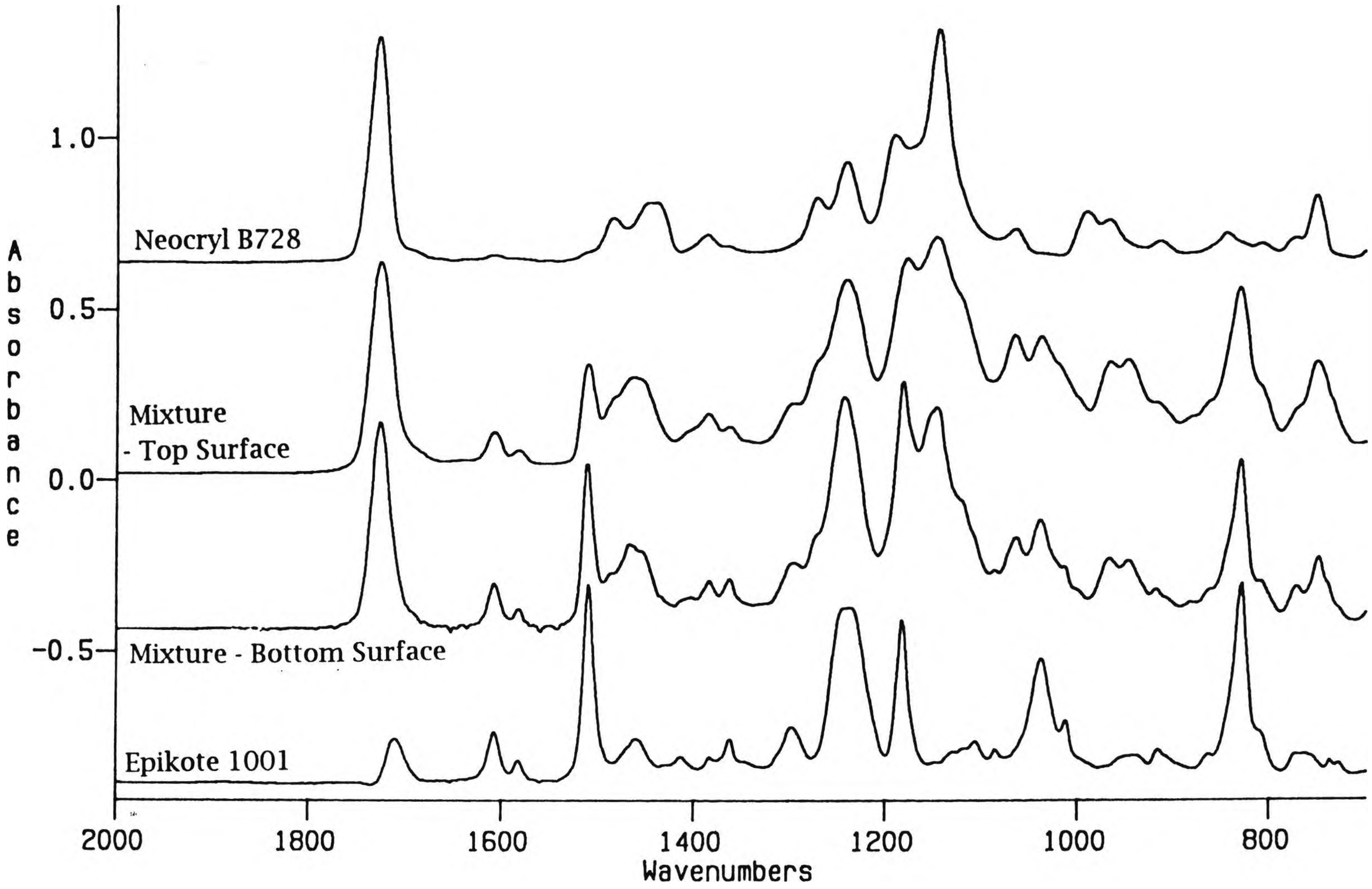

Figure 13. FTIR-HATR Spectrum
Unpigmented Epikote 1001 / Neocryl B728 Coating

These results correlate well with the studies made on powder coatings where it was stated that for multilayer formation to occur there should be a surface energy difference between the polymer powders in the fused state of at least 0.2 J cm^{-1} and preferably 5.0 J cm^{-1}.

4.2.3.4. Effect of Resin Compatibility

4.2.3.4.1. Phase Behaviour

Phase separation is considered to be a prerequisite for stratification. However, it would be advantageous to have systems that were one phase at application solids to give good in-can-stability and ease of application. An ideal system would phase separate at 60 - 80% solids since at higher concentrations viscosity may inhibit the separation of the two phases into layers. Therefore, a knowledge of the phase behaviour of these resin combinations in solution is required. It is possible to determine experimentally the approximate resin concentration at phase separation for different compositions and generate a ternary phase diagram.

The phase behaviour of pairs of resins in various solvents was examined. In each case one of the resins in the pair was an epoxy resin.

4.2.3.4.2. Phase Diagrams

Ternary phase diagrams were built using information from three resin ratios 4:1, 1:1 and 1:4 by weight on resin solids (Table 19).

Resin Combination	Solvent	Ratio Epikote : Resin 2 1:4 %	 1:1 %	 4:1 %
Epikote 828 / Neocryl B700	MiBK	38	65	>65
Epikote 1001 / Neocryl B700	MiBK	30	30	29
Epikote 1001 / Neocryl B700	MEK	33	31	36
Epikote 1007 / Neocryl B700	MiBK	<5	<5	<5
Epikote 1007 / Neocryl B700	MEK	<5	<5	<5
Epikote 828 / Lumiflon LF200	MiBK	60	>65	>65
Epikote 1001 / Lumiflon LF200	MiBK	25	25	<10
Epikote 1007 / Lumiflon LF200	MiBK	<5	<5	<5

Table 19. Resin Solids at Point of Phase Separation

Figure 14 shows the results from the combination Epikote 1001 / Neocryl B700 / MEK expressed diagramatically.

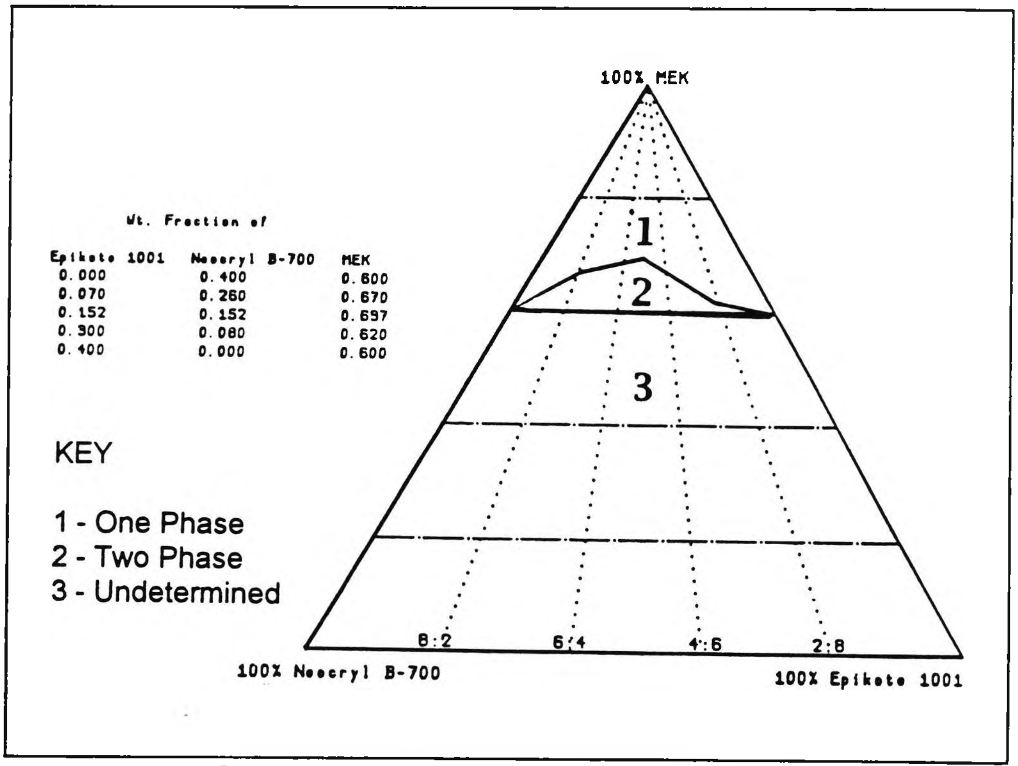

Wt. Fraction of

Epikote 1001	Neocryl B-700	MEK
0.000	0.400	0.600
0.070	0.260	0.670
0.152	0.152	0.697
0.300	0.080	0.620
0.400	0.000	0.600

KEY

1 - One Phase
2 - Two Phase
3 - Undetermined

Figure 14. Experimental Phase Diagram

Epikote 1001 / Neocryl B700 / MEK

In most systems the solids content at the point of phase separation showed more dependence on the molecular weight of the epoxy than the solvent used. For the system Epikote 1001 / Neocryl B700 at a 1:1 ratio the solids content at the point of phase separation was 31% in MEK, 30% in MiBK and 25% in n-butyl acetate.

The molecular weight of the resins had an very noticeable effect on the phase behaviour of resin pairs. For a given combination phase separation occurred at a lower total resin concentration when the Epikote resin was changed from Epikote 828 (Mw = 379) to Epikote 1007 (Mw = 9114). For the systems including an Epikote resin in combination with Lumiflon LF200 in MiBK phase separation occurred at above 65% solids with Epikote 828 but less than 5% solids with Epikote 1007. Similar trends were observed in Epikote / Neocryl B700 systems.

Therefore it is seen that compatibility decreases rapidly as the molecular weight of the resins increases. Table 20 shows the results for the solids content at the point of phase separation (cloud point) for all systems at a 1:1 resin ratio using the solvent blend XDM (50% MiBK, 30% xylene, 20% methoxy propanol). These results clearly show the effect that the molecular weight of the epoxy resin has on the phase behaviour of the system.

Resin 1	Resin 2	Solids %	Dry Film Appearance	Solution Appearance*
Epikote 828	Alkyd VAS 9223	78	Hazy	Clear
Epikote 828	Crodaplast AC500	100	Clear	Clear
Epikote 828	Crodaplast AC550	100	Clear	Clear
Epikote 828	Hypalon 20	<3	Cloudy	Cloudy
Epikote 828	Hythane 9	100	Clear	Clear
Epikote 828	Lumiflon LF200	>65	Cloudy	Cloudy
Epikote 828	Lumiflon LF916	64	Cloudy	Clear
Epikote 828	Neocryl B700	65	Cloudy	Clear
Epikote 828	Neocryl B728	100	Clear	Clear
Epikote 828	Neocryl B804	45	Cloudy	Clear
Epikote 828	Neocryl B811	100	Clear	Clear
Epikote 828	Neocryl B813	100	Hazy	Clear
Epikote 828	Plastokyd AC4X	100	Clear	Clear
Epikote 828	Plastokyd SC140	100	Clear	Clear
Epikote 828	Plastokyd SC400	100	Clear	Clear
Epikote 828	Plastokyd SC7	100	Clear	Clear
Epikote 828	Synolac 6016	100	Clear	Clear
Epikote 828	Synolac 9090	100	Clear	Clear
Epikote 1001	Alkyd VAS 9223	41	V Large Lenses	Cloudy
Epikote 1001	Crodaplast AC500	48	Small Lenses	Hazy
Epikote 1001	Crodaplast AC550	50	Small Lenses	Clear
Epikote 1001	Hypalon 20	<3	Clear	Cloudy
Epikote 1001	Hythane 9	42	Small Lenses	Cloudy
Epikote 1001	Lumiflon LF200	25	V Large Lenses	Cloudy
Epikote 1001	Lumiflon LF916	35	Medium Lenses	Cloudy
Epikote 1001	Neocryl B700	30	Large Lenses	Cloudy
Epikote 1001	Neocryl B728	100	Clear	Clear
Epikote 1001	Neocryl B804	28	Medium Lenses	Cloudy
Epikote 1001	Neocryl B811	100	Clear	Clear
Epikote 1001	Neocryl B813	35	Hazy	Cloudy
Epikote 1001	Plastokyd AC4X	>67	Hazy	Clear
Epikote 1001	Plastokyd SC140	38	Cloudy	Cloudy
Epikote 1001	Plastokyd SC400	>67	Hazy	Clear
Epikote 1001	Plastokyd SC7	>60	Hazy	Clear
Epikote 1001	Synolac 6016	100	Clear	Clear
Epikote 1001	Synolac 9090	>54	Cloudy	Clear
Epikote 1007	Alkyd VAS 9223	18	Small Lenses	Cloudy
Epikote 1007	Crodaplast AC500	20	Medium Lenses	Cloudy
Epikote 1007	Crodaplast AC550	23	Medium Lenses	Cloudy
Epikote 1007	Hypalon 20	<3	Medium Lenses	Cloudy
Epikote 1007	Hythane 9	20	Hazy	Cloudy
Epikote 1007	Lumiflon LF200	14	Medium Lenses	Cloudy
Epikote 1007	Lumiflon LF916	15	Large Lenses	Cloudy
Epikote 1007	Neocryl B700	<5	Large Lenses	Cloudy
Epikote 1007	Neocryl B728	30	Cloudy	Hazy
Epikote 1007	Neocryl B804	9	Hazy	Cloudy
Epikote 1007	Neocryl B811	31	Cloudy	Cloudy
Epikote 1007	Neocryl B813	17	Small Lenses	Cloudy
Epikote 1007	Plastokyd AC4X	24	Small Lenses	Cloudy
Epikote 1007	Plastokyd SC140	20	Small Lenses	Cloudy
Epikote 1007	Plastokyd SC400	28	Hazy	Cloudy
Epikote 1007	Plastokyd SC7	52	Hazy	Cloudy
Epikote 1007	Synolac 6016	34	Hazy	Clear
Epikote 1007	Synolac 9090	37	Hazy	Cloudy

* Solution appearance at 50% solids

Table 20. Phase Data

From the results shown in Table 20 it appears that the ideal situation in terms of molecular weight lies somewhere between Epikote 828 and Epikote 1001 depending on which second resin is employed. Most resin combinations using Epikotes 1004 and 1007 phase separate at too low a resin concentration to enable one-phase mixtures to be produced at solids contents typical of those used in the surface coatings industry. However, some compromise must be reached as stratification is seen to improve with increasing molecular weight.

4.2.3.4.3. Phase Equilibria

Phase separation does not guarantee that the phases will be rich in one of the component resins. To investigate phase composition more closely a detailed analytical study of a limited number of systems was made.

The phase behaviour of Epikotes 828, 1001, 1004 and 1007 with Lumiflon LF200 and Epikote 1001 with Neocryl B700 at equilibrium was studied experimentally.

Ratios of Epikote / resin 2 of 1:1, 3:1, 5:1 and 9:1 were studied at 30% solids in a 1:1 mixture of xylene and MiBK. This solvent mixture was chosen for its solubility of this resin combination at this solids concentration and also its simplicity of analysis by GC-MS. After agitation in an ultrasonic bath systems were sealed and left to equilibrate at 25°C for a period of two weeks. If phase separation was observed the layers were separated as far as possible using a hypodermic syringe and analysed for solids content, solvent composition (GC-MS), surface energy (Wilhelmy plate at 25°C) and resin composition (FTIR).

At this concentration all systems containing Epikote 828 were one phase at equilibrium. This would suggest that combinations containing Epikote 828 are not potential stratifying systems since phase separation is not exhibited. Systems containing Epikote 828 also dry to give clear films suggesting that phase separation does not occur up to 100% solids. Infrared results also showed these systems had little tendency toward stratification.

Systems containing Epikote 1007 did not give good separation - perhaps due to the higher viscosity of Epikote 1007 compared to the other Epikotes. This meant the phases were difficult to separate and the reliability of the results was low.

Where phase separation occurred, one of the phases was found to contain predominantly epoxy resin whereas the other could contain significant amounts of both resins (Tables 21,22 and 23). This implies that both resins could be present at both interfaces even though the system has fully stratified. This has important implications for infrared studies which may detect a mixture of resins even though stratification has occurred.

The best separation was found at 1:1 resin ratios. This is in disagreement with Verkholantsev's work where he suggested that for the materials he used far from equal ratios would improve stratification[17].

Ratio Epikote : Lumiflon	Phase	Epikote	Lumiflon	MiBK	Xylene
1:1	I	40	0	30	30
	II	11	31	29	29
3:1	I	44	0	28	28
	II	18	37	22	22
5:1	I	46	0	27	27
	II	8	42	25	25
9:1	I	47	0	27	27
	II	22	27	26	26

Table 21. Phase Separation Data - Epikote 1001 / Lumiflon LF200

Ratio Epikote : Lumiflon	Phase	Epikote	Lumiflon	MiBK	Xylene
1:1	I	42	0	29	29
	II	4	47	24	24
3:1	I	35	5	30	30
	II	0	47	26	26
5:1 ʃʃ	I	39	3	29	29
	II	29	28	16	16
9:1 ʃʃ	I	39	0	30	30
	II	36	31	16	16

ʃʃ Layers not well separated

Table 22. Phase Separation Data - Epikote 1004 / Lumiflon LF200

Ratio Epikote : Lumiflon	Phase	Solids	Epikote	Neocryl	MiBK	Xylene	Surface Energy (mN m-1)
1:1	I	29	10	19	26	45	26.5
	II	*	28	2	23	47	*
3:1	I	30	15	15	25	45	25.5
	II	36	35	1	21	43	26.2
5:1	I	29	16	13	25	46	26.3
	II	33	33	0	22	45	26.4
9:1	I	30	28	2	20	50	27.8
	II	32	31	1	25	43	26.3

*There was insufficient material in this layer for these measurements to be carried out. It was assumed that this layer contained 30% solids and 70% solvent.

Table 23. Phase Separation Data - Epikote 1001 / Neocryl B700

4.2.3.5. Resin Ratio

In order to verify the results obtained above for the phase separation behaviour at different resin ratios of Epikote resin : topcoat resin of 1:1, 3:1 and 9:1 were studied to determine the effect of resin ratio on stratification.

Generally it was found that stratification occurred at a similar level from both 1:1 and 3:1 ratios but was seriously impaired at ratios of 9:1 (Table 24). This shows good agreement with the work on phase equilibria shown in Tables 21, 22 and 23 where it was shown that the best separation of layers was produced using ratios close to 1:1. Figure 15 shows an example of an FTIR-PAS spectrum of an unpigmented Epikote 1001 / Lumiflon LF200 film at 1:1 resin ratio.

Resin 1	Resin 2	Ratio	IR
Epikote 1001	Lumiflon LF200	1:1	3
Epikote 1001	Lumiflon LF200	3:1	3
Epikote 1001	Lumiflon LF200	9:1	1

Table 24. Effect of Resin Ratio on Stratification

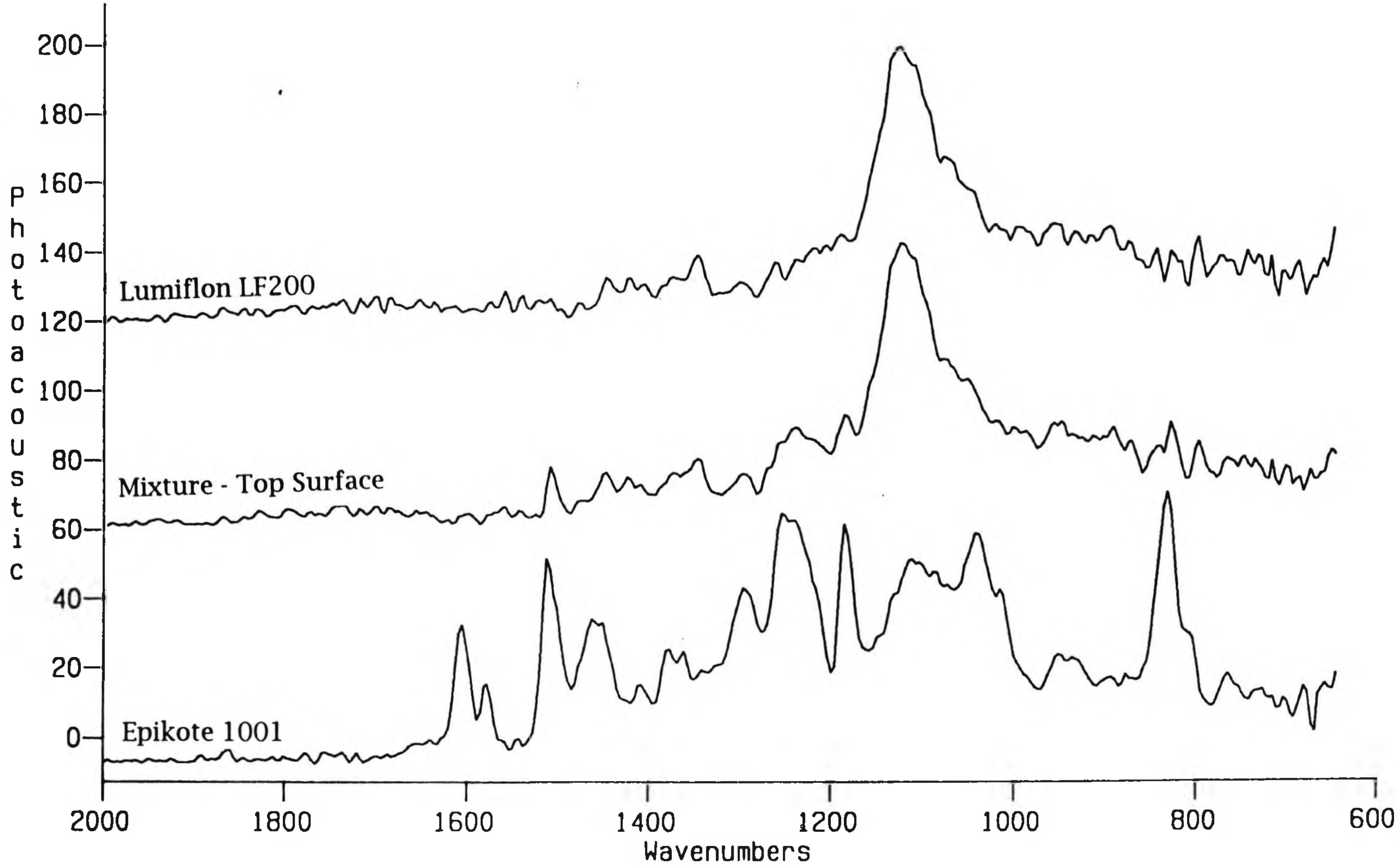

Figure 15. FTIR-PAS Spectra
Unpigmented Epikote 1001 / Lumiflon LF200

4.2.3.5.1. Kinetics of Drying

Selected systems were studied during drying using an optical microscope with a video camera attached. A portion of the system to be studied was spread onto a microscope slide and viewed and recorded at 50 to 100x magnification.

An Epikote 1001 / Neocryl B700 system diluted to give a one phase solution was studied by this method. As solvent evaporated from the film, spheres of one phase could be clearly seen within a second continuous phase. The spheres moved across each other in a continuous circulatory motion. On colliding the spheres joined together and increased in size, before disappearing. It became evident that the disappearing spheres were forming a lower layer in the film. This motion lasted for several minutes after which the formation of hexagonal convection cells (Bérnard cells) was apparent .

An Epikote 1001 / Lumiflon LF200 system showed slightly different behaviour. After the spheres had joined their respective continuous phase some of the material in the lower layer re-emerged in the layer at the air interface appearing as lenses which again with time shrunk but did not completely rejoin the lower layer (Table 25).

Time	Observation
20 seconds	Rapid motion of small spheres starts at film edge
30 seconds	Rapid motion of small spheres visible across body of film
40 seconds	Large spheres observed - motion still rapid
50 seconds	Large spheres start joining with lower layer
80 seconds	Motion beginning to slow down
5 minutes	Bernard Cells apparent - film appears almost stationary but spheres still joining lower layer
7 minutes	Re-emerging of material from lower layer
9 minutes	Material shrinks almost entirely back to lower layer
10 minutes	No detectable movement

Table 25. Observations During Drying - Epikote 1001 / Lumiflon LF200

4.2.3.6. Film Thickness

Unpigmented systems with dry film thicknesses of between 50μm and 200μm all gave similar results. Stratification was found to be seriously impaired at 25μm. This may be because the solvent evaporates too quickly in thinner films where there is a larger surface area (relative to the total film volume) available for solvent evaporation than in thicker films.

4.2.3.7. Temperature

The effect of temperature on stratification was studied using Epikote / Lumiflon LF200 / Jeffamine D230 in MiBK, xylene, methoxy propanol (50,30,20) systems. A 1:1 resin ratio and 50% non-volatile content were used throughout. After application the films were dried at varying temperatures (30, 23 and 7°C) for 24 hours prior to curing at 110°C for 1 hour. The results showed that stratification is seriously impaired at 7°C when the films start to exhibit lensing instead of separation into distinct layers. The high viscosity of the drying film at 7°C may prevent stratification by reducing the movement of the separating phases.

This effect of temperature may have a detrimental effect on the potential for stratifying coatings to be used externally in cold or mild climates.

4.2.3.8. Starting Phase

The aim of this study was to determine whether systems which are initially two phases are necessary, or preferable to those which are initially homogeneous.

Unpigmented systems containing Epikote / Lumiflon LF200 and Epikote / Neocryl B700 were studied. For each system the resins were prepared at a ratio of 1:1 and at approximately 50% solids in xylene, MiBK, methoxy propanol (30:50:20). One film was prepared that was initially two phase in nature. A second film was prepared after diluting the 50% mixture until a clear one phase solution resulted.

In all cases when examined by FTIR systems prepared from homogeneous initial mixtures were comparable with those obtained from two phase mixtures. However, the low non-volatile content of homogeneous mixtures and hence low viscosity made preparation of films from these materials difficult. In an attempt to produce mixtures that would allow higher solids and still be homogeneous some work was carried out using mixtures of the commercial Epikote resins. The mixtures studied were:

"Epikote 901"	828:1001 1:1
"Epikote 903"	828:1001 1:3
"Epikote 781	828:1007 1:1
"Epikote 783"	828:1007 1:3

Mixtures containing Epikote 1007 lowered the solids achievable before the occurrence of phase separation but the mixtures containing Epikote 828 and 1001 slightly raised the solids achievable before the onset of phase separation when compared to Epikote 1001 (Table 26). However, the achievable solids are still below the solids that would be required to give adequate application viscosity in homogeneous unpigmented systems. This may not be a problem in real systems where pigments and other additives would increase the solids content and hence the viscosity of the system to an acceptable level.

"Epikote"	Solids at point of phase separation / % Lumiflon LF200	Solids at point of phase separation / % Neocryl B700
1001	24	23
901	28	31
903	25	26
781	19	14
783	13	13

Table 26. Phase Separation Behaviour - Epikote Resins

Table 27 shows that these Epikote mixtures are still able to produce stratifying systems when used in combination with either Neocryl B700 or Lumiflon LF200.

Resin 1	Resin 2	IR
Epikote 901	Neocryl B700	3
Epikote 901	Lumiflon LF200	3
Epikote 903	Neocryl B700	3
Epikote 903	Lumiflon LF200	3
Epikote 781	Neocryl B700	4
Epikote 781	Lumiflon LF200	3
Epikote 783	Neocryl B700	4
Epikote 783	Lumiflon LF200	3

Table 27. FTIR Results - Epikote Mixtures

4.2.4. Conclusions

The parameters shown to favour stratification from liquid unpigmented resin combinations on metallic substrates are:

1. Low compatibility between the resin pair. This may conveniently be carried out by increasing the molecular weight of the epoxy component.

2. Curing the epoxy component with a polar curing agent.

3. A large surface energy difference between the resin components.

4. A resin ratio that is near to unity.

5. A dry film thickness of at least 100 microns.

4.3. Prediction of Stratification Based on Surface Energy

4.3.1. Prediction of Stratification from Solid Surface Energies

It is possible that the surface energies of the pure solid resins may be used to predict stratification from the equations below:

$$(\gamma_{sl} - \gamma_{s2}) \geq \gamma_{12} \qquad \textbf{(37)}$$

$$\gamma_2 - \gamma_{s2} - \gamma_1 + \gamma_{s1} > 0 \qquad \textbf{(42)}$$

$$\gamma_s - \gamma_{s2} - \gamma_{12} - \gamma_1 > 0 \qquad \textbf{(39)}$$

Table 28 shows predictions made using solid surface energy data for the resins. However, it is seen that the predicted and experimental results are quite different. In particular, systems with Lumiflon LF200 are not predicted to stratify using this method, but experimentally they are observed to do so. The probable reason for this is that the effect of the solvent on the surface energy has not been taken into account. Stratification occurs before all the solvent has evaporated, so it is the surface energies of the separating phases rather than the solid resins which are important.

Resin 1	**Epikote 828**		**Epikote 1001**		**Epikote 1007**	
Resin 2	**Theory**	**Exp**	**Theory**	**Exp**	**Theory**	**Exp**
Neocryl B700	✓		✓	✓	✓	✓
Neocryl B728						
Neocryl B804	✓	✓				
Neocryl B811						
Neocryl B813						
Crodaplast AC500		✓		✓		✓
Crodaplast AC550	✓		✓		✓	✓
Lumiflon LF200				✓		✓
Lumiflon LF916				✓		✓
Plastokyd SC7	✓					
Plastokyd SC140	✓					
Plastokyd SC400						
Plastokyd AC 4X						
Alkyd VAS 9226				✓		✓
Hythane 9						
Synolac 6016						
Synolac 9090						
Plastoprene 1S						
Alloprene R10	✓		✓		✓	
Hypalon 20	✓		✓		✓	

Table 28. Prediction of Stratification on Aluminium Foil.

4.3.2. Prediction of Stratification from Solution Surface Energies

Assuming that the concentration of the two phases is always the same, it is possible to predict whether stratification should occur during solvent evaporation. This is illustrated below in Figure 16 for the system Epikote 1001 / Neocryl B700 in n-butyl acetate. The three conditions for stratification (Equations 37, 39 and 42) are plotted against the resin concentration. Where all three conditions are fulfilled it is predicted that the system will stratify. It is seen that this system is predicted to stratify at all concentrations (provided it is two phase) and this is in agreement with experimental results.

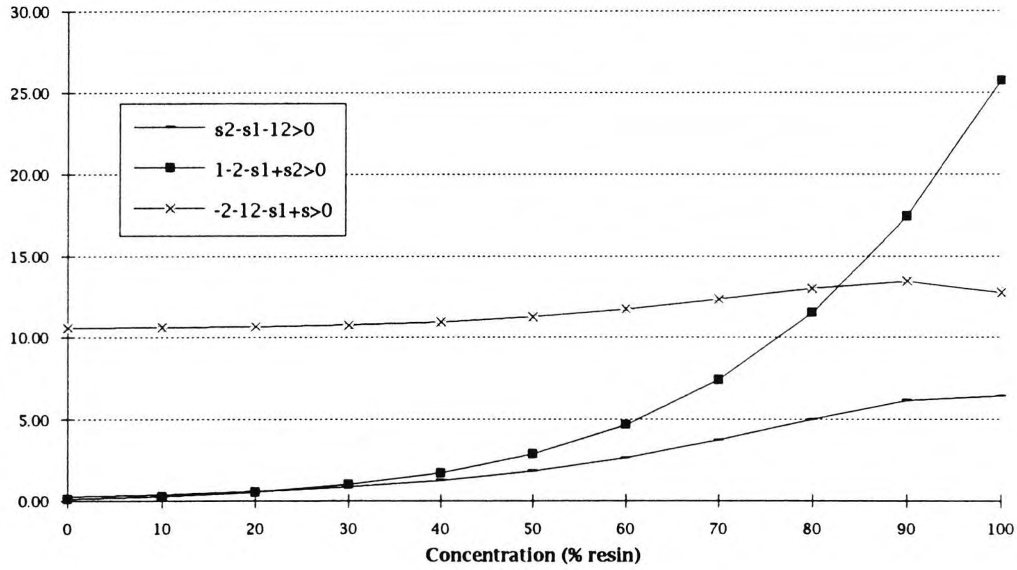

Figure 16. Prediction of Stratification for Epikote 1001 / Neocryl B700.

For the system Epikote 1001 / Lumiflon LF200 stratification is predicted for concentrations up to 80% total solids. Above 80% resin solids one of the conditions becomes negative (Figure 17) and stratification is no longer predicted. This would explain why the system is not predicted to stratify using pure resin surface energies but is observed to stratify experimentally. Below 80% solids the two phase system will form into two layers. At 80% solids the conditions for stratification are no longer satisfied but the viscosity is too high to allow much disruption of the layers. This is also consistent with optical examination of film formation from an unpigmented Epikote Lumiflon system where two layers appeared to form at low concentrations but some disruption was observed at high resin concentrations (PRA video PRAVSSC1).

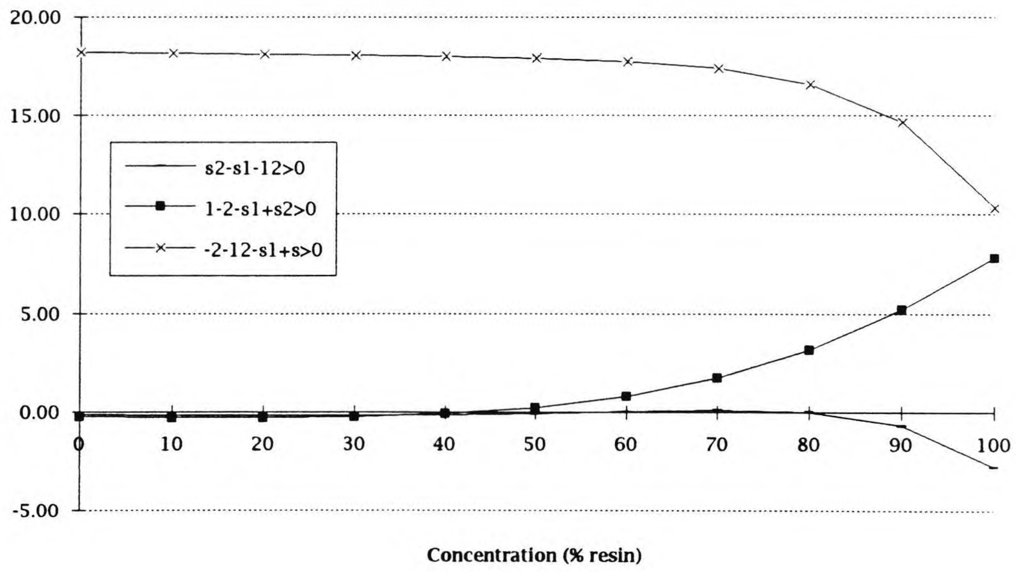

Figure 17. Prediction of Stratification for Epikote 1001 / Lumiflon LF200.

Figure 18 shows the prediction of stratification for an Epikote 1001 / Neocryl B728 combination. The graph shows that two out of three of the requirements for stratification are never fulfilled, predicting that this combination would not exhibit stratification. This is in agreement with the experimental results where stratification was not observed.

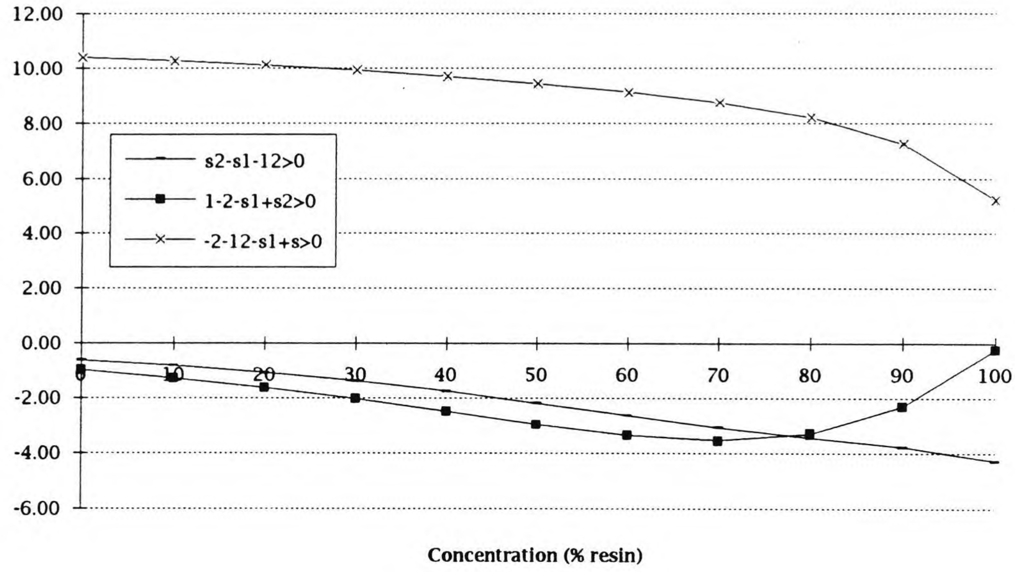

Figure 18. Prediction of Stratification for Epikote 1001 / Neocryl B728

The concentration ranges where stratification is predicted are listed in Table 29. The correlation with experimental data is good except in the case of Epikote 828. This is because it is assumed that phase separation has occurred for the prediction of stratification. For most systems containing

Epikote 828 as one component the system remains homogeneous until it reaches high concentrations[92] which probably precludes stratification.

Resin 1	Resin 2	Solvent	Predicted Range % Solids	Experiment IR
Epikote 828	Lumiflon LF200	Methyl iso-Butyl Ketone	0 - 100	
	Neocryl B700	n-Butyl Acetate	0 - 100	1
	Neocryl B728	n-Butyl Acetate	0 - 30	0
	Neocryl B804	n-Butyl Acetate	60 -100	3
	Neocryl B811	n-Butyl Acetate	0	0
	Neocryl B813	n-Butyl Acetate	70 - 100	0
Epikote 1001	Lumiflon LF200	Methyl iso-Butyl Ketone	0 - 80	4
	Neocryl B700	n-Butyl Acetate	0 - 100	3
	Neocryl B728	n-Butyl Acetate	0	0
	Neocryl B804	n-Butyl Acetate	0	2
	Neocryl B811	n-Butyl Acetate	0	0
	Neocryl B813	n-Butyl Acetate	0	1
Epikote 1007	Lumiflon LF200	Methyl iso-Butyl Ketone	0 - 80	4
	Neocryl B700	n-Butyl Acetate	0 - 100	3
	Neocryl B728	n-Butyl Acetate	0	0
	Neocryl B804	n-Butyl Acetate	90 -100	2
	Neocryl B811	n-Butyl Acetate	0	0
	Neocryl B813	n-Butyl Acetate	0	1

Table 29. Predicted Concentration Ranges for Stratification

4.3.3. Summary

This section has reviewed the possibility of predicting stratification from surface energy values.

It has been shown that in some cases the tendency of a system to stratify can be predicted from the surface energies of the solid resins. However, this was found to be unreliable because it is the solution surface energies of the separating phases rather than the solid surface energies that must be considered. Where solution surface energy data are available, reliable predictions concerning stratification can be made. In the case of Epikote and Lumiflon these data shows why stratification is not predicted using the solid surface energy data. It also offers an explanation of the unusual behaviour of this system as seen by optical microscopy.

4.4. Prediction of Stratification Based on Solubility Parameters

It has already been seen that Hansen three dimensional solubility parameters can predict resin solubility with reasonable accuracy, giving good agreement with experimental results. This section will look at the possibilities of correlating Hansen solubility parameter data with properties such as phase behaviour, film and solution appearance and stratification behaviour. After some preliminary studies it became clear that the two functions that appeared to give some correlation with Hansen Solubility Parameter data were V (the volume of the solubility sphere overlap) and B (the sum of the volumes of the spheres divided by the distance between their centres). These two functions were used in the following analysis.

Tables 30 and 31 summarise data where epoxy / topcoat resin combinations are arranged firstly in order of increasing percentage overlap volume (V) and then in order of increasing total volume/sphere separation (B). In each case the data are shown against experimental data on film and solution appearance, solids at phase separation and stratification behaviour as determined from FTIR measurements.

4.4.1. Correlation with Solubility Sphere Overlap (V)

The results in Table 30 show that there appears to be a low degree of correlation between solubility sphere overlap and film appearance. Above 55% overlap a majority (59%) of homogeneous films (designated clear or hazy) were produced. Below 55% overlap a majority (61%) of heterogeneous films (designated cloudy or with lenses) were produced.

Systems exhibiting a low percentage overlap of the solubility spheres (less than 55%) produced mainly heterogeneous solutions at 50% solids, whereas systems with larger common volumes (percentage overlaps greater than 55%) generally gave homogeneous solutions. Of the 54 systems studied 67% followed this trend.

The results in Table 30 also show that all those systems giving good stratification had percentage overlaps of 50% or less. This would suggest that stratification is favoured if the two resins have significantly different solubility behaviour and few common solvents which may cause formulation difficulties in commercial systems.

4.4.2. Correlation with B

Some correlation of B with film and solution appearance and solids achievable before phase separation can be seen in Table 31. Generally, if B is less than 2,000, resin solutions are cloudy in appearance, films appear heterogeneous and phase separation occurs below 50% solids. All systems giving full stratification and most giving good stratification fall within this group.

If B is greater than 2,000 generally both films and solutions are homogeneous in appearance and the resin pairs are compatible up to 100% solids. Most systems in this group do not exhibit stratification.

The results show that both V and B predict stratification to a similar degree. Either is capable of selecting a group of systems which contains most of the experimental stratifying systems. However, in each case the group also contains a high number of experimentally non-stratifying systems.

Resin 1	Resin 2	R1	R2	D	V %	Solids %	Film Appearance	Solution Appearance	Degree of Stratification
Epikote 1001	Crodaplast AC500	10.9	12.3	15.88	16.01	48	Small Lenses	Hazy	3
Epikote 1001	Hypalon 20	10.9	11.3	13.91	19.33	<3	Clear	Cloudy	
Epikote 828	Crodaplast AC500	16.7	12.3	19.96	20.60	100	Clear	Clear	2
Epikote 828	Hythane 9	16.7	16.6	19.83	21.43	100	Clear	Clear	
Epikote 828	Plastokyd SC400	16.7	20.0	23.31	22.93	100	Clear	Clear	
Epikote 1007	Plastokyd SC7	8.8	20.0	6.39	23.48	52	Hazy	Cloudy	1
Epikote 1007	Neocryl B804	8.8	8.5	9.52	27.16	9	Hazy	Cloudy	2
Epikote 1001	Lumiflon LF200	10.9	8.5	11.96	27.78	25	V Large Lenses	Cloudy	4
Epikote 1007	Neocryl B700	8.8	7.3	9.27	30.53	<5	Large Lenses	Cloudy	3
Epikote 1007	Lumiflon LF200	8.8	8.5	8.45	34.29	14	Medium Lenses	Cloudy	4
Epikote 1007	Neocryl B813	8.8	7.3	8.78	34.62	17	Small Lenses	Cloudy	1
Epikote 1001	Hythane 9	10.9	16.6	16.91	35.80	42	Small Lenses	Cloudy	2
Epikote 828	Plastokyd SC140	16.7	20.0	19.29	37.01	100	Clear	Clear	0
Epikote 1007	Hypalon 20	8.8	11.3	11	37.59	<3	Medium Lenses	Cloudy	0
Epikote 828	Plastokyd AC4X	16.7	19.9	18.78	38.50	100	Clear	Clear	
Epikote 1001	Neocryl B804	10.9	8.5	10.36	39.50	28	Medium Lenses	Cloudy	2
Epikote 1001	Plastokyd SC400	10.9	20.0	19.86	40.68	>67	Hazy	Clear	1
Epikote 1001	Lumiflon LF916	10.9	8.8	10.08	40.88	35	Medium Lenses	Cloudy	4
Epikote 828	Hypalon 20	16.7	11.3	15.48	44.70	<3	Cloudy	Cloudy	
Epikote 1007	Lumiflon LF916	8.8	8.8	6.78	45.07	15	Large Lenses	Cloudy	4
Epikote 1007	Crodaplast AC500	8.8	12.3	10.88	47.61	20	Medium Lenses	Cloudy	4
Epikote 1001	Plastokyd SC140	10.9	20.0	18.41	50.23	38	Cloudy	Cloudy	0
Epikote 1001	Neocryl B700	10.9	7.3	9.26	53.24	30	Large Lenses	Cloudy	3
Epikote 828	Lumiflon LF916	16.7	8.8	14.5	58.36	64	Cloudy	Clear	0
Epikote 828	Plastokyd SC7	16.7	20.0	13.56	60.75	100	Clear	Clear	0
Epikote 828	Lumiflon LF200	16.7	8.5	14.26	61.53	>65	Cloudy	Cloudy	0
Epikote 828	Neocryl B728	16.7	4.8	9.51	63.68	100	Clear	Clear	0
Epikote 1001	Plastokyd AC4X	10.9	19.9	16.29	63.99	>67	Hazy	Clear	1
Epikote 828	Alkyd VAS 9223	16.7	19.9	12.7	63.99	78	Hazy	Clear	0
Epikote 1001	Neocryl B813	10.9	7.3	7.95	66.61	35	Hazy	Cloudy	1
Epikote 1001	Synolac 9090	10.9	10.7	4.85	68.74	>54	Cloudy	Clear	0
Epikote 1007	Neocryl B811	8.8	4.5	7.02	69.57	31	Cloudy	Cloudy	0
Epikote 1007	Alkyd VAS 9223	8.8	19.9	16.44	70.80	18	Small Lenses	Cloudy	3
Epikote 1001	Synolac 6016	10.9	10.8	4.21	72.25	100	Clear	Clear	1
Epikote 1007	Neocryl B728	8.8	4.8	6.37	76.91	30	Cloudy	Hazy	0
Epikote 1007	Hythane 9	8.8	16.6	12.03	78.13	20	Hazy	Cloudy	0
Epikote 1001	Neocryl B811	10.9	4.5	8.35	83.29	100	Clear	Clear	0
Epikote 828	Crodaplast AC550	16.7	12.9	7.99	83.98	100	Clear	Clear	0
Epikote 828	Neocryl B804	16.7	8.5	11.45	85.11	45	Cloudy	Clear	3
Epikote 1007	Plastokyd SC400	8.8	20.0	14.54	86.27	28	Hazy	Cloudy	0
Epikote 828	Synolac 6016	16.7	10.8	8.87	89.71	100	Clear	Clear	0
Epikote 1007	Plastokyd SC140	8.8	20.0	13.98	89.96	20	Small Lenses	Cloudy	0
Epikote 1007	Synolac 6016	8.8	10.8	3.94	90.18	34	Hazy	Clear	-1
Epikote 1001	Alkyd VAS 9223	10.9	19.9	11.68	92.58	41	V Large Lenses	Cloudy	3
Epikote 1007	Synolac 9090	8.8	10.7	3.4	93.23	37	Hazy	Cloudy	0
Epikote 828	Synolac 9090	16.7	10.7	7.96	94.85	100	Clear	Clear	0
Epikote 828	Neocryl B811	16.7	4.5	11.32	95.57	100	Clear	Clear	0
Epikote 828	Neocryl B700	16.7	7.3	10.69	96.47	65	Cloudy	Clear	1
Epikote 1001	Plastokyd SC7	10.9	20.0	10.65	97.22	>60	Hazy	Clear	0
Epikote 1001	Neocryl B728	10.9	4.8	6.77	97.71	100	Clear	Clear	0
Epikote 1001	Crodaplast AC550	10.9	12.9	2.73	98.42	50	Small Lenses	Clear	0
Epikote 828	Neocryl B813	16.7	7.3	8.8	99.02	100	Hazy	Clear	0
Epikote 1007	Crodaplast AC550	8.8	12.9	4.65	99.19	23	Medium Lenses	Cloudy	3
Epikote 1007	Plastokyd AC4X	8.8	19.9	10.99	99.98	24	Small Lenses	Cloudy	1

Legend

Stratification	0 - no Stratification; → 4 - Full Stratification
Solids	Percentage solids at point of phase separation
Solution Appearance	Appearance of solution of resins at a ratio of 1:1 on resin solids, total solids 50% in xylene, MiBK, methoxy propanol (30:50:20)

Table 30. Correlation of Solubility Sphere Overlap with other Parameters

Resin 1	Resin 2	R1	R2	D	B	Solids %	Film Appearance	Solution Appearance	Degree of Stratification
Epikote 1007	Neocryl B811	8.8	4.5	7.0	461.00	31	Cloudy	Cloudy	0
Epikote 1007	Neocryl B700	8.8	7.3	9.3	483.72	<5	Large Lenses	Cloudy	3
Epikote 1007	Neocryl B813	8.8	7.3	8.8	510.71	17	Small Lenses	Cloudy	1
Epikote 1007	Neocryl B728	8.8	4.8	6.4	520.85	30	Cloudy	Hazy	0
Epikote 1007	Neocryl B804	8.8	8.5	9.5	570.06	9	Hazy	Cloudy	2
Epikote 1007	Lumiflon LF200	8.8	8.5	8.5	642.25	14	Medium Lenses	Cloudy	4
Epikote 1001	Lumiflon LF200	10.9	8.5	12.0	668.65	25	V Large Lenses	Cloudy	4
Epikote 1001	Neocryl B811	10.9	4.5	8.4	695.37	100	Clear	Clear	0
Epikote 1001	Neocryl B700	10.9	7.3	9.3	761.78	30	Large Lenses	Cloudy	3
Epikote 1001	Neocryl B804	10.9	8.5	10.4	771.92	28	Medium Lenses	Cloudy	2
Epikote 1007	Hypalon 20	8.8	11.3	11.0	808.96	<3	Medium Lenses	Cloudy	0
Epikote 1001	Lumiflon LF916	10.9	8.8	10.1	821.34	35	Medium Lenses	Cloudy	4
Epikote 1001	Hypalon 20	10.9	11.3	13.9	824.49	<3	Clear	Cloudy	
Epikote 1001	Crodaplast AC500	10.9	12.3	15.9	832.45	48	Small Lenses	Hazy	3
Epikote 1007	Lumiflon LF916	8.8	8.8	6.8	842.05	15	Large Lenses	Cloudy	4
Epikote 1001	Neocryl B728	10.9	4.8	6.8	869.70	100	Clear	Clear	0
Epikote 1001	Neocryl B813	10.9	7.3	8.0	887.31	35	Hazy	Cloudy	1
Epikote 1007	Crodaplast AC500	8.8	12.3	10.9	978.80	20	Medium Lenses	Cloudy	4
Epikote 828	Crodaplast AC500	16.7	12.3	20.0	1367.93	100	Clear	Clear	2
Epikote 1001	Hythane 9	10.9	16.6	16.9	1453.90	42	Small Lenses	Cloudy	2
Epikote 828	Lumiflon LF916	16.7	8.8	14.5	1542.32	64	Cloudy	Clear	0
Epikote 828	Lumiflon LF200	16.7	8.5	14.3	1548.50	>65	Cloudy	Cloudy	0
Epikote 828	Hypalon 20	16.7	11.3	15.5	1650.72	<3	Cloudy	Cloudy	
Epikote 828	Neocryl B811	16.7	4.5	11.3	1757.14	100	Clear	Clear	0
Epikote 1007	Hythane 9	8.8	16.6	12.0	1830.03	20	Hazy	Cloudy	0
Epikote 828	Neocryl B804	16.7	8.5	11.5	1928.52	45	Cloudy	Clear	3
Epikote 828	Hythane 9	16.7	16.6	19.8	1950.07	100	Clear	Clear	
Epikote 1001	Plastokyd SC400	10.9	20.0	19.9	1960.47	>67	Hazy	Clear	1
Epikote 828	Neocryl B700	16.7	7.3	10.7	1977.42	65	Cloudy	Clear	1
Epikote 1007	Synolac 6016	8.8	10.8	3.9	2063.76	34	Hazy	Clear	-1
Epikote 828	Neocryl B728	16.7	4.8	9.5	2100.15	100	Clear	Clear	0
Epikote 1001	Plastokyd SC140	10.9	20.0	18.4	2114.88	38	Cloudy	Cloudy	0
Epikote 1001	Synolac 9090	10.9	10.7	4.9	2176.51	>54	Cloudy	Clear	0
Epikote 1007	Alkyd VAS 9223	8.8	19.9	16.4	2181.55	18	Small Lenses	Cloudy	3
Epikote 828	Plastokyd SC400	16.7	20.0	23.3	2274.54	100	Clear	Clear	
Epikote 1007	Synolac 9090	8.8	10.7	3.4	2348.82	37	Hazy	Cloudy	0
Epikote 1001	Plastokyd AC4X	10.9	19.9	16.3	2359.41	>67	Hazy	Clear	1
Epikote 828	Neocryl B813	16.7	7.3	8.8	2402.12	100	Hazy	Clear	0
Epikote 1007	Plastokyd SC400	8.8	20.0	14.5	2501.02	28	Hazy	Cloudy	0
Epikote 1001	Synolac 6016	10.9	10.8	4.2	2541.87	100	Clear	Clear	1
Epikote 1007	Crodaplast AC550	8.8	12.9	4.7	2547.65	23	Medium Lenses	Cloudy	3
Epikote 1007	Plastokyd SC140	8.8	20.0	14.0	2601.21	20	Small Lenses	Cloudy	0
Epikote 828	Plastokyd SC140	16.7	20.0	19.3	2748.55	100	Clear	Clear	0
Epikote 828	Synolac 6016	16.7	10.8	8.9	2794.34	100	Clear	Clear	0
Epikote 828	Plastokyd AC4X	16.7	19.9	18.8	2796.56	100	Clear	Clear	
Epikote 828	Synolac 9090	16.7	10.7	8.0	3095.55	100	Clear	Clear	0
Epikote 1007	Plastokyd AC4X	8.8	19.9	11.0	3263.40	24	Small Lenses	Cloudy	1
Epikote 1001	Alkyd VAS 9223	10.9	19.9	11.7	3290.65	41	V Large Lenses	Cloudy	3
Epikote 828	Crodaplast AC550	16.7	12.9	8.0	3567.11	100	Clear	Clear	0
Epikote 1001	Plastokyd SC7	10.9	20.0	10.7	3655.86	>60	Hazy	Clear	0
Epikote 828	Plastokyd SC7	16.7	20.0	13.6	3909.99	100	Clear	Clear	0
Epikote 828	Alkyd VAS 9223	16.7	19.9	12.7	4135.38	78	Hazy	Clear	0
Epikote 1001	Crodaplast AC550	10.9	12.9	2.7	5280.82	50	Small Lenses	Clear	0
Epikote 1007	Plastokyd SC7	8.8	20.0	6.4	5690.90	52	Hazy	Cloudy	1

Legend

Stratification	0 - no Stratification; → 4 - Full Stratification
Solids	Percentage solids at point of phase separation
Solution Appearance	Appearance of solution of resins at a ratio of 1:1 on resin solids, total solids 50% in xylene, MiBK, methoxy propanol (30:50:20)

Table 31. Correlation of Solubility Parameter Data with other Properties

4.4.3. Summary

This section has reviewed the possibility of using Hansen three dimensional solubility parameter data to predict stratification from pairs of commercial resins in common solvents or solvent blends.

Experimentally determined Hansen three - dimensional solubility parameter data for resins in the form of V (the volume of the overlap of the spheres assessed as a percentage of the volume of the smaller sphere) and B (a function of the radii of the spheres and the separation of the centres of the spheres) were correlated with experimental data obtained on the appearance of dry films, the appearance of a mixture of resins in a common solvent at a given concentration, the phase behaviour and stratification in unpigmented systems. Stratification was assessed from photo acoustic FTIR data.

The results show that some trends can be identified. However it does not appear possible to predict the behaviour of a pair of resins with accuracy from these data alone. Although these data show that 67% of stratifying systems are found in the groups V< 55% *or* B< 2000 these groups also contain a high number of non-stratifying systems.

Thus, it would appear that the information gained from Hansen three dimensional solubility parameters is of limited use in the quest of selecting suitable resins for stratifying coatings.

Hansen solubility parameters were primarily designed to predict resin solubility. The results have shown that this can generally be experimentally determined simply and used to predict resin solubility with some accuracy. However, it is also evident that solubility parameter data alone cannot adequately predict resin compatibility or stratification.

5. PIGMENTED SYSTEMS

5.1. Introduction

The results for unpigmented systems have shown that for solvent based systems containing an epoxy resin as one of the components, stratification is favoured by:-

1. Polar curing agents
2. Top coat resins with low surface energies
3. Epoxy : top coat resin ratios of 1:1 or 3:1
4. Dry film thicknesses of at least 100 microns.

Consequently studies of pigmented systems were carried out on systems fulfilling these requirements.

5.2. Characterisation of Materials

5.2.1. Pigments

A range of commercial pigments was selected that provided either the anti-corrosive properties required by a primer or the opacity and durability that would be required by a topcoat.

Zinc phosphate and red iron oxide pigments were selected as typical anti-corrosive pigments for a primer on a metallic substrate. Various grades of rutile titanium dioxide (Table 32) were selected to provide the opacity and durability that would be required from a topcoat. Most commercial grades of titanium dioxide have surface treatments added during manufacture. The grades used were selected by the manufacturers as being typical of grades used in solvent borne coatings whilst providing a range of inorganic and organic surface treatments.

Grade	%TiO_2	Inorganic Coating	Organic Coating	Surface Area m^2/g	Crystal Size μm	Relative Density
R-SM2	98.5	None	None	7	0.21	4.20
R-FC5	98.0	Alumina	Siloxane	7	0.18	4.05
R-TC4	90.0	Alumina / Silica	Present	17	0.23	3.95
R-TC90	94.0	Alumina	Present	15	0.22	4.05

Table 32. Titanium Dioxide Grades

5.3. Detection of Stratification

5.3.1. FTIR

Pigmented films were analysed using FTIR-PAS analysis in a similar manner to unpigmented films. A similar ranking system was used:-

Rank	Description
0	**No Stratification**
2	**Partial Stratification** (increased concentration of resin 2 at air interface)
3	**Good Stratification** (high concentration of resin 2 at air interface)
4	**Full Stratification** (only resin 2 at air interface)

All pigmented systems were cured, so Rank 1, which was used where both sides of the film were measured for unpigmented systems was not used for pigmented systems.

5.3.2. SEM-EDS

This technique was used to study the distribution of pigments in pigmented systems where the inorganic pigments could be easily detected by EDS. For cross-section studies of pigmented systems a ranking system was devised from the "elemental map" produced for a particular element:-

Rank	Description
*	Pigment(s) located through whole film
**	Some evidence of pigment separation
***	Pigment(s) remain totally in one resin

5.3.3. Optical Microscopy

Optical microscopy was used in conjunction with SEM-EDS and FTIR to view cross-sections of pigmented films.

5.4. Systems containing One Pigment

5.4.1. Pigmenting Primer Resins

Systems were initially studied that contained a protective pigment in the primer layer and a clear topcoat layer. This type of coating where one layer (usually the lower layer) is pigmented and the other clear are encountered industrially especially in automotive applications in what are often termed "base coat / clear coat" systems.

Studies concentrated on pigmentation of only the Epikote resin with either the protective pigments zinc phosphate (Delaphos 2M) or red iron oxide (Bayer 130B). Systems were chosen that had shown promise as unpigmented systems. Jeffamine D230 was used as a cross-linking agent for the epoxy resin since this curing agent was seen to improve stratification compared to systems without Jeffamine D230 in the corresponding unpigmented systems.

Epikote 1001 / Neocryl B700 / Jeffamine D230 systems were studied initially. The zinc phosphate was dispersed into the Epikote layer by ball milling prior to mixing with both resin 2 and curing agent. These results showed that similar results could be obtained using pigment volume concentrations (PVC's) of 10, 20 and 30% (based on the mass of Epikote resin solids). A PVC of 30% was used for further studies. The iron oxide was used at 10% PVC based on the Epikote resin.

Pigmentation of the epoxy resins with either of the protective pigments generally produced films showing similar trends to those exhibited by the appropriate unpigmented systems (Table 33). The most promising systems were found to be those containing Epikote 1001 with either Lumiflon LF200 or Neocryl B700 where the pigment was clearly located in the epoxy layer.

Resin 1	Resin 2	Pigment 1	IR	SEM
Epikote 828	Lumiflon LF200	Zinc Phosphate	0	*
Epikote 1001	Lumiflon LF200	Zinc Phosphate	4	***
Epikote 828	Neocryl B700	Zinc Phosphate	0	*
Epikote 1001	Neocryl B700	Zinc Phosphate	3	***
Epikote 1001	Neocryl B700	Iron Oxide	2	***
Epikote 828	Neocryl B813	Zinc Phosphate	0	*
Epikote 1001	Neocryl B813	Zinc Phosphate	0	*

Table 33. Results from Pigmented Systems

Figure 19 shows an electron micrograph showing an Epikote 1001 / Lumiflon LF200 resin combination pigmented with zinc phosphate. The zinc phosphate can be seen in the epoxy layer at the substrate, the separation of the resins is seen in the FTIR-PAS spectrum of the top surface of this coating shown in Figure 21.

Figure 20 shows a photograph taken using an optical microscope showing an Epikote 1001 / Neocryl B700 / red iron oxide coating. The iron oxide is clearly seen in the epoxy layer at the substrate. Figure 22 shows the FTIR-PAS spectrum of the top surface of this combination clearly showing the separation of the resins.

It was generally found that systems containing one pigment in the epoxy resin showed the same trends as the equivalent unpigmented system - those systems which had stratified when unpigmented continued to do so when one pigment was added to the epoxy resin. Those systems which had not stratified as unpigmented systems showed similar results when pigmented.

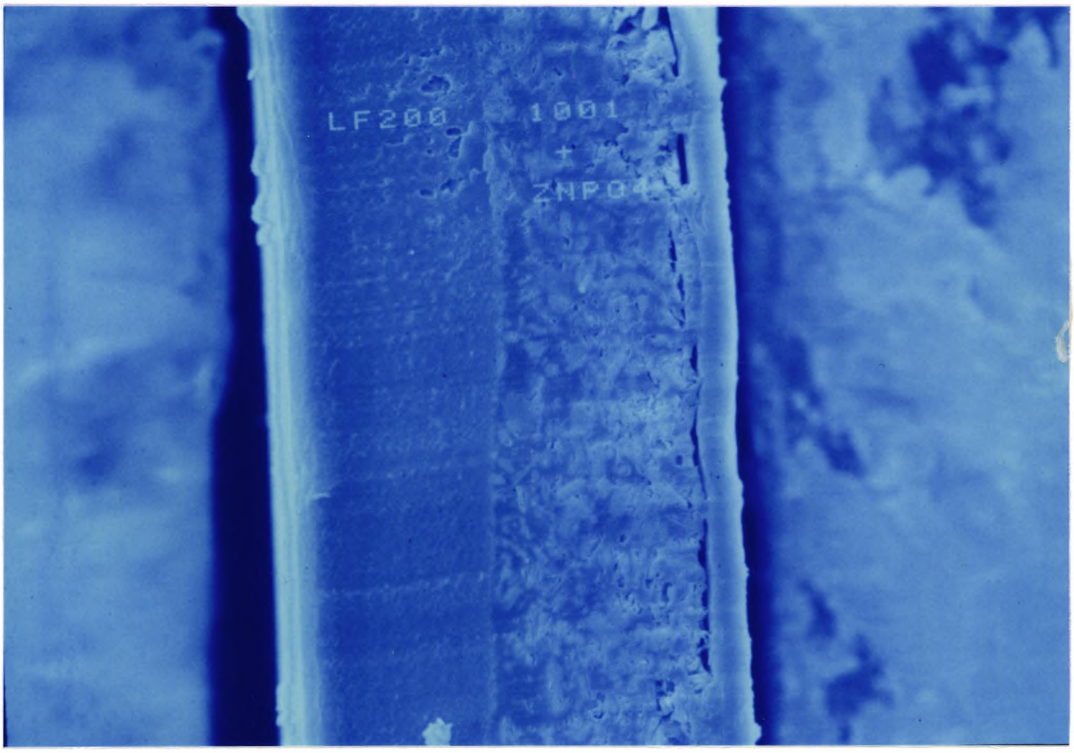

Figure 19 - Epikote 1001 / Lumiflon LF200 / Zinc Phosphate Coating

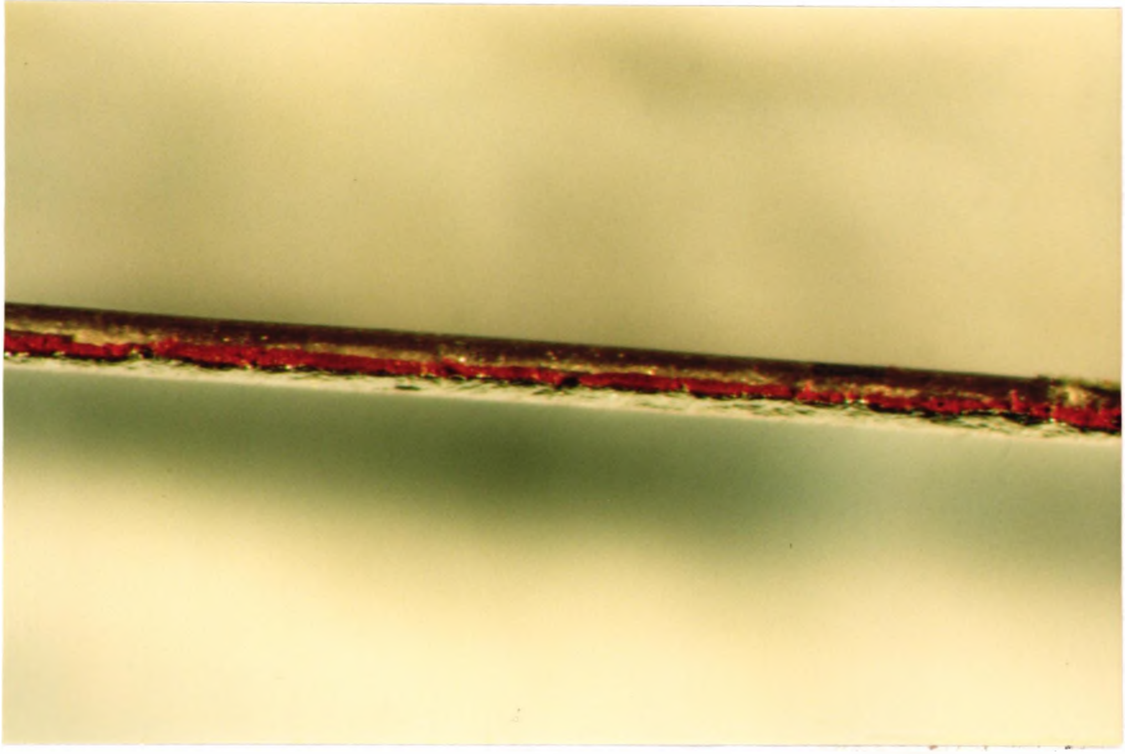

Figure 20 - Epikote 1001 / Neocryl B700 / Red Iron Oxide Coating

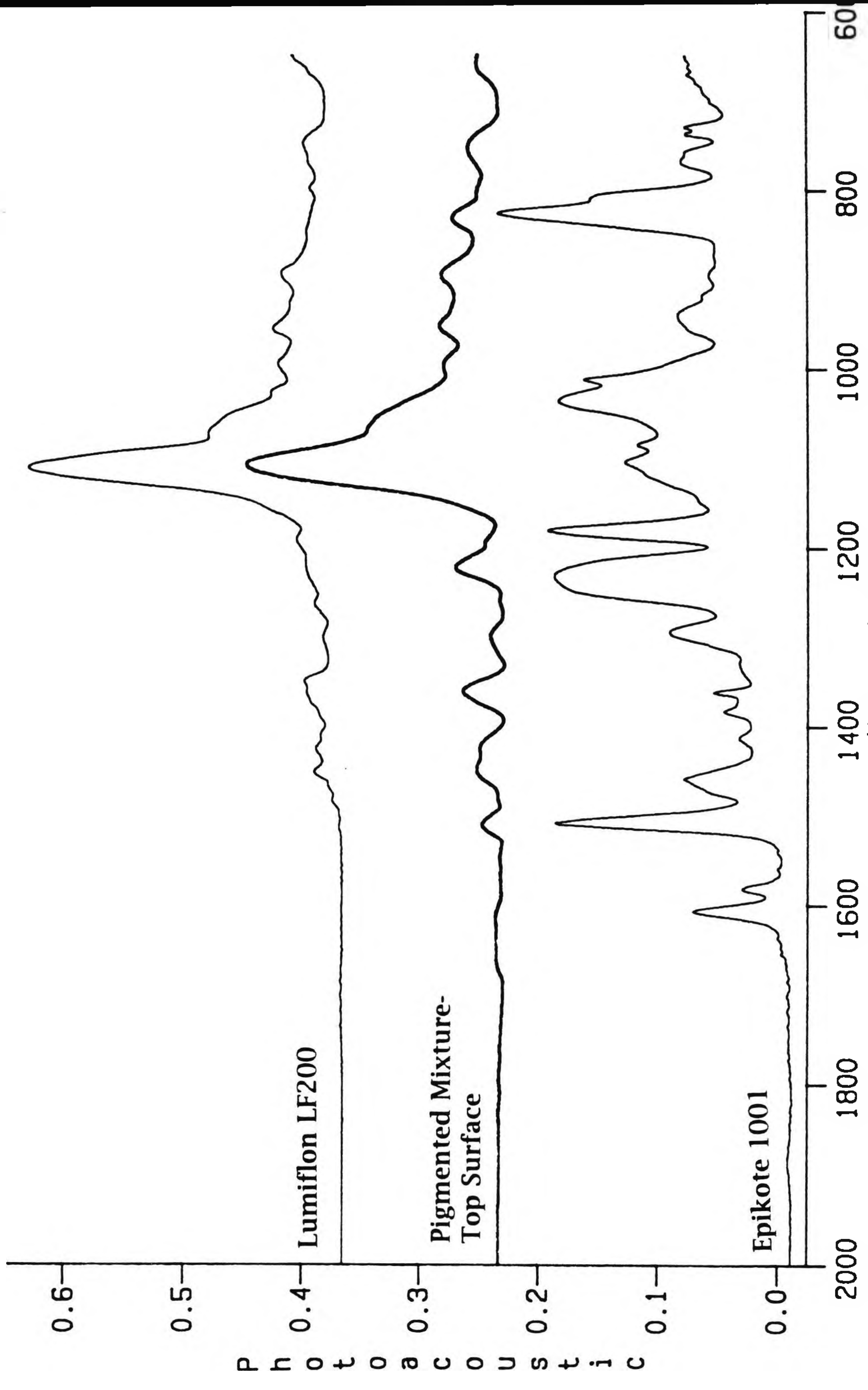

Figure 21. FTIR-PAS Spectrum
Epikote 1001 / Lumiflon LF200 / Zinc Phosphate Coating

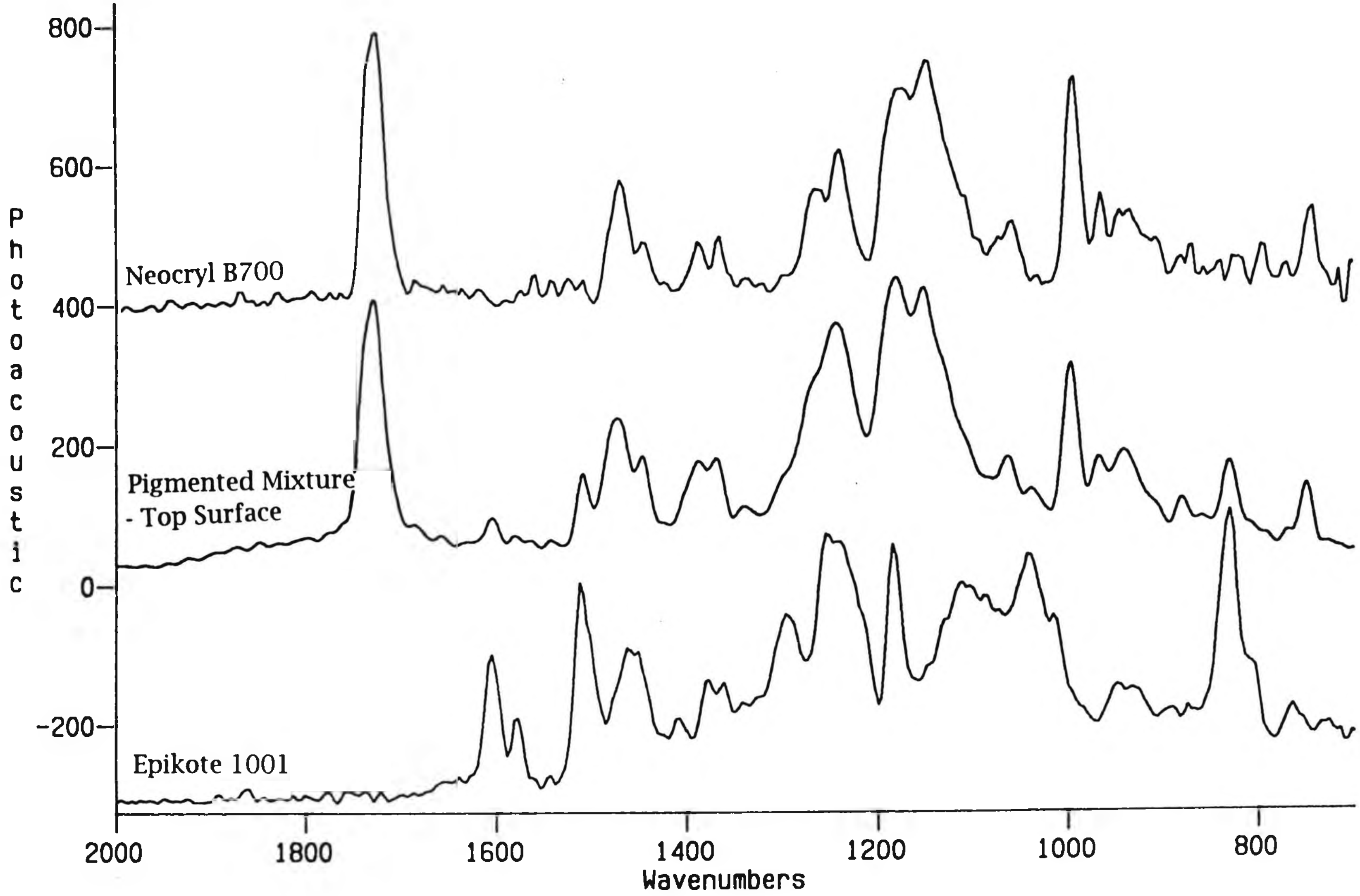

Figure 22. FTIR-PAS Spectrum
Epikote 1001 / Neocryl B700 / Iron Oxide Coating

5.4.2. Pigmenting Topcoat Resins

Some experiments were carried out pigmenting only the topcoat resin. Although such systems would not generally be acceptable industrially information might be gained on the mechanism of pigment distribution in stratifying films.

Zinc phosphate was dispersed at 5% and 30% PVC in either Neocryl B700 or Lumiflon LF200 prior to mixing with Epikote 1001 and Jeffamine D230. After stoving the zinc phosphate was always located in the Epikote layer indicating that this pigment has a strong affinity for the highly polar epoxy resin (Table 34).

Resin 1	Resin 2	Pigment 2	IR	SEM
Epikote 1001	Neocryl B700	5% Zinc Phosphate	4	***
Epikote 1001	Neocryl B700	30% Zinc Phosphate	4	***

Table 34. Location of Pigment Dispersed in resin 2

Similar work was carried out pigmenting the topcoat resin with titanium dioxide. It was generally found that the pigment was found to be located through the whole film, in some cases it appeared that resin stratification was also impaired (Table 35).

Resin 1	Resin 2	Pigment	IR	SEM
Epikote 828	Neocryl B700	TiO_2 (R-TC4)	2	*
Epikote 828	Neocryl B700	TiO_2 (R-FC5)	2	*
Epikote 1001	Neocryl B700	TiO_2 (R-TC4)	5	*
Epikote 1001	Neocryl B700	TiO_2 (R-FC5)	2	*

Table 35.

It would appear that titanium dioxide pigments do not have the same affinity for the epoxy resin that was exhibited by iron oxide and zinc phosphate. In addition titanium dioxide pigments do not show any affinity for the topcoat resin.

Studies were carried out to determine whether gravity or pigment density are driving forces in determining the final location of the pigment. This was studied primarily by inverting films after application to observe whether the pigment was found to be located in the lower topcoat layer in which it was milled or the upper epoxy layer. Location of the pigment in the epoxy layer would tend to indicate that the pigment had an affinity for this resin.

Systems were prepared with zinc phosphate dispersed into the topcoat resin prior to mixing with the epoxy resin. Systems were also prepared with the zinc phosphate dispersed into the epoxy resin, then mixed with the topcoat resin and curing agent. After application of the film to an aluminium foil substrate it was immediately turned upside down to dry. After staying inverted for 24 hours the films were stoved.

In all these cases the zinc phosphate was found in the epoxy layer which would suggest that pigment density or gravity are not the driving forces for this process but that the pigment has a definite affinity for the epoxy resin (Table 36).

Resin 1	Resin 2	Pigment	IR	SEM
Epikote 1001	Neocryl B700	5% Zinc Phosphate	4	***
Epikote 1001	Neocryl B700	30% Zinc Phosphate	4	***

Table 36. Effect of Gravity and Pigment Density

Further experiments involved dispersing the pigment (either $ZnPO_4$ or Fe_2O_3) in a mixture of Epikote 1001 and Neocryl B700 prior to addition of Jeffamine D230. In both cases good stratification of the resins was observed and the pigment located almost exclusively in the epoxy layer (Table 37) which supports the preceding results that suggest that it is not gravity or pigment density that decide the final location of the pigment. It would appear that there is a definite affinity between the protective pigments and the polar epoxy resin.

Resin 1	**Resin 2**	**Pigment**	**IR**	**SEM**
Epikote 1001	Neocryl B700	Iron Oxide	3	***
Epikote 1001	Neocryl B700	Zinc Phosphate	3	***

Table 37. Affinity of protective pigments for epoxy resins

5.4.3. Additives

5.4.3.1. Anti-Terra-U

Wetting and dispersion additives are often added to paints to improve the dispersion and stabilisation of the pigment. Absence of dispersing agents can lead to paint defects such as sedimentation and flocculation. An important part of this study was therefore the effect of paint additives on the stratification process. Addition of 1% dispersing agent on weight of pigment is generally considered to give at least monolayer coverage.

The addition of a typical dispersing agent, Anti-Terra-U, 1% on weight of pigment, to the pigment dispersions was not found to impair stratification (Table 38). However, pigment dispersion did not appear to improve significantly and thus Anti-Terra U was not included in subsequent systems.

Resin 2	Pigment 2	Resin 1	IR	SEM
Lumiflon LF200	Zinc Phosphate / A-T	Epikote 828	0	*
Lumiflon LF200	Zinc Phosphate / A-T	Epikote 1001	4	**
Lumiflon LF200	Zinc Phosphate	Epikote 1001	4	***
Neocryl B700	Zinc Phosphate / A-T	Epikote 828	0	*
Neocryl B700	Zinc Phosphate / A-T	Epikote 1001	2	***
Neocryl B700	Zinc Phosphate	Epikote 1001	3	***
Neocryl B700	Zinc Phosphate / A-T	Epikote 1007	4	***

Table 38. Effect of Pigment Dispersing Agent (1% Anti-Terra-U) on Stratification

5.4.3.2. PiBMA

The use of a co-resin as a thickening aid was explored since one phase systems were generally found to have low viscosities. PiBMA (Neocryl B700) was added as a co-resin to Epikote / Lumiflon systems at levels of 5% and 20%. The PiBMA was added to thicken the Epikote resin during the milling stage with zinc phosphate.

At 5% the thickening effect of the PiBMA was not sufficient to produce a marked increase in viscosity. At 20% the viscosity had improved but stratification had deteriorated significantly (Table 39). This is presumably because Epikote / PiBMA systems were not observed to stratify experimentally.

Resin 2	Resin 1	Pigment 1	IR
Lumiflon LF200	Epikote 903	Zinc Phosphate	4
Lumiflon LF200	Epikote 903 + 5% B700	Zinc Phosphate	3
Lumiflon LF200	Epikote 903 + 20% B700	Zinc Phosphate	2

Table 39. Effect of Thickener on Stratification

5.5. Systems containing Two Pigments

These studies aimed to introduce a pigment into the topcoat resin at the air interface as well as the protective pigment in the primer layer. This would provide the desired degree of opacity and durability to the top coat.

The Epikote resin (Epikote 1001) was pigmented with either iron oxide or zinc phosphate. The TiO_2 (TiO_2 grade R-TC4 or R-FC5) was dispersed into the second resin (either Lumiflon LF200 or Neocryl B700) at 15% PVC prior to mixing with pigmented Epikote and the addition of Jeffamine D-230. Systems were applied to aluminium foil and stoved.

It was generally found that the addition of TiO_2 to systems which had previously shown good stratification with a single pigment had a severely detrimental effect on the films, with little or no stratification of the pigments recorded by SEM (Table 40). In most cases the IR results show that some stratification of the resins was still occurring.

Resin 1	Pigment	Resin 2	Pigment	IR	SEM
Epikote 828	Zinc Phosphate	Neocryl B700	TiO_2 (R-TC4)	0	*
Epikote 828	Zinc Phosphate	Neocryl B700	TiO_2 (R-FC5)	0	*
Epikote 1001	Zinc Phosphate	Neocryl B700	TiO_2 (R-TC4)	2	**
Epikote 1001	Zinc Phosphate	Neocryl B700	TiO_2 (R-FC5)	2	**
Epikote 1007	Zinc Phosphate	Neocryl B700	TiO_2 (R-TC4)	4	**
Epikote 1007	Zinc Phosphate	Neocryl B700	TiO_2 (R-FC5)	2	**
Epikote 828	Zinc Phosphate	Neocryl B813	TiO_2 (R-TC4)	0	*
Epikote 828	Zinc Phosphate	Neocryl B813	TiO_2 (R-FC5)	0	*
Epikote 1001	Zinc Phosphate	Neocryl B813	TiO_2 (R-TC4)	0	*
Epikote 1001	Zinc Phosphate	Neocryl B813	TiO_2 (R-FC5)	0	*
Epikote 1007	Zinc Phosphate	Neocryl B813	TiO_2 (R-TC4)	3	*
Epikote 1007	Zinc Phosphate	Neocryl B813	TiO_2 (R-FC5)	3	*

Table 40. Systems pigmented with two Pigments

5.5.1. Silane Adhesion Promoters

It had been suggested[93] that the use of silane adhesion promoters might be an aid to locating TiO_2 in resin 2. Materials of this nature are often employed as adhesion promoters since they have the ability to bond two dissimilar material together - in this case an inorganic material (TiO_2) and the organic resin (Figure 23). An uncoated grade of titanium dioxide (Tioxide R-SM2) was used for this study to ensure that any effect was due to the coupling agent and not to the coating on the pigment. Prior to coating with adhesion promoter the titanium dioxide pigment was used in formulations to ensure that the uncoated pigment alone would not improve pigment separation (Table 41).

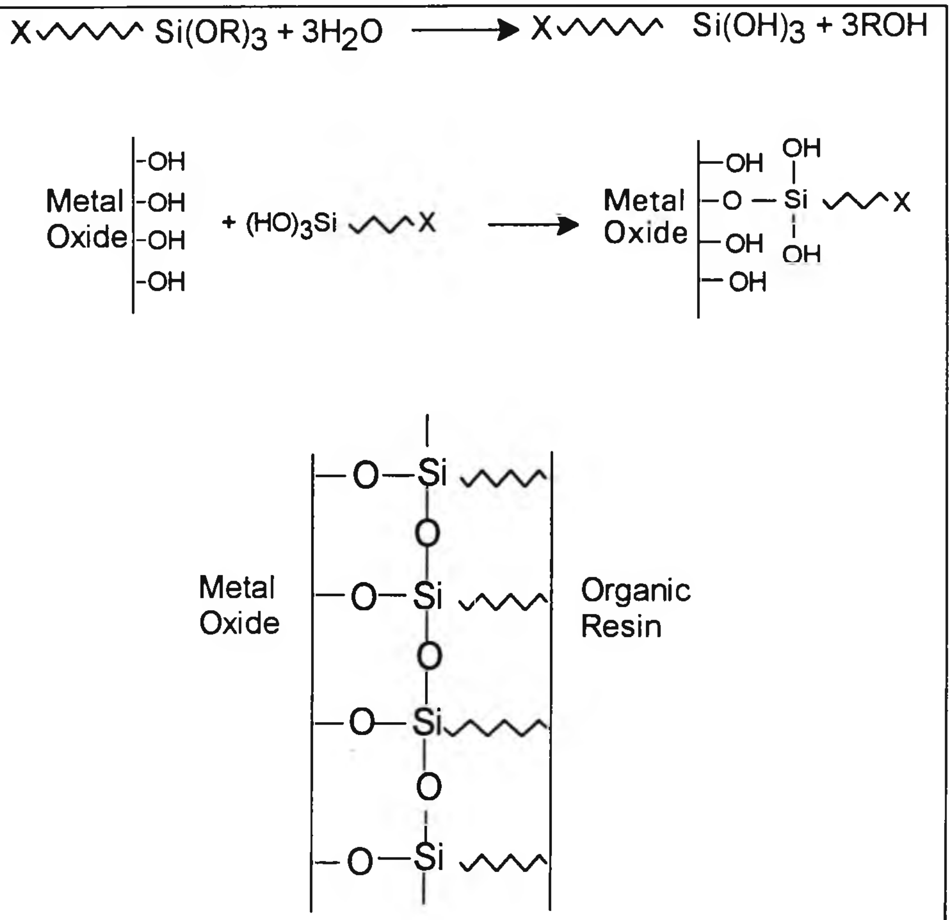

In this case:-
$X = NH_2$
$R = C_2H_5$

Figure 23. Simplified Depiction of Bonding Through a Silane Coupling Agent

Resin 2	Pigment 2	Resin 1	Pigment 1	IR	SEM
Lumiflon LF200	-	Epikote 828	R-SM2	1	*
Lumiflon LF200	-	Epikote 903	R-SM2	2	**
Lumiflon LF200	-	Epikote 1001	R-SM2	3	**
Neocryl B700	-	Epikote 828	R-SM2	1	*
Neocryl B700	-	Epikote 903	R-SM2	2	*
Neocryl B700	-	Epikote 1001	R-SM2	3	*
Lumiflon LF200	R-SM2	Epikote 828	-	0	*
Lumiflon LF200	R-SM2	Epikote 903	-	1	*
Lumiflon LF200	R-SM2	Epikote 1001	-	2	*
Neocryl B700	R-SM2	Epikote 828	-	1	*
Neocryl B700	R-SM2	Epikote 903	-	3	*
Neocryl B700	R-SM2	Epikote 1001	-	2	*

Table 41. Use of Uncoated Titanium Dioxide R-SM2

Table 41 shows that the uncoated TiO_2 grade R-SM2 was located across the whole of the dried film.

The surface of the R-SM2 grade TiO_2 was initially coated with the adhesion promoter amino propyl triethoxy silane (AMEO) (Figure 23) at a level of 13% (on weight of pigment), by stirring the pigment / silane mixture in technical grade MEK and then drying and grinding in a pestle and mortar prior to incorporating into formulations. Technical grade MEK was used as some water is required for the stepwise hydrolysis of the silane. Figure 23 shows the reaction of the silane with the pigment surface.

It was found that in some cases the coated pigment could be successfully located in the topcoat resin (Table 42). Systems containing iron oxide dispersed in Epikote 1001 and TiO_2 coated with AMEO dispersed in Lumiflon LF200 were the most successful. Figures 24 and 25 show cross sections of systems containing Epikote 828 and 1001 with Lumiflon LF200 photographed using an optical microscope.

Resin 2	Pigment 2	Resin 1	IR	SEM
Lumiflon LF200	TiO_2 coated with AMEO	Epikote 828	1	**
Lumiflon LF200	TiO_2 coated with AMEO	Epikote 903	4	***
Lumiflon LF200	TiO_2 coated with AMEO	Epikote 1001	4	***
Neocryl B700	TiO_2 coated with AMEO	Epikote 828	1	*
Neocryl B700	TiO_2 coated with AMEO	Epikote 903	3	*
Neocryl B700	TiO_2 coated with AMEO	Epikote 1001	3	**

Table 42. Addition of AMEO coated R-SM2 to Resin 2

It is suggested that the since both chlorinated rubber and Lumiflon are chlorine containing resins the AMEO may be reacting with the C-Cl bonds. This idea was reinforced by attempts to locate the AMEO coated pigment in PiBMA (Neocryl B700) which were unsuccessful - in all cases TiO_2 was spread through the whole film.

However, attempts to locate pigment coated with iso butyl triethoxy silane (IBTEO) or coated with less than 13% AMEO, or coated with 13% AMEO and subsequently washed were not successful (Table 43).

Epoxy Resin	Topcoat Resin	TiO_2 Coating	IR	SEM
Epikote 828	Lumiflon LF200	IBTEO	0	*
Epikote 903	Lumiflon LF200	IBTEO	4	*
Epikote 1001	Lumiflon LF200	IBTEO	4	*
Epikote 828	Neocryl B700	IBTEO	0	*
Epikote 903	Neocryl B700	IBTEO	3	(**)
Epikote 1001	Neocryl B700	IBTEO	3	(***)

Figures in parentheses indicate that the pigment was located in the epoxy resin.

Table 43. Addition of IBTEO Coated TiO_2 to Topcoat Resins

Figure 24 - Epikote 828 / Iron Oxide / Lumiflon LF200 / AMEO coated TiO_2

Figure 25 - Epikote 1001 / Iron Oxide / Lumiflon LF200 / AMEO coated TiO_2

5.6. Physical Testing

Although the development of commercial stratifying systems was outside the scope of this study it was considered feasible to undertake a series of standard paint tests on a selection of pigmented laboratory formulations to compare their performance with systems applied conventionally as two separate coats. The same resin pairs were used for both the stratifying and the conventionally applied coatings. The most promising stratifying systems were selected for testing.

The systems tested were Epikote 1001/Lumiflon LF200 and Epikote 1001/Neocryl B700. In each case the Epikote was pigmented with zinc phosphate (Delaphos 2M) and resin 2 pigmented with titanium dioxide according to the following scheme:-

(i)	Epikote 1001	40.0g	PVC~20%
	XDM*	40.0g	
	Zinc Phosphate	27.4g	
	Jeffamine D230	4.8g	
(ii)	Neocryl B700	25.0g	PVC~10%
	XDM*	37.5g	
	TiO_2 (Tioxide R-FC5)	11.4g	

(iii)	Lumiflon LF200	60.0g	PVC~10%
	XDM*	16.8g	
	Cymel 303	1.1g	
	TiO_2 (Tioxide R-SM2/13% AMEO)	17.5g	

* XDM refers to a solvent mixture containing 50% MiBK, 30% xylene and 20% Dowanol PM (methoxy propanol).

Each resin / pigment mixture was dispersed using a ball-mill for 24 hours. The Epikote dispersion was then mixed with each resin 2 dispersion using a 1:1 ratio on resin solids and the curing agent added. The mixture was then ball-milled for a further 1 hour prior to application.

Each Epikote / resin 2 system was applied to the substrate both as two separate coats and as a stratifying film. In each case approximately 100μm total dry film thicknesses were used. The substrates used for the tests were steel and aluminium panels as appropriate to the test.

Stoving times and temperatures were 24 hours at room temperature followed by 110°C for 1 hour for Epikote/Neocryl systems and 140°C for 1 hour for Epikote / Lumiflon systems. In the case of the coatings applied as separate layers the Epikote layer was stoved as above before addition of resin 2.

The following physical tests were carried out on the panels:-

5.6.1. Gloss

Gloss measurements were made at an angle of 60° according to BS 3900 : Part D5[85], using a Rhopoint gloss meter calibrated using Rhopoint standards and are the average of six readings.

5.6.2. Pencil Hardness

Pencil hardness was carried out according to ASTM D3363[86].

5.6.3. Pendulum Damping

Measurements were carried out using the König pendulum, which would give a 6° to 3° damping time of 250 ± 10 seconds on a polished glass panel according to BS 3900 Part E5[87].

5.6.4. Cross Cut Adhesion

Eight parallel cuts 2 mm apart were made in each direction. The rating for film adhesion is described below according to the pictorial representations in BS 3900 : Part E6[88].

Classification	Description
0	Edges of cuts completely smooth; no lattice squares detached
1	Detachment of small flakes at intersections of cuts. A cross-cut area no greater than 5% is affected.
2	Flaking along edges and/or intersections of cuts. A cross-cut area between 5% and 15% is affected.
3	Flaking in ribbons along edges of cuts and/or flaking within squares. A cross- cut area between 15% and 35% is affected.
4	Flaking along edges of cuts and some detachment of squares. A cross-cut area between 15% and 35% is affected.
5	Flaking greater than 65% of cross-cut area.

5.6.5. Bend Test (Conical Mandrel)

The test panel and coating were bent using a conical mandrel test apparatus. The coating was then examined for the extent of cracking from the small end of the mandrel according to BS 3900 : Part E11[89].

All plates were observed to crack along the entire length of the film. The length therefore refers to the length of the paint film.

5.6.6. Resistance to Liquids

This test was carried out according to BS3900 : Part G5 (ISO 2812)[90] using method 3. A drop of the test solvent was spotted onto the panel and left for 10 minutes. After this time the solvent was rinsed off and the degree of deterioration noted according to the following scheme:-

Classification	Description
*	Coating unmarked by solvent
**	Slight erosion of coating
***	Moderate erosion of coating
****	Severe erosion of coating
*****	Coating completely destroyed by solvent

5.6.7. Artificial Weathering (QUV)

Panels were subjected to continuous 4 hourly UV/ condensation cycles using a Q-Panel Company QUV Accelerated Weathering Tester and UVA lamps (315-400 nm). The panels were examined at regular intervals for signs of deterioration.

The panels were exposed for 2594 hours (108 days).

5.6.8. Artificial Weathering (Marr)

Panels were weathered in a Marr Enclosed Carbon Arc Weatherometer according to BS 3900 : Part F3[91]. The panels were subjected to water atomisation and a drying fan in cycles whilst exposed to UV light produced by a carbon arc. The panels were examined at regular intervals for signs of deterioration.

The panels were exposed for a total of 1750 hours (73 days).

System	**Epikote 1001 Neocryl B700**	**Epikote 1001 Neocryl B700**	**Epikote 1001 Lumiflon LF200**	**Epikote 1001 Lumiflon LF200**
Type	Two Coats	Stratifying	Two Coats	Stratifying
Gloss / units	73.4	37.1	73.8	58.3
Pencil Hardness	H/2H	4H/5H	2H/3H	H/2H
Pendulum Damping/s	168	122	157	140
Cross-Cut Adhesion	0	2	1	2
Mandrel Bend	127 mm (flaky)	129 mm (flaky)	129 mm (fine cracks)	138 mm (fine cracks)
Resistance to Liquids				
Toluene	****	**	***	**
MEK	***	**	***	***
Acetone	***	**	***	**
Methylene Chloride	***	**	***	**
Methanol	*	*	*	*
Butyl Acetate	***	**	***	**
Ethylene Glycol	***	***	*****	*****
Xylene	****	***	****	****
Weathering (QUV)				
420 hours		Some Yellowing		Some Yellowing
526 hours	Slight Marking			
752 hours			Slight Marking	
876 hours				
2594 hours	Loss of Gloss	Loss of Gloss		Some Yellowing
Weathering (Marr)				
836 hours	No Damage	No Damage	No Damage	No Damage
1750 hours	Loss of Gloss	Loss of Gloss	Loss of Gloss	Loss of Gloss

Table 44. Physical Testing Results

The results in this section have shown that the stratifying systems are comparable to their two-coat counterparts when subjected to a series of standard paint tests. The stratifying systems generally exhibited lower gloss and poorer cross-cut adhesion but were comparable in all other areas. The solvent resistance of the stratifying systems appeared slightly better than those applied as two separate coats.

5.7. Conclusions

This work has shown the feasibility of adding pigments to resin combinations that were experimentally observed to stratify when unpigmented. The most successful systems were those to which a protective pigment was added to the primer resin located at the substrate interface. Such systems could be usefully employed industrially in pigmented base coat / clear topcoat type applications.

Addition of a second pigment to improve durability proved more difficult, in some cases resins still exhibited stratification while the pigments were spread through both layers. Some success was achieved using a silane coated titanium dioxide pigment which could be located in the Lumiflon resin. However, this was an isolated case.

The coatings produced were found to perform at least as well as their two-coat counterparts when subjected to standard paint testing methods.

6. CONCLUSIONS

This work has clearly shown the feasibility of producing unpigmented systems that spontaneously stratify when applied to a metallic substrate.

Stratification of such systems requires that pairs of commercial resins must be soluble in common solvents or solvent blends, but, after application must phase separate, followed by layer formation.

It has been shown that the information gained from Hansen three dimensional solubility parameters is of limited use in the quest of selecting suitable resins for stratifying coatings. Hansen solubility parameters were primarily designed to predict resin solubility. It has been shown that this can generally be predicted simply and with some accuracy. However, it is also evident that solubility parameter data alone cannot adequately predict resin compatibility as an aid to the prediction of stratification.

The phase behaviour of resin pairs in common solvents can be experimentally determined and usefully expressed using phase diagrams.

It has been shown that in some cases the tendency of a system to stratify can be predicted from the surface energies of the solid resins. However, this has been found to be unreliable. This is because it is the solution surface energies of the separating phases rather than the solid surface energies that must be considered. Where solution surface energy data are available, reliable predictions concerning stratification can be made. However, the build up of the viscosity of the system has been seen to have an important impact on the reliability of these predictions.

The practical systems which most favoured stratification were epoxy / acrylic and epoxy / fluorinated polyether systems with the epoxy component of either cured with a proprietary polyoxypropyleneamine curing agent. Such systems offer a degree of incompatibility as well as their solutions having suitable surface energy differences. The most favourable conditions were found to be a resin ratio of 1:1 and a dry film thickness of at least 100 microns.

Extension of this work to systems containing a protective pigment in the layer at the substrate interface has also been successful. Pigments were added to resin combinations that were experimentally observed to stratify when unpigmented. The most successful systems were those to which a protective pigment was added to the primer resin located at the substrate interface. Such systems could be usefully employed industrially in pigmented base coat / clear topcoat type applications.

Addition of a second pigment to improve durability proved more difficult, in some cases resins still exhibited stratification while the pigments were spread through both layers. Some success was achieved using a silane coated titanium dioxide pigment which could be located in the Lumiflon resin. However, this was an isolated case.

The coatings produced were found to perform at least as well as their two-coat counterparts when subjected to standard paint testing methods.

Following the establishment of guidelines for self-stratification from solvent borne liquid systems it is envisaged that the technology of self stratification may be transferred to other areas. Multi-functional films from a single application have obvious benefits in many surface coatings systems as well as other related areas. For example, adhesives, where two dissimilar materials are to be bonded together could greatly benefit from the advantages of self-stratification. Similarly, printing inks where different interfaces are required to have different characteristics could benefit from this approach.

7. REFERENCES

1 Boxall, J., *Paint Manuf., 1978,* ***48,*** *(3), 18*

2 Lambourne, R., *'Paint and Surface Coatings - Theory and Practise'*, 1987, (Chichester: Ellis Horwood Ltd)

3 Morgans, W.M., *'Outlines of Paint Technology'*, Third Edition, 1990 (London : Edward Arnold)

4 Oil and Colour Chemists' Association, Australia, *'Surface Coatings'* - Volume 1, Second Edition, 1983, (London : Chapman & Hall)

5 Boxall, J., *Paint Manuf., 1978,* ***48,*** *(5) 23*

6 Armitage, F., *'The British Paint Industry'*, 1967 (London : Pergamon)

7 Turner, G.P.A., *'Introduction to Paint Chemistry and Principles of Paint Technology'*, Third Edition, 1988, (London : Chapman & Hall)

8 Nylen, P. and Sunderland, E., *'Modern Surface Coatings'*, 1965, (London : John Wiley)

9 Oil and Colour Chemists' Association, Australia, *'Surface Coatings'* - Volume 2, Second Edition, 1984, (London : Chapman & Hall)

10 Steel Structures Painting Council, *'Painting Manual'*, Volume 2, 1991 (USA : SSPC)

11 Meeus, F., *J. Oil Colour Chem. Assoc.*, 1990, **5**, 186

12 Oil and Colour Chemists' Association, *'Introduction to Paint Technology'*, Fourth Edition, 1976, (Middlesex : Oil and Colour Chemists' Association)

13 Harrison, J.B., *Corros. Coatings S. Afr., 1975,* ***2****, (6), 11*

14 Harrison, J.B., *Corros. Coatings S. Afr., 1976,* ***3****, (1), 11*

15 Harrison, J.B., *Corros. Coatings S. Afr., 1981,* ***8****, (4), 27*

16 Funke, W., *J. Oil Colour Chem. Assoc.*, 1976, **59**, 398

17 Verkholantsev, V. V., *Prog. Org. Coat.*, 1985, **13**, 71

18 Murase, H., and Funke, W., *XVth FATIPEC Congress, Amsterdam*, 1980, **2**, 387

19 UK Patent 1570 540 to Kansai Paint Co. Ltd., 1980

20 UK Patent 2046 765 A to Kansai Paint Co. Ltd., 1980

21 Funke, W., *Prog. Org. Coat.*, 1974, **2**, 289

22 Grozinskaya, Z. P., Streckachinskaya., L. S. and Verkholantsev, V. V., *Lakokras. Mater. ikh Prime.,* 1979, **5**, 30
Translated by Helma Jotischky

23 Verkholantsev, V. V., *Prog. Org. Coat.*, 1990, **18**, 43

24 Verkholantsev, V. V., *J. Coat. Tech.*, 1992, **64**, 51

25 UK Patent 2 046 765 A to Kansai Paint Company Ltd., 1980

26 Van Krevelen, D. W., '*Properties of Polymers*', 1990, (Oxford : Elsevier)

27 Seymour, R. B., *Popular Plastics*, 1984, **29**, 25

28 Hildebrand, J.H. and Scott, R.L., *'The Solubility of Non-Electrolytes'*, 3rd Ed.,1950, (New York : Rheinhold)

29 Burrell, H., *Off. Dig.*, 1957, **29**, 1069

30 Burrell, H., *Off. Dig*, 1955, **27**, 726

31 Crowley, J.D., Teague, G.S. and Lowe J.W., *J. Paint Technol.*, 1966, **38**, 269

32 Crowley, J.D., Teague, G.S. and Lowe J.W., *J. Paint Technol.*, 1967, **39**,19

33 Gordy, W., *J. Chem. Phys.,* 1940, **8**, 170

34 Nelson, R.C, Hemwell, R.W. and Edwards, G.D., *J. Paint Technol.*, 1970, **42**, 636

35 Hansen, C.M., *J. Paint Technol.*, 1967, **39**, 104

36 Hansen, C.M., *Farg och Lack*, 1971, **4**, 69

37 Barton, A.F., *Handbook of Solubility Parameters and Other Cohesion Parameters*, 1983, (Florida : CRC Press)

38 Wallström, E., and Svenningsen, I., *Handbook of Solvent Properties*, 1984, (Denmark : Scandinavian Paint and Printing Ink Research Institute)

39 Wallström, E., *Farg och Lack Scand.*, 1984, **19**, 127

40 Huyskens, P.L., Haulait-Pirson, M.C., Brandts Buys, L.D and Van der Borght, X.M, *J. Coatings Technol.*, 1985, **57**, 57

41 Fredenslund, A., Jones, R.L. and Prausnitz, J.M., *AIChE J.*, 1975, **21**, 1086

42 Fredenslund, A., Gmehling, J., and Rasmussen, P., *"Vapour-Liquid Equilibria using UNIFAC"*, 1977, (Amsterdam : Elsevier)

43 Skjold-Jørgensen, S., Kolbe, B., Gmehling, J. and Rasmussen, P., *Ind. Eng. Process Des. Dev.*, 1979, **18**, 714

44 Koehnen, D.M. and Smolders, C.A., *J. Appl. Polym. Sci.*, 1975, **19**, 1163

45 Mieczkowski, R., *Eur. Polym. J.*, 1988, **24**, 1185

46 Mieczkowski, R., *Eur. Polym. J.*, 1989, **25**, 1055

47 BRITE Project RI 1B 0246 C(H) Technical Review of Research, July - December, 1989, TNO Report p12.

48 Wu, D.T., *XVIIth FATIPEC Congress, Lugano, Switzerland*, 1984, **3**, 347

49 Martuscelli, E., *XIVth Int. Conf. Org. Coat. Sci. Technol., (Athens),* 1988, 207

50 Holten-Andersen, J., *XIIth Int. Conf. Org. Coat. Sci. Technol.,* 1986, 13

51 Flory, P.J.,*"Principles of Polymer Chemistry"*, 1953, (New York : Cornell University Press)

52 Tompa, H, '*Polymer Solutions*', 1956 (London : Butterworths)

53 Howe, S.E., and Coleman, M.M., *Macromolecules*, 1986, **19**, 72

54 Painter, P.C., Park, Y., and Coleman, M.M., *Macromolecules*, 1986, **19**, 66

55 Coleman, M.M., *Polymer.*, 1988, **29**, 1659

56 Patterson, D., *Polym. Eng. Sci.*, 1982, **22**, 64

57 Painter, P.C., Park, Y., and Coleman, M.M., *Macromolecules*, 1989, **22,** 580

58 Painter, P.C., Park, Y., and Coleman, M.M., *Macromolecules*, 1988, **21,** 66

59 Patterson, D., *Macromolecules*, 1978, **11**, 690

60 Harkins, W. D. and Jordan., *J. Amer. Chem. Soc.*, 1930, **52**, 1751

61 Ellison, A.H. and Zisman, W.A., *J. Phys. Chem.*, 1954, **58**, 260.

62 Zisman, W. A., *J. Paint Technol.* 1972, **44**, 42

63 Neumann, A.W., Good, R.J., Hope, C.J. and Sejpal, M., *J. Colloid Interface Sci.*, 1974, **49**, 291.

64 Spelt, J.K. and Neumann, A.W., *Langmuir*, 1987, **3**, 588.

65 Spelt, J.K. and Neumann, A.W., *Prog. Colloid Polymer Sci.*, 1988, **77**, 26.

66 Sell, P.J. and Neumann, A.W., *Angew. Chem. Internat. Edit.*, 1966, **5**, 299.

67 Good, R.J. and Girifalco, L.A., *J. Phys. Chem.*, 1957, **61**, 904.

68 Good, R.J. and Girifalco, L.A., *J. Phys. Chem.*, 1960, **64**, 561

69 Good, R.J. Girifalco, L.A. and Kraus, G., *J. Phys. Chem.*,1957, **61**, 904.

70 Fowkes, F.M., *J. Phys. Chem.*, 1962, **66**, 382.

71 Fowkes, F.M., *Ind. Eng. Chem.*, 1964, **56**, 15.

72 Fowkes, F.M. and Mostafa, M.A., *Ind. Eng. Chem., Prod. Res. Dev.*, 1978, **17**, 3.

73 Wu, S., *J. Adhesion,* 1973, **5**, 39.

74 Van Oss, C.J., Chaudhurry, M.K. and Good, R.J., *Chem. Rev.,* 1988, **88**, 927.

75 Van Oss, C.J., Chaudhurry, M.K. and Good, R.J., *Adv. Colloid Interface Sci.*, 1987, **35**, 28.

76 Good, R.J., Chaudhurry, M.K. and Van Oss, C.J., *'Fundamentals of Adhesion'* (ed. Lee, L.H.), 1991 (New York : Plenum)

77 Van Oss, C.J. Chaudhurry, M.K., and Good, R.J., *Sep. Sci. Technol.*, 1989, **24**, 15.

78 Van Oss, C.J. and Good, R.J., *J. Macromal, Sci., Chem.*, 1989, **A26(8)**, 1183

79 Urban, M. W., *J. Coat. Techn.*, 1987, **59** (745), 29

80 Urban, M. W., *Prog. Org. Coat.* 1989, **16**, 321

81 Carter, R. O., Paputa Peck, M. C., and Bauer, D. R., *Polym. Degradation & Stability*, 1989, **23**, 121

82 McTurk, G., Bulman, S. and Ockleford, C. D., *J. Micros.*, 1982, **127**, 233

83 Wallström, E., and Svenningsen, I., *Handbook of Solvent Properties*, 1984, (Denmark : Scandinavian Paint and Printing Ink Research Institute)

84 British Standards Institution.
Determination of volatile matter and non-volatile matter
BS 3900 : Part B2 : 1970 (1991)

85 British Standards Institution.
Measurement of specular gloss of non-metallic paint film at 20°, 60° and 85°. BS 3900 : Part D5 : 1980 (1987)

86 American Society for Testing and Materials
Test method for film hardness by pencil test. ASTM D-3363-74 (1989)

87 British Standards Institution.
Pendulum Damping Test. BS 3900 : Part E5 : 1973 (1991)

88 British Standards Institution.
Cross-cut test. BS 3900 : Part E6 : 1974 (1989)

89 British Standards Institution.
Bend Test (Conical Mandrel). BS 3900 : Part E11 : 1985 (1991)

90 British Standards Institution.
Determination of resistance to liquids. BS 3900 : Part G5 : 1976 (1991)

91 British Standards Institution.
Resistance to artificial weathering (enclosed carbon arc)
BS 3900 : Part F3 : 1971 (1986)

92 BRITE Project RI 1B 0246 C(H). Technical Review of Research, June - December 1990, PRA Report

93 BRITE Project RI 1B 0246 C(H) Technical Review of Research, July-December, 1990, TNO Report, P18